



UNIVERSIDADE FEDERAL DE ALAGOAS
INSTITUTO DE CIÊNCIAS BIOLÓGICAS E DASAÚDE
PROGRAMA DE PÓS-GRADUAÇÃO EM CIÊNCIAS DA SAÚDE

VICTOR MENEZES SILVA

**ANÁLISE BIOINFORMÁTICA DAS CÉLULAS DE SCHWANN NA PROGRESSÃO
DO CÂNCER DE PULMÃO**

MACEIÓ

2019

VICTOR MENEZES SILVA

**ANÁLISE BIOINFORMÁTICA DAS CÉLULAS DE SCHWANN NA PROGRESSÃO
DO CÂNCER DE PULMÃO**

Dissertação apresentada ao Programa de Pós-Graduação em Ciências da Saúde da Universidade Federal de Alagoas para obtenção do título de Mestre em Ciências da Saúde.

Orientadora: Prof.^a Dr.^a Aline Cavalcanti de Queiroz

Maceió

2019

Catálogo na fonte
Universidade Federal de Alagoas
Biblioteca Central
Divisão de Tratamento Técnico

Bibliotecário: Marcelino de Carvalho Freitas Neto – CRB-4 – 1767

- S586a Silva, Victor Menezes.
Análise bioinformática das células de *Schwann* na progressão do câncer de pulmão / Victor Menezes Silva. – 2019.
117 f. : il.
- Orientadora: Aline Cavalcanti de Queiroz.
Dissertação (mestrado em Ciências da Saúde) – Universidade Federal de Alagoas. Instituto de Ciências Biológicas e da Saúde. Maceió, 2019.
- Bibliografia: f. 110-117.
1. Células de *Schwann*. 2. Microambiente tumoral. 3. Neoplasias pulmonares. 4. Biologia computacional. I. Título.

CDU: 616.24-006



Universidade Federal de Alagoas
Instituto de Ciências Biológicas e da Saúde
Programa de Pós-graduação em Ciências da Saúde

ICBS - UFAL – Campus A. C. Simões
Av. Lourival Melo Mota, S/N
Cidade Universitária – Maceió-AL
CEP: 57072-900
E-mail: ppgcs9@gmail.com
Fone: 82 3214 1850

Folha de Aprovação

Victor Menezes Silva

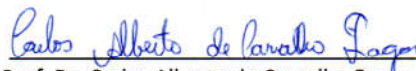
Análise bioinformática das células de Schwann na progressão do câncer de pulmão

Dissertação submetida ao corpo docente do Programa de Pós-Graduação em Ciências da Saúde da Universidade Federal de Alagoas e aprovada em 20 de março de 2019.

Banca Examinadora



Profa. Dra. Aline Cavalcanti de Queiroz (Orientador)



Prof. Dr. Carlos Alberto de Carvalho Fraga – (UFAL)



Profa. Dra. Bruna Del Vecchio Koike – (UNIVASF)

Dedico esse trabalho aos que lutam para que todos tenham oportunidades de vivenciar os privilégios sociais que vivi.

AGRADECIMENTOS

Ao Prof. Dr. Carlos Alberto de Carvalho Fraga, por todo empenho na colaboração desse trabalho. Espero que esse seja apenas o início de uma longa história de amizade e compromisso!

Aos meus amigos Rafael Dannylo, Emerson Xavier, Carol Marques, Amanda Karine Ferreira e Jussara Baggio (os siameses). Não tinha noção de que criaria um vínculo tão forte e verdadeiro com vocês! Muito obrigado por todo apoio!

Agradeço, novamente, aos meus grandes amigos Emerson e Rafael. Meus dias aqui são mais alegres com a presença de vocês! Obrigado pelo acolhimento!

Às integrantes do grupo URSAL, Daniele Silva e Eloiza Tanabe. Que conseguem fazer brotar sorrisos no meu rosto, até quando estou estressado.

À Aline Cavalcanti de Queiroz, quem acreditou em mim desde minha chegada ao campus. “Medicina não é fácil, Victor, se prepare!”. Muito obrigado pelos vários votos de confiança!

A toda turma do IESC, em especial aos amigos Carlos Dornels, Jamile Ferro, Michael Machado, Rafael Silva, Raquel Santos e Deysiany Porto. Sinto-me honrado em compartilhar conhecimento e aprender tanto com vocês!

À Paula, por toda história vivida. Que nosso respeito e afeto durem pra sempre.

Aos colegas do LABMEG Edilson, Carolzinha e Ithallo, pelos sorrisos sinceros e pelos ensinamentos compartilhados.

À Bruna Del Vechio Koike, uma das minhas referências de pessoa guerreira.

Ao amigo Luiz Araújo, por todo suporte durante minha vinda. Jamais esquecerei das suas maluquices!

Ao colega Daniel Coimbra. Desfruto daquela sua ajuda até hoje. Muito Obrigado!

Às alunas Jéssica e Karen, pelas contribuições na produção desse trabalho.

Ao Grupo de Pesquisa em Neurociências e Tempo – GENTE, em especial ao amigo Leandro Lourenção Duarte, que promoveu meu interesse na ciência. Sou fã do seu trabalho e te desejo muito sucesso.

À Fundação de Amparo à Pesquisa do Estado de Alagoas (FAPEAL), por todo investimento na minha formação acadêmica.

E, finalmente, um agradecimento especial ao Grupo de Estudos em Biociências e Saúde – GEBS, particularmente à minha amiga Cristiane.

“Nem médico, nem doutô, me chame de professor.”

Victor Menezes

RESUMO

O fenômeno da carcinogênese é um processo complexo que ocorre por meio de múltiplos eventos genéticos que alteram as funções normais dos oncogenes e genes supressores de tumor. Estudos mostraram que as células de Schwann participam do microambiente tumoral, produzindo vários fatores que beneficiam as células cancerígenas. Durante esse processo, as células de Schwann são desdiferenciadas e auxiliam o processo de proliferação das células cancerígenas. Essas células então migram para a região próxima ao tecido tumoral e auxiliam o desenvolvimento da célula neoplásica. Nesse contexto, o objetivo do presente estudo foi avaliar a influência das células de Schwann sobre os cânceres de pulmão. Realizamos uma visão bioinformática e observamos que a "interação neuroativo ligante-receptor" foi regulada positivamente em LUSC e regulada negativamente em LUAD. A "via de sinalização do p53" estava ativa em ambos os cânceres de pulmão, uma vez que o CCNE1, CDKN2A e PERP estavam sobre-regulados. Enquanto isso, os miRNAs regulados inativam a via de "orientação dos axônios", visando os genes ROBO2 e SLIT2. Ambos os genes também estão associados à inibição da migração das células de Schwann. Além disso, o GFAP e o GAP43 são superexpressos, levando à desdiferenciação das células de Schwann. Além disso, tanto Schwann quanto as células cancerígenas são estimuladas via cascata de fosforilação para proliferar e migrar. Acreditamos também que a desdiferenciação e proliferação de células de Schwann são induzidas por tecido neoplásico; Consequentemente, as células de Schwann produzem diferentes fatores que participarão de vários processos de progressão tumoral. Esses processos também podem estar envolvidos na invasão do tumor no tecido perineural, especialmente em LUSC.

Palavras-Chave: Células de Schwann. Microambiente Tumoral. Progressão Tumoral. Câncer de Pulmão.

ABSTRACT

The phenomenon of carcinogenesis is a complex process that occurs through multiple genetic events that alter the normal functions of oncogenes and tumor suppressor genes. Studies have shown that Schwann cells participate in the tumor microenvironment, producing several factors that benefit cancer cells. During this process, Schwann cells are dedifferentiated and help the process of cancer cell proliferation. These cells then migrate to the region close to the tumor tissue and assist the development of the neoplastic cell. In this context, the aim of the present study was to evaluate the influence of Schwann cells over lung cancers. We performed a bioinformatic insights and we observed that the "neuroactive ligand-receptor interaction" pathway was upregulated in LUSC and downregulated in LUAD. The "p53 signaling pathway" was active in both lung cancers, since CCNE1, CDKN2A, and PERP were upregulated. Meanwhile, upregulated miRNAs inactivate the "axon guidance" pathway, targeting ROBO2 and SLIT2 genes. Both genes are also associated with Schwann cells migration inhibition. Also, GFAP and GAP43 are overexpressed, leading to Schwann cells dedifferentiation. Besides, both Schwann and cancer cells are stimulated via phosphorylation cascade to proliferate and migrate. We also believe that Schwann cells' dedifferentiation and proliferation are induced by neoplastic tissue; Consequently, Schwann cells produce different factors that will participate in various processes of tumor progression. These processes may also be involved in tumor invasion into the perineural tissue, especially in LUSC.

Key-Words: Schwann cells. Tumor microenvironment. Tumoral progression. Lung cancer.

LISTA DE FIGURAS

Figura 1- Representação esquemática de um microambiente tumoral.....	13
Figura 2- Representação esquemática da EMT (transição epitélio-mesenquimal) e MET (transição mesenquimal-epitelial) no contexto da progressão tumoral.	16
Figura 3- Resposta de uma fibra nervosa à lesão	19
Figura 4- Diagrama esquemático da resposta à lesão neuronal nos sistemas nervosos periférico e central.....	21

LISTA DE SIGLAS

- BDNF** – Brain Derived Neurotrophic Factor (Fator de Crescimento Derivado do Cérebro)
- BRCA** – Breast Invasive Carcinoma (Carcinoma Invasivo da Mama)
- CNF** – Ciliary Neurotrophic Factor (Fator Neurotrófico Ciliar)
- DEGs** – differentially Expressed Genes (Genes Diferencialmente Expressos)
- GDNF** – Glial Derived Neurotrophic Factor (Fator de Crescimento Derivado da Glia)
- GEO** – Gene Expression Omnibus
- GFAP** – Glial Fibrillary Acidic Protein (Proteína Ácida Fibrilar Glial)
- GO** – Gene ontology (Ontologia Genética)
- IGF** – Insulin – like Growth Factor (Fator de Crescimento associado à Insulina)
- KEGG** – Kyoto Encyclopedia of Genes and Genomes
- LUAD** – Lung Adenocarcinoma (Adenocarcinoma Pulmonar)
- LUSC** – Lung Squamous Cell Carcinoma (Carcinoma de Células Escamosas do Pulmão)
- MET** – Mesenchymal–Epithelial Transition (Transição Mesênquima-Epitélio)
- MMPs** – Matrix Metalloproteinases (Metaloproteinases de Matriz)
- NCAM1** – Neural Cell Adhesion Molecule 1 (Molécula de Adesão Celular Neural 1)
- NGF** – Nerve Growth Factor (Fator de Crescimento Neural)
- PRAD** – Prostate Adenocarcinoma (Adenocarcinoma da Próstata)
- SNC** – Sistema Nervoso Central
- SNP** – Sistema Nervoso Periférico
- TCGA** – The Cancer Genome Atlas
- TIMER** – Tumor Immune Estimation Resource
- TNF α** – Tumor Necrosis Factor- α (Fator de Necrose Tumoral α)
- VEGF** – Vascular Growth Endothelial Factor (Fator Endotelial de Crescimento Vascular)

SUMÁRIO

1.	Introdução.....	11
i.	Fenômeno neoplásico.....	11
ii.	Câncer de pulmão.....	17
iii.	Resposta dos neurônios periféricos a lesão.....	21
iv.	Células de Schwann	23
v.	Sistema nervoso periférico, células de Schwann e câncer	23
vi.	Análise computacional	23
2.	Objetivos.....	28
v.	Objetivo geral.....	28
vi.	Objetivos específicos	28
3.	Metodologia.....	30
4.	Referências	111

1. INTRODUÇÃO

i. Fenômeno neoplásico

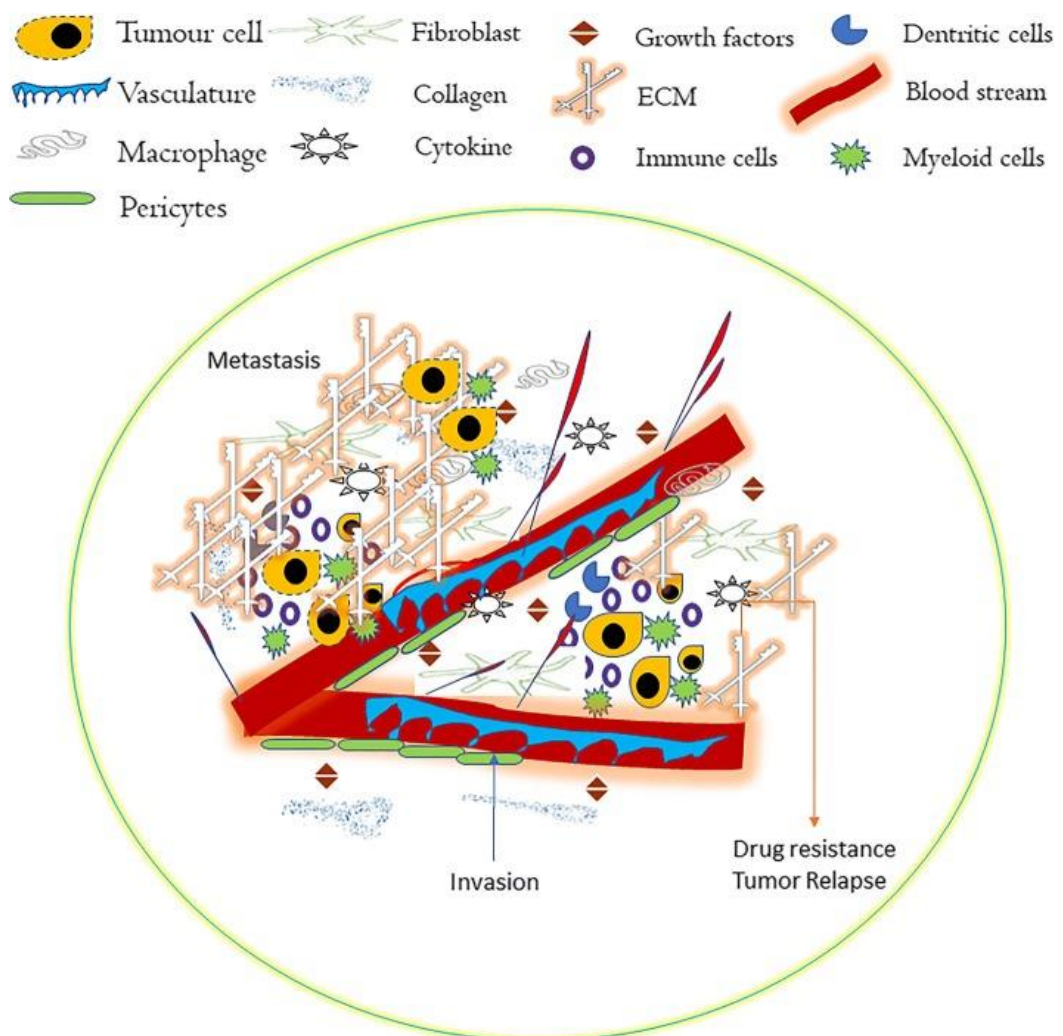
O câncer é a segunda principal causa de mortalidade a nível global. No Brasil, foi estimado pelo Instituto Nacional do Câncer (INCA), que no biênio 2018-2019 a taxa de incidência é de 600 mil novos casos por ano (BRASIL, 2017). Esse fato se deve, principalmente, pela especificidade da doença a nível tecidual, sendo um grande desafio para o diagnóstico específico e eficácia dos tratamentos (KOGURE; KOSAKA; OCHIYA, 2019; GATENBY; GILLIES, 2008). Em homens, os maiores percentuais de tipos de câncer ocorrem na próstata, pulmão e brônquios, cólon e reto, e bexiga, respectivamente (XIAO *et al.*, 2019). Em mulheres, a prevalência de câncer é mais alta na mama, pulmão e brônquios, cólon e reto, corpo uterino e tireoide, respectivamente (VILLARREAL-GARZA *et al.*, 2019). Tais dados indicam que o câncer de próstata e de mama constitui uma parcela importante do câncer em homens e mulheres, respectivamente (ZHOU; HUANG, 2011).

O fenômeno da carcinogênese é um processo complexo que ocorre através de múltiplos eventos genéticos que alteram as funções normais dos oncogenes e dos genes supressores de tumor (DU; CHENG; SU, 2019). Essas alterações podem resultar em produção aumentada de fatores de crescimento ou do número de receptores celulares de superfície, dos sinalizadores intracelulares, e/ou produção aumentada de fatores de transcrição (PAXTON *et al.*, 2019). A perda da atividade supressora de tumor leva a um fenótipo celular capaz de aumentar a proliferação celular e a perda da adesão celular, habilitando essas células mutadas a se infiltrarem nos tecidos locais e a se espalharem para sítios distantes (GRÜNDKER *et al.*, 2019). Metástase é a causa de 90% de mortes de câncer e configuram um conjunto diverso de manifestações clínicas (NOGUTI *et al.*, 2012; ZHOU; HUANG, 2011) Metástases são formadas por células neoplásicas malignas que deixam o sítio primário e trafegam via vasos sanguíneos e linfáticos até novos sítios no organismo onde disseminam novas colônias (KOGURE; KOSAKA; OCHIYA, 2019). As células do câncer, então, empregam diversas estratégias de auxílio à adaptação e, posteriormente, expansão e progressão em um novo sítio. A formação e progressão do câncer é um processo multissistêmico, envolvendo o sistema imunológico, vascularização e disseminação (DROMAIN, *et al.*, 2019). A capacitação

metastática caracteriza-se pelo crescimento tumoral, invasão da membrana basal em tecidos da submucosa, formação vascular e linfática, invasão tecidual sistêmica e posterior (LO; ZHANG, 2018; NOGUTI *et al.*, 2012; ZHOU; HUANG, 2011).

As células que circundam um tumor formam um microambiente molecular conhecido como estroma (Figura 1). O estroma pode ser influenciado e, por sua vez, influencia o crescimento, migração e invasão tumoral, além da resistência farmacológica (DE OLIVEIRA *et al.*, 2009; MILLER *et al.*, 2007).

Figura 1 – Representação esquemática de um microambiente tumoral.



Fonte: THOMAS; RADHAKRISHNAN, 2019.

Dependendo das características do tumor primário, do estroma e a capacidade intrínseca de células tumorais metastáticas a se adaptarem em um novo local, as células

malignas usam mecanismos distintos na proliferação, sobrevivência e disseminação (NAJI *et al.*, 2019).

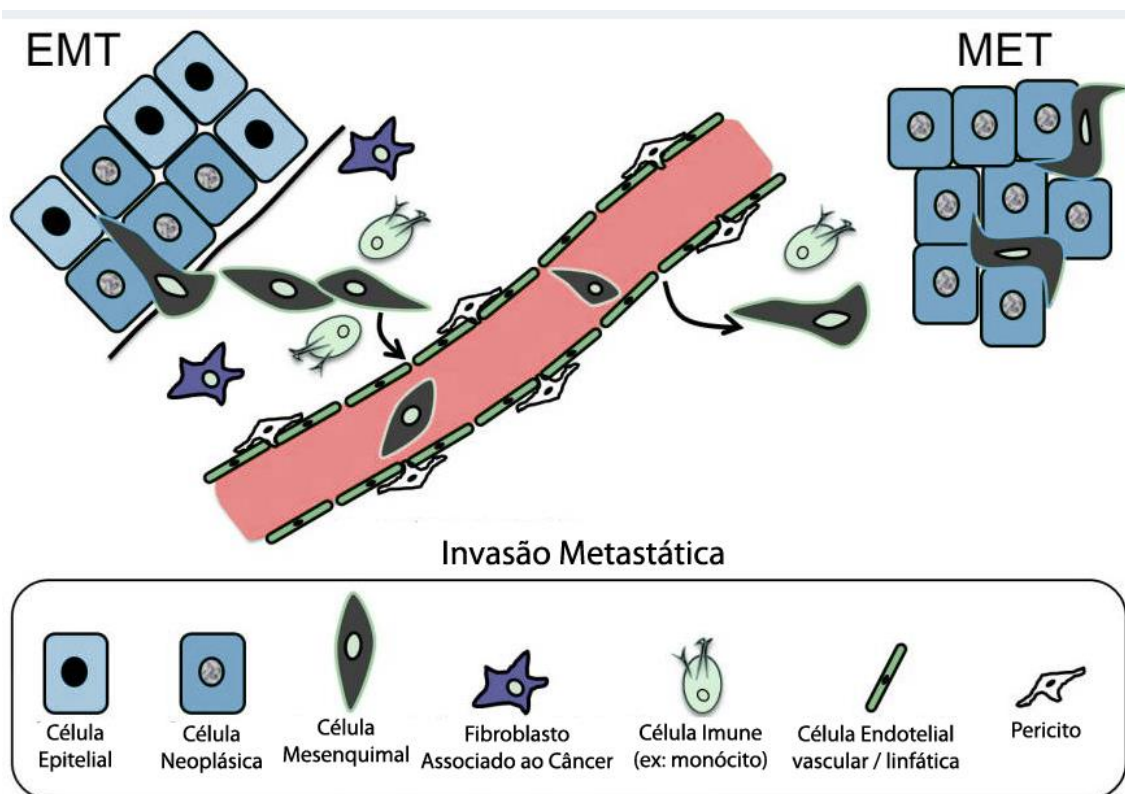
Essas células frequentemente reativam a expressão de genes que são empregados por células normais durante o processo de embriogênese (THOMAS; RADHAKRISHNAN, 2019; LO; ZHANG, 2018; NOGUTI *et al.*, 2012). Para deixar o tumor primário e disseminar em órgãos distantes, as células metastáticas perdem a habilidades de aderência às células adjacentes, potencializando a capacidade migratória e invasiva. Esse mecanismo é acompanhado por várias modificações na expressão de genes, como por exemplo, perda da expressão de receptores epiteliais e aumento da expressão de marcadores mesenquimais, fenômeno também conhecido como transição epitélio-mesenquimal (AIELLO *et al.*, 2018; LARNE *et al.*, 2015).

A matriz extracelular desempenha um papel crítico no microambiente tumoral. Durante a formação tumoral, as células neoplásicas se ligam a moléculas presentes na matriz extracelular, o que facilita a comunicação com outras células, tais como neutrófilos, fibroblastos, macrófagos e linfócitos (MCCUBREY *et al.*, 2007). A matriz extracelular é especialmente importante na formação e invasão tumoral à medida que as células respondem e se adaptam ao microambiente local. Isto envolve tanto a proliferação desregulada de células tumorais como a modificação do ambiente imediato para favorecer a sobrevivência celular, a angiogênese e o crescimento tumoral (KOGURE; KOSAKA; OCHIYA, 2019). A superexpressão de citocinas, tal como o fator de necrose tumoral α (TNF α), uma citocina envolvida em várias vias de sinalização e no processo inflamatório, potencializa o processo metastático (RANDOLPH; JAKUBZICK; QU, 2008). Fatores que podem degradar a matriz extracelular também facilitam a formação e invasão tumoral. Por exemplo, as metaloproteinases de matriz (MMPs) têm sido associadas na degradação de membranas basais e matriz extracelular, facilitando a invasão e metástase de células tumorais, bem como promovendo proliferação celular, metástases e angiogênese (HINGORANI *et al.*, 2018; YAO *et al.*, 2018). Além das degradações de membranas basais e da matriz, outro aspecto importante na formação e invasão do tumoral é o processo denominado transição epitélio-mesenquimal, o qual possibilita que uma célula epitelial associada a um tumor comece a secretar fatores típicos da matriz extracelular (KANG *et al.*, 2019).

O tecido epitelial é caracterizado pela presença de células epiteliais justapostas fortemente unidas por glicoproteínas de adesão, e pela ausência ou pouca presença de matriz extracelular (PAKULA *et al.*, 2019; MASCOLO *et al.*, 2012). Aderida na base do tecido epitelial está localizada a membrana basal, camada que divide as células epiteliais das células mesenquimais (NAJI *et al.*, 2019). As células mesenquimais são geralmente fusiformes e indiferenciadas, possuindo um relevante potencial de diferenciação com objetivo de suprir a demanda homeostática no tecido em que se localiza (AIELLO *et al.*, 2018; PASTUSHENKO *et al.*, 2018).

Um fenômeno conhecido como transdiferenciação ocorre sempre que exista necessidade de alguma transição fenotípica celular (MARKIEWICZ *et al.*, 2019). Uma clássica transdiferenciação no tecido epitelial é conhecido como transição epitélio-mesenquimal (EMT), que confere a capacidade de mudanças morfofuncionais das células epiteliais, apresentando fenótipos de células mesenquimais semelhante aos fibroblastos, organizados livremente com intensa mobilidade (ZHANG *et al.*, 2019; TSUBAKIHARA; MOUSTAKAS, 2018). Uma vez transdiferenciada no processo de EMT, a célula começa a apresentar funções migratórias e invasivas (PAKUŁA *et al.*, 2019). Para uma EMT bem sucedida, são necessárias complexas modificações estruturais e funcionais na célula (PASTUSHENKO *et al.*, 2018). Além da modificação do epitélio para mesênquima (EMT), também é possível que o processo reverso aconteça, fenômeno denominado como transição mesênquima-epitélio (MET), o qual confere a transdiferenciação de uma célula mesenquimal migratória em fenótipos de célula epitelial (figura 2), após possível realocação em um novo ambiente (MARKIEWICZ *et al.*, 2019; HUANG; WU; XU, 2015).

Figura 2 – Representação esquemática da EMT (transição epitélio-mesenquimal) e MET (transição mesenquimal-epitelial) no contexto da progressão tumoral.



Fonte: adaptação de MOUSTAKAS; HELDIN, 2016.

As EMTs são processos comumente encontrados durante a embriogenese além de diversos processos fisiopatológicos e reparo tecidual, por exemplo, nos processos inflamatórios, cicatrização e fibrose (NAJI *et al.*, 2019; LO; ZHANG, 2018). Atualmente distingue-se três tipos de EMTs: o tipo I, que são atuantes em condições não patológicas, como exemplo no cenário embrionário; o tipo II que operam durante a regeneração tecidual, fibrose e cicatrização de feridas; e tipo III que participam durante a progressão tumoral através de mutações genéticas ou modificações epigenéticas no DNA e histonas (ZHANG *et al.*, 2019; PAKULA *et al.*, 2019; MOUSTAKAS, 2018). As manifestações de EMT do tipo III são mais frequentes em compostos supressores de tumor, através de processos de acetilação, metilação, e fosforilação, conferindo maior capacidade migratória e invasiva (LO; ZHANG, 2018).

ii. Câncer de pulmão

A base molecular do câncer de pulmão é complexa e heterogênea. Melhorias na compreensão das alterações moleculares em múltiplos níveis (genética, epigenética, expressão proteica) e sua significância funcional têm o potencial de influenciar o diagnóstico, o prognóstico e o tratamento da doença. Os cânceres de pulmão desenvolvem-se através de um processo de múltiplas etapas envolvendo o desenvolvimento de múltiplas alterações genéticas e epigenéticas, particularmente a ativação de vias promotoras do crescimento e a inibição de vias supressoras de tumor (GUO *et al.*, 2015; ZHOU *et al.*, 2018). A maior compreensão das múltiplas vias bioquímicas envolvidas na patogênese molecular do câncer de pulmão é crucial para o desenvolvimento de estratégias de tratamento que possam direcionar as aberrações moleculares e suas vias ativadas a jusante. Alterações moleculares específicas que impulsionam o crescimento do tumor e fornecem alvos para a terapia foram melhor definidas em adenocarcinomas, mas há um interesse crescente nas vias moleculares do carcinoma de células escamosas, destacando novos potenciais alvos terapêuticos. No câncer de pulmão, como em outras malignidades, a tumorigênese relaciona-se à ativação de proteínas promotoras do crescimento [por exemplo, v-Ki-ras2, homólogo do oncogene viral do sarcoma de rato Kirsten (KRAS), receptor do fator de crescimento epidérmico (EGFR), BRAF, MEK-1, HER2, MET, ALK e rearranjado durante a transfecção (RET), bem como a inativação de genes supressores de tumor [por exemplo, P53, fosfatase com homologia da tensina (PTEN), LKB-1]. A ativação de oncogenes promotores do crescimento pode ocorrer por amplificação gênica ou outras alterações genéticas, incluindo mutações pontuais e rearranjos estruturais que levam à sinalização descontrolada através de vias oncogênicas (GUO *et al.*, 2015). As mutações condutoras oncogênicas foram identificadas em mais de 50% dos carcinomas de células escamosas de pulmão.

Alterações epigenéticas são comuns no câncer de pulmão. A hipermetilação da citosina em grupos de dinucleídeos CpG na sequência promotora de DNA de genes codificadores de proteases pode levar perda de expressão genica. No câncer de pulmão, mais de 80 genes foram identificados como hipermetilados, incluindo genes supressores de tumores, como por exemplo o p16INK4 α . A detecção do DNA metilado pode ser um biomarcador útil para a detecção precoce do câncer de pulmão. Estudos mostraram que a detecção de três ou mais genes metilados de um painel de seis genes selecionados se

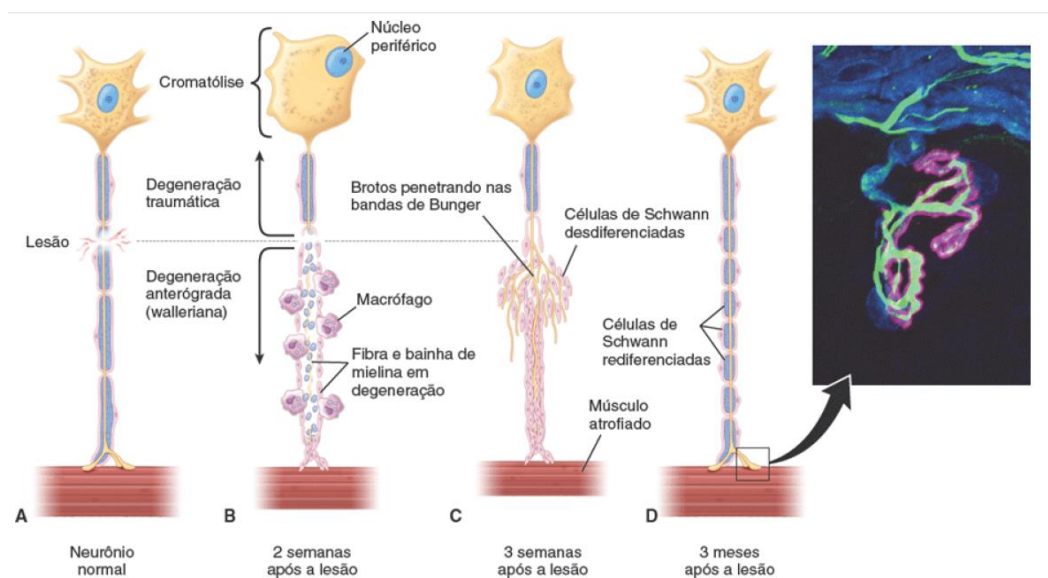
correlacionou com um aumento de 6,5 vezes no câncer de pulmão. Além disso, outra alteração epigenética que inibe a expressão gênica é a desacetilação de histonas. A metilação do promotor e a desacetilação da histona são processos reversíveis; assim, a inibição farmacológica é uma potencial estratégia terapêutica inovadora que pode reverter o silenciamento gênico e, portanto, ser eficaz em neoplasias (GUO et al., 2015; ZHOU et al., 2018).

iii. Resposta dos neurônios periféricos a lesão

Um nervo periférico, quando sofre uma axonotmese, caracterizada pela ruptura axonal, é dividido em duas partes a partir do local lesionado: coto proximal e coto distal, tomando como referência a distância entre os cotos e o corpo celular (OGATA, 2004; KANDEL *et al.*, 2003). É fundamental entender as diferenças de processos que ocorrem em cada segmento, pois uma sequência de eventos morfofuncionais (Figura 3), essenciais no processo de regeneração nervosa, acontece em ambas as partes logo após a lesão (KUMAMARU *et al.*, 2018; MAGGI, LOWE E MACKINNON, 2003).

Imediatamente após a lesão, o corpo celular já inicia uma série de respostas metabólicas, reorganização citoplasmática e alterações específicas de expressão gênica, conhecidas como reação neuronal (NAVARRO, 2015). São características da reação neuronal do corpo celular, singulares retrações dos dendritos; considerável intumescimento do volume celular provocada pela elevada síntese de mRNA e proteínas (JESSEN E MIRSKY, 2016); superregulação do gene c-JUN, o qual a transcrição está relacionada com os estágios regenerativos (ROSS E PAWLINA, 2016); migração do núcleo em direção a periferia (ZOCHODNE, 2000); e dispersão do retículo endoplasmático rugoso, responsável pela formação da substância de Nissl, evento que promove a deriva dos ribossomos no citoplasma, caracterizando o fenômeno conhecido como cromatólise (SIMONS; NAVE, 2015; NAVARRO, VIVÓ E VALERO-CABRÉ, 2007; EVANS, 2001). Se o processo de regeneração for eficiente, as alterações morfofuncionais do corpo celular são comumente reversíveis após a conclusão do processo (FRIK *et al.*, 2018; GEMINIANI *et al.*, 2018; KUMAMARU *et al.*, 2018; BOYD E GORDON, 2003).

Figura 3 – Resposta de uma fibra nervosa à lesão. A. Uma fibra nervosa normal que sofreu lesão; B. Fibra nervosa após lesão; C. Células de Schwann promovendo a formação dos cordões de Bungier; D. Regeneração bem sucedida.



Fonte: Ross e Pawlina, 2016.

No coto proximal, se inicia um processo de degeneração traumática retrograda do axônio através da ação de células de Schwann e macrófagos, que fagocitam a estrutura axonal e mielínica residual em direção ao corpo celular, até que seja alcançado o próximo nódulo de Ranvier (FRIK *et al.*, 2018; PENAS; NAVARRO, 2018). O processo de degeneração também tem capacidade de progredir através de vários segmentos internodais, podendo até atingir o corpo celular, provocando consequentemente a morte do nervo lesionado (JOHNSON, ZOBOS E SOUCACOS, 2005; BURNET E ZAGER, 2004). As células de Schwann presentes na estrutura do axônio associado ao coto proximal, também iniciam a secreção de fatores de crescimento que são fundamentais moduladores celulares de proliferação, migração e sobrevivência aos agentes envolvidos no processo de reparo axonal (HEINEN *et al.*, 2015; CHEN, COHEN E HALLETT, 2002). Partindo da idéia de quando a degeneração retrograda do coto proximal é interrompida em algum dos nódulos de Ranvier, não comprometendo o corpo celular que apresenta basicamente toda função de síntese

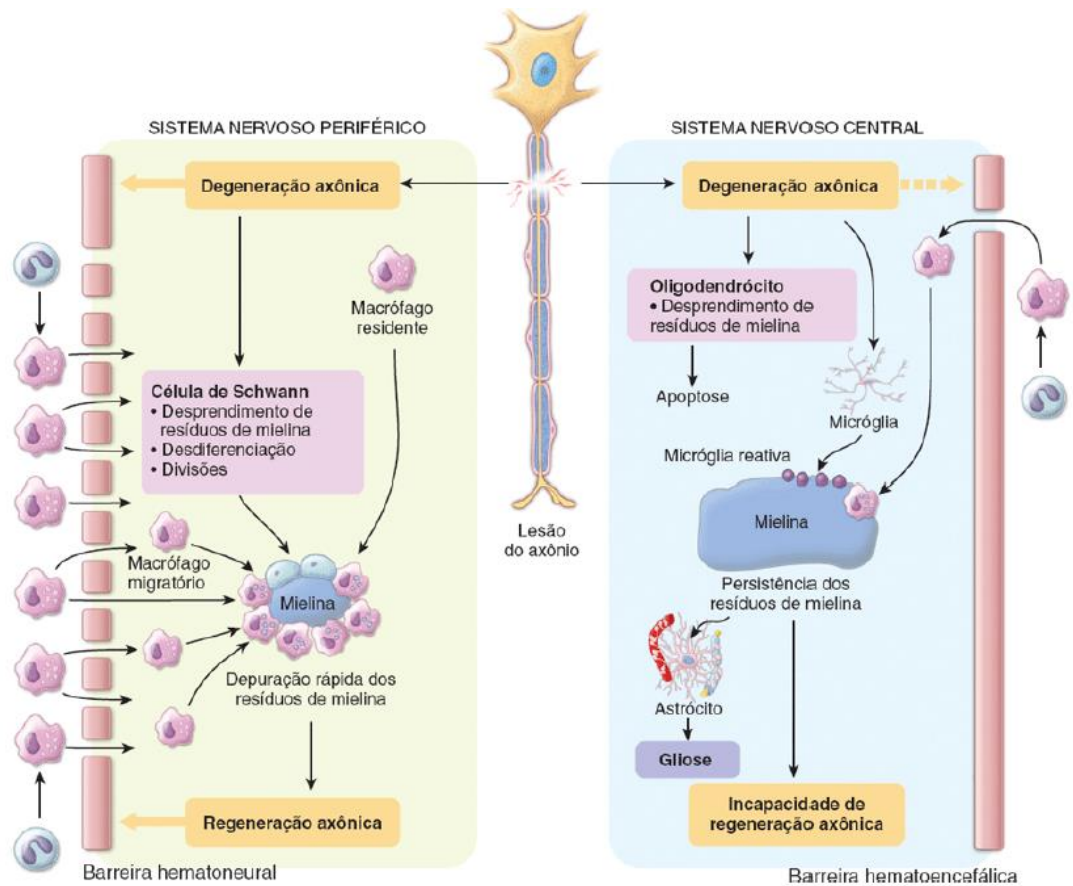
protéica, o desligamento entre os dois cotos implica na degeneração anterógrada do coto distal (GRIFFIN E THOMPSON, 2008).

A degeneração do coto distal, primeiramente descrita por Waller (WALLER, 1850), e hoje conhecida como degeneração walleriana, é um complexo processo que envolve o rearranjo total do seguimento, que se entende entre o sítio da lesão e o órgão alvo do nervo lesionado (Figura 3). Nesse processo, as múltiplas ações das células de schwann são determinantes no processo regenerativo (PORRELLO *et al.*, 2014; NAPOLI *et al.*, 2012; MARTINS *et al.*, 2005; SIQUEIRA, 2007). Logo após a injúria nervosa periférica é possível verificar o processo de tumefação do axônio distal, seguido de um evento de desintegração, além da ruptura de barreira hematoneural ao logo de toda região axônica lesionada, permitindo o influxo de macrófagos derivados de monócitos nos vasos sanguíneos (ZHANG *et al.*, 2017; GAUDET, POPOVICH E RAMER, 2011). Os macrófagos circulantes nas camadas internas dos nervos periféricos, conhecidas como macrófagos residentes, migram e proliferam ativamente logo após a ocorrência da lesão, antes dos primeiros macrófagos atravessarem a barreira hematoneural, respondendo mais rapidamente aos sinais quimiotáticos das células de Schwann (FRIK *et al.*, 2018; CONSTANTIN E TACHE, 2012). As células de Schwann iniciam a ação fagocitária dos resíduos mielínicos e axonal enquanto, simultaneamente, liberam fatores que, por quimiotaxia, atraem células fagocitárias, principalmente os macrófagos, sendo esta de extrema importante no processo de eliminação dos mielínicos-derivados, promovendo a decomposição do citoesqueleto e agregados, fenômeno chamado de desintegração granular do citoesqueleto axonal (ROSS E PAWLINA, 2016; GARMAN, 2011).

Quando perdem o contato com o axônio, as células de Schwann se desdiferenciam e intensificam a secreção de fatores de crescimento ao passo que diminuem bruscamente a expressão das proteínas mielínicas (ALLODI, UDINA E NAVARRO, 2012; GARMAN, 2011). O fator de crescimento glial (GGF, do inglês Glial Growth Factor) é um intenso estimulador de proliferação celular das células de Schwann, e, quando expresso, inicia uma potente ação de divisão das células de Schwann, com disposição linear direcionada as suas lâminas externas (DORON-MANDEL, FAINZILBER E TERENCE, 2015). Uma vez que ocorreu a desintegração granular do citoesqueleto axônico, a proliferação das células de Schwann, sob influência do GGF, promove a formação de um lúmen vazio e rodeado pelas

lâminas externas, que servirá de origem para regeneração do axônio, constituindo a primeira etapa do processo de regeneração nervosa (Figura 4) (RASBAND; PELES, 2015; PETRUSKA; MENDEL, 2004). Uma vez iniciado o processo de regeneração através da proliferação das células de Schwann desdiferenciadas, a conformação linear vai se moldando ao lúmen vazio, formando os componentes que são conhecidos como cordões celulares de Bungner, ou simplesmente bandas de Bungner, que servem como orientação norteadora que direciona a invasão do novo broto axônico em processo regenerativo (JESSEN, MIRSKY; LLOYD, 2015; SALZER, 2008).

Figura 04 – Diagrama esquemático da resposta à lesão neuronal nos sistemas nervosos periférico e central.



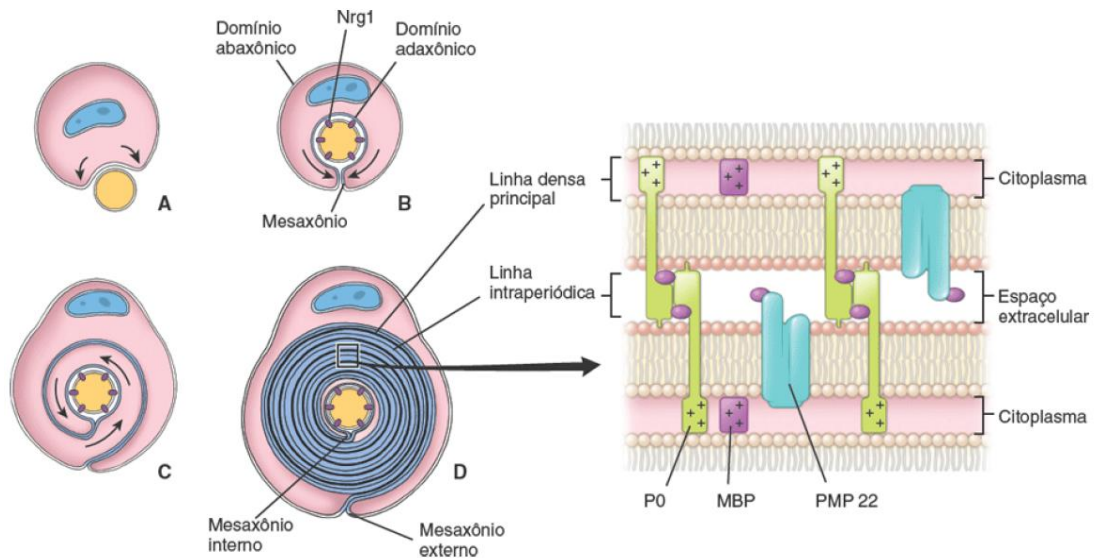
Fonte: Ross e Pawlina, 2016.

iv. Células de Schwann

O protagonismo das células de Schwann no reparo de lesões nervosas e condução da orientação do crescimento axonal evidencia suas diferenças funcionais com os oligodendrócitos (Figura 04), do sistema nervoso central (GORDON; WOOD; SULAIMAN, 2019). As células de Schwann são popularmente descritas como unidades celulares da neuroglia, presentes no sistema nervoso periférico e amplamente conhecidas pela capacidade de formar mielina, uma camada lipoproteica que promove o isolamento elétrico do axônio e, por consequência, o aumento da velocidade no impulso nervoso conhecido como o fenômeno de condução saltatória (RAASAKKA *et al.*, 2019; EL SOURY *et al.*, 2018). Existem diversos subtipos derivados da crista neural, incluindo células satélites dos gânglios da raiz dorsal e gânglios autonômicos, as células de Schwann perisinápticas da junção neuromuscular e as células de Schwann não formadoras de mielina que envolvem as fibras não mielinizadas do sistema nervoso periférico (TRICAUD, 2019; FLEDRICH *et al.*, 2018). Tais subtipos derivados da crista neural são diferenciados através da expressão do fator de transcrição Sox-10, o principal marcador de células da crista neural (SAKAUE; ENGLAND, 2015; ROSS; PAWLINA, 2016).

A bainha de mielina é, possivelmente, uma adaptação evolutiva dos seres vertebrados que permitiu um desenvolvimento mais complexo dos sistemas nervosos (JESSEN; MIRSKY; LLOYD, 2015). Durante a produção do complexo lipoproteico de mielina, fenômeno conhecido como mielinização (Figura 5), as células de Schwann envolvem um segmento do axônio, inicialmente num sulco periférico da membrana; posteriormente, conforme progressão no envolvimento do segmento axonal, ocorre a polarização em dois domínios membranosos: abaxônico (domínio exposto ao endoneuro) e adaxônico (domínio exposto ao axônio); um terceiro domínio membranoso é criado após o completo envolvimento do segmento axonal: o mesaxônio, uma dupla membrana que abrange e liga as membranas adaxônica e abaxônica (BENITO *et al.*, 2017; ZHANG *et al.*, 2017; ROSS E PAWLINA, 2016; NAPOLI *et al.*, 2012; SALZER, 2008).

Figura 05 – Diagrama dos estágios da formação da mielina por uma célula de Schwann. A. axônio posicionado num sulco periférico da célula de Schwann. B. Célula de Schwann envolvendo o axônio. C. Camadas concêntricas da bainha de mielina em desenvolvimento; D. Fusão das membranas, formando a mielina.



Fonte: Ross e Pawlina, 2016.

A bainha de mielina é formada a partir do momento que o axônio é completamente envolvido pelo mesaxônio, momento o qual uma das lâminas do mesaxônio inicia o processo de enrolamento sobre o eixo do axônio, numa circulação espiralada e controlada pela expressão da proteína transmembrana axonal Nrg1 (JESSEN; MIRSKY; LLOYD, 2015; GARMAN, 2011). Conforme progressão das voltas, quase todo volume citoplasmático da célula de Schwann é mecanicamente conduzido para fora das camadas mielinizadas (ZHANG *et al.*, 2017; SALZER, 2008).

O citoplasma de células de Schwann não mielinizadas também pode envolver porções axonais do nervo periférico, este envolvimento acontece dentro de invaginações na superfície da membrana que podem envolver mais de um axônio. Estudos comprovam que mais de 20 axônios podem estar envolvidos numa única invaginação da célula de Schwann não mielinizada (GORDON; WOOD; SULAIMAN, 2019; GARMAN, 2011).

v. Sistema nervoso periférico, células de Schwann e câncer

As taxas de sobrevida para uma variedade de tumores malignos são relativamente menores quando há invasão perineural, fenômeno que influencia diretamente na qualidade de vida do paciente, promovendo paralisia, dores entre outros fatores determinantes na morbidade (FENG *et al.*, 2018; BOCKMAN; BÜCHLER, 1994). Sabe-se que a invasão perineural está associada a múltiplos tipos de processos neoplásicos, sendo um importante sinal de metástase e invasão tumoral (CHEN *et al.*, 2019; KUANG *et al.*, 2019). Apesar da clara compreensão do conceito de invasão perineural, as vias moleculares envolvidas com o fenômeno e o mecanismo da expressão dos fenótipos móveis e invasivos ainda estão sendo investigados, sendo uma etapa essencial para idealização de estratégias terapêuticas mais eficazes (ESPAÑA-FERRUFINO; LINO-SILVA; SALCEDO-HERNÁNDEZ, 2018).

A invasão neoplásica é um evento que envolve ação de células presentes no microambiente tumoral, que promovem a progressão tumoral através da biointeração com as células neoplásicas circundantes (AZAM; PECOT, 2016; NAPOLI *et al.*, 2012). Quando se trata de uma invasão neoplásica num tecido nervoso, as células nervosas constituem o microambiente tumoral inteiro (WANG *et al.*, 2017). Células cancerosas e células nervosas se misturam e, em alguns casos, há uma perda completa dos elementos neurais (BOCKMAN; BÜCHLER; BEGER, 1994). No contexto de uma progressão tumoral, apesar de vários tipos celulares nervosos poderem contribuir para sua evolução, estudos recentes indicam que as células de Schwann estão profundamente associadas com a interação das células cancerígenas nos nichos tumorais em que há presença de tecido nervoso periférico (DEBORDE; WONG, 2017; BUNIMOVICH *et al.*, 2016).

Estudos afirmam que a plasticidade das células de Schwann exerce uma forte influência no desenvolvimento de diversas doenças humanas, por exemplo hanseníase e neurofibromatose (FURLANA; ADAMEYKO, 2018). As múltiplas funções das células de Schwann são atribuídas pela sua capacidade de desdiferenciação e rediferiação, a exemplo da atuação durante o reparo da lesão nervosa periférica (GOKEY *et al.*, 2012). As células de Schwann também degradam matriz extracelular que, por consequência, formam lúmens revestidos com laminina, que são utilizadas como ductos de migração por células neoplásicas (DEBORDE; WONG, 2017).

As células de Schwann expressam metaloproteinases da matriz tipo 2 e 9 (MMP2 e MMP9), que são gelatinases fundamentais no processo de degradação da matriz, além de expressarem moléculas de adesão celular neural 1 (NCAM1), indicando uma possível direta contribuição na invasão tumoral (DEBORDE *et al.*, 2016; GOKEY *et al.*, 2012; NAPOLI *et al.*, 2012; WEBBER *et al.*, 2011). Levando em consideração que células imunes podem infiltrar um nicho tumoral e modular a invasão neoplásica, vale ressaltar que diante do estímulo de lesão nervosa, as células de Schwann também recrutam macrófagos (ROSS; PAWLINA, 2016; JESSEN; MIRSKY; LLOYD, 2015).

Fibroblastos são componentes presentes no microambiente tumoral que podem regular a invasão através da expressão de fatores que estimulam o remodelamento da matriz (MIYAZAKI *et al.*, 2019). Se durante o processo de regeneração nas lesões nervosas as células de Schwann biointeragem com fibroblastos, que colaboram com o crescimento do axônio lesionado, é possível que durante o processo neoplásico essa biointeração também seja mimetizada. (LO; ZHANG, 2018)

Estudos tem demonstrado que as células de Schwann atuam em vários processos durante a cancerização (FURLANA; ADAMEYKO, 2018; BUNIMOVICH *et al.*, 2016). As células neoplásicas parecem produzir fatores que mimetizam o processo de resposta dos axônios periféricos a lesão. Dessa forma, as células de Schwann podem se desdiferenciar, migrando para a região próxima as células neoplásicas e, estas sendo carregadas para a região perineural, já nos estágios iniciais da carcinogênese (AIELLO *et al.*, 2018; LO; ZHANG, 2018; PASTUSHENKO *et al.*, 2018).

vi. Análise computacional

A pesquisa translacional é uma tendência metodológica que se iniciou a partir dos anos 2000, e desde então, apresenta um crescimento exponencial no cenário científico mundial (HSU *et al.*, 2019). Os estudos translacionais permitem que as práticas investigativas possam usufruir de uma variedade de fontes derivadas das distintas áreas (BROOM *et al.*, 2019). Essa tendência unida ao grande aumento na geração de dados e poder computacional, confere destaque a área da bioinformática, que é um campo de pesquisa que tem contribuído nas descobertas de novos fundamentos genômicos e proteômicos de numerosas doenças complexas (MULDER *et al.*, 2018). Poderosos recursos da bioinformática também foram desenvolvidos para produzir uma perspectiva molecular detalhada dos processos morfofuncionais celulares (ROSENWALD; PAULEY; WELCH, 2016). Ao combinar esses recursos com os avanços biotecnológicos, é possível afirmar que existe uma tendência ao melhor entendimento de diversos mecanismos de ação e regulação celular no processos saúde-doença (MEISEL *et al.*, 2018; WAGNER *et al.*, 2018). Novos conhecimentos subjacentes aos dados do genoma humano estão se acumulando num ritmo intenso, parte desse progresso está sendo protagonizado por cientistas atuantes nas áreas que envolvem o fenômeno neoplásico e suas associações genéticas potencialmente relacionados com a doença (NUSSINOV *et al.*, 2019; KATO *et al.*, 2018).

Um fator determinante no crescimento em larga-escala das pesquisas da bioinformática é a disponibilidade gratuita de acesso aos bancos de dados públicos, como por exemplo o Gene Expression Omnibus (GEO), que foi iniciado em 1999 devido ao aumento da demanda por repositórios de dados públicos gerados por sequenciamento e outras formas de dados genômicos funcionais (CHEN *et al.*, 2019). O GEO permite a consulta e armazenamento de muitos tipos de coleta de dados, como dados obtidos por meio de altas taxas de expressão gênica e hibridização (KIM *et al.*, 2019).

O GEO2R é uma ferramenta web interativa que permite aos usuários comparar dois ou mais grupos de amostras em uma série GEO, a fim de identificar genes que são diferencialmente expressos em condições experimentais. Os resultados são apresentados como uma tabela de genes ordenados por significância. O GEO2R realiza comparações em tabelas de dados processados fornecidas pelo requisitante usando os pacotes GEOquery e limma R do projeto Bioconductor. O pacote GEOquery R analisa dados

GEO em estruturas de dados R que podem ser usadas por outros pacotes R. O pacote *limma* (modelos lineares para análise de microarranjos) R surgiu como um dos testes estatísticos mais amplamente utilizados para a identificação de genes diferencialmente expressos. Ele lida com uma ampla variedade de designs experimentais e tipos de dados e aplica correções de testes múltiplos nos valores P para ajudar a corrigir a ocorrência de falsos positivos. Assim, o GEO2R fornece uma interface simples que permite aos usuários executar a análise estatística R sem experiência em linha de comando (KIM *et al.*, 2019).

Ao contrário das outras ferramentas de análise DataSet da GEO, o GEO2R não depende de DataSets com curadoria e interroga diretamente o arquivo de dados original da Matriz da Série. Isso permite que uma proporção maior de dados GEO seja analisada em tempo hábil. No entanto, é importante perceber que essa ferramenta pode acessar e analisar quase todas as séries GEO, independentemente do tipo e da qualidade dos dados, de modo que o usuário deve estar ciente das limitações e advertências do GEO2R (CHEN *et al.*, 2019).

Outro importante banco de dados público é o The Cancer Genome Atlas (TCGA), um projeto desenvolvido e mantido pelo National Cancer Institute (NCI) em 2005, financiado pelo governo dos Estados Unidos, com o objetivo de catalogar em larga escala as modificações genéticas responsáveis pelos principais tipos de câncer utilizando diversas técnicas, entre elas o sequenciamento de nova geração (SPAINHOUR *et al.*, 2019). Esta base de dados representa um esforço para melhorar a capacidade de diagnosticar, tratar e prevenir o câncer através de uma melhor compreensão das bases moleculares da doença (HE *et al.*, 2019).

Diversas ferramentas e pacotes têm sido desenvolvidos recentemente, como por exemplo, o TCGAbiolinks e TCGAbiolinksGUI. Ambos são pacotes do software R, licenciado sob a Licença Pública Geral (GPLv3), e estão disponível gratuitamente através do repositório Bioconductor. Em conformidade com as diretrizes rígidas para submissão de pacotes ao Bioconductor, Tanto o TCGAbiolinks quanto o TCGAbiolinksGUI incorporam pacotes e estatísticas existentes no Bioconductor para auxiliar na identificação de regiões genômicas diferentemente definidas por mutação, número de cópias, expressão ou metilação do DNA; para reproduzir estudos anteriores de marcadores TCGA; e integrar tipos de dados tanto dentro do TCGA como em outros

tipos de dados fora do TCGA. Os pacotes consistem em funções que podem ser agrupadas em três níveis principais: Dados, Análise e Visualização. Além disso, os pacotes oferecem análise integrativa aprofundada de múltiplas plataformas, como número de cópias e expressão ou expressão e metilação do DNA. Essas funções podem ser usadas independentemente ou em combinação para fornecer ao usuário pipelines de análise totalmente compreensíveis aplicados aos dados do TCGA (COLAPRICO *et al.*, 2016; SILVA *et al.*, 2018).

2. OBJETIVOS

Objetivo geral

- Identificar marcadores moleculares associados às células de Schwann e amostras de adenocarcinoma pulmonar e carcinoma de células escamosas do pulmão.

Objetivos específicos

- Analisar, através da bioinformática, a expressão diferencial de genes em amostras de células de Schwann tratadas com fatores de crescimento produzidos por células neoplásicas;
- Comparar a expressão dos genes em células de Schwann e amostras de câncer de pulmão;
- Identificar as vias moleculares dos genes com expressão diferenciadas;
- Compreender o mecanismo pela qual as células de Schwann auxiliam na proliferação, motilidade, apoptose e viabilidade da célula neoplásica.

3. METODOLOGIA

Este trabalho foi descrito sob a forma de artigo científico, cuja metodologia e discussão encontram-se descritas, em sua totalidade, no texto do artigo a ser submetido à publicação em periódico indexado.

- Título: “Are Schwann cells associated with lung cancer progression control? Insights from the meta-analysis of transcriptomics data”, formatado segundo as normas para publicação do periódico Clinical Cancer Research.

O artigo foi estruturado com base nas normas de publicação do periódico. Após sua apresentação, seguir-se-ão as considerações finais, bem como as referências relacionadas à dissertação em geral.

Are Schwann cells associated with lung cancer progression control? Insights from the meta-analysis of transcriptomics data

Victor Menezes Silva¹, Jessica Alves Gomes¹, Genilda Castro de Omena Neta¹, Karen da Costa Paixão¹, Ana Kelly Fernandes Duarte¹, Gabriel Cerqueira Braz da Silva¹, Ricardo Jansen Santos Ferreira¹, Rafael Danyllo da Silva Miguel¹, Carolinne de Sales Marques¹, Aline Cavalcanti de Queiroz^{1#}, Carlos Alberto de Carvalho Fraga^{1*#}

*¹ Federal University of Alagoas, Campus Arapiraca. Av. Manoel Severino Barbosa, Bom Sucesso, Arapiraca, AL 57309-005, Brazil.

*Corresponding authors Carlos Alberto de Carvalho Fraga and Aline Cavalcanti de Queiroz. Federal University of Alagoas, Campus Arapiraca, Av. Manoel Severino Barbosa, Bom Sucesso, Arapiraca, AL 57309-005, Brazil Tel. +55 82 991931405; E-mail: carlos.fraga@arapiraca.ufal.br

Equally Contributing Authors

Abstract

Studies have shown that Schwann cells participate in the tumor microenvironment, producing several factors that benefit cancer cells. During this process, Schwann cells are dedifferentiated and help the process of cancer cellular proliferation. These cells then migrate to the region close to the tumor tissue and assist the development of the neoplastic cell. In this context, the aim of the present study was to evaluate the influence of Schwann cells over lung cancers. We performed a bioinformatic insights and we observed that the “neuroactive ligand-receptor interaction” pathway was upregulated in LUSC and downregulated in LUAD. The “p53 signaling pathway” was active in both lung cancers, since *CCNE1*, *CDKN2A*, and *PERP* were upregulated. Meanwhile, upregulated miRNAs inactivate the “axon guidance” pathway, targeting *ROBO2* and *SLIT2* genes. Both genes are also associated with Schwann cells migration inhibition. Also, *GFAP* and *GAP43* are overexpressed, leading to Schwann cells dedifferentiation. Besides, both Schwann and cancer cells are stimulated via a phosphorylation cascade to proliferate and migrate. We also believe that Schwann cells’ dedifferentiation and proliferation are induced by neoplastic tissue; consequently, Schwann cells produce different factors that will participate in various processes of tumor progression. These processes may also be involved in tumor invasion into the perineural tissue, especially in LUSC.

Introduction

The phenomenon of carcinogenesis is a complex process that occurs through multiple genetic and epigenetic events altering the normal functions of oncogenes and tumor suppressor genes. Such changes may result in an increased production of growth factors or transcription factors, or an increased number of cell surface receptors and intracellular flags ¹. The loss of tumor suppressor activity leads to a cellular phenotype capable of increasing cell proliferation and loss of cell adhesion, enabling such mutated cells to infiltrate local tissues and to spread to distant sites. Metastasis is the cause of 90% of cancer deaths and results in a diverse set of clinical manifestations ²⁻⁴. Metastases occur when malignant neoplastic cells leave the primary site and travel via blood and lymph vessels to new sites in the body where they disseminate new colonies. Cancer cells then employ various strategies to aid adaptation and subsequent expansion and progression in new sites. Formation and progression of cancer is a multisystemic process, involving the immune system, vascularization, and dissemination. Metastatic training is characterized by tumor growth, invasion of the basement membrane into submucosal tissues, vascular and lymphatic formation, perineural and systemic tissue invasion, and subsequent progression ⁵.

The extracellular matrix plays a critical role in tumor microenvironment. During tumor formation, neoplastic cells bind to molecules present in the extracellular matrix, which facilitates communication with other cells, such as neutrophils, fibroblasts, macrophages, lymphocytes, and peripheral nervous system cells ^{6,7}. The extracellular matrix is especially important in tumor formation and invasion as cells respond and adapt to the local microenvironment. This involves both the unregulated proliferation of tumor cells and the modification of the immediate environment to favor cell survival, angiogenesis, and tumor growth. Factors that can degrade the extracellular matrix also facilitate tumor formation and invasion ^{7,8}. For example, matrix metalloproteinases (MMPs) have been associated with the degradation of basement membranes and extracellular matrix, facilitating the invasion and metastasis of tumor cells, as well as promoting cell proliferation, metastasis, and angiogenesis ^{9,10}. In addition to the degradation of the matrix, another important aspect in the formation and invasion of the tumor is the process called epithelial-mesenchymal transition. The epithelial-mesenchymal transition allows the tumors' epithelial cells to produce factors generally found in the extracellular matrix ⁹⁻¹¹.

Studies have shown that Schwann cells participate in the tumor microenvironment,

producing several factors that benefit cancer cells. During this process, Schwann cells are dedifferentiated and help the process of cancer cellular proliferation. These cells then migrate to the region close to the tumor tissue and assist the development of the neoplastic cell ^{12,13}. In this context, the aim of the present study was to evaluate the influence of Schwann cells over lung cancers.

Methods

Data collection and study inclusion criteria

The Gene Expression Omnibus (GEO) project was initiated in 1999 due to an increasing demand for public data repositories. Its large volume of data may be effectively explored, queried, and visualized through user-friendly web-based tools¹⁴. Taking advantage of this facility, we downloaded the expression profiles of a gene array, GSE4030, and further analyzed them with GEO2R (<http://www.ncbi.nlm.nih.gov/geo/geo2r/>), to screen for differentially expressed mRNAs (DEGs). GEO2R is an interactive web tool for comparing two groups of data; it can analyze any GEO series. Adjusted p values, using Benjamini and Hochberg false discovery rate method by default, were applied to correct for the occurrence of false positive results. An adj. $p < 0.05$ and a $\log_{2}FC \geq 1$ were set as the cut-off criteria.

Functional and pathway enrichment analysis

Gene ontology (GO) analysis of the relevant biological processes, cellular components, and molecular functions was performed using the protein analysis through evolutionary relationships program (PANTHER, www.pantherdb.org), a curated database of protein families, functions, and pathways. GO terms assigned into identified molecules were classified according to their functions¹⁵.

The Kyoto Encyclopedia of Genes and Genomes (KEGG) is an integrated database resource for biological interpretation of genome sequences and other high-throughput data¹⁶. KEGG analyses were available at the DAVID database (<https://david.ncifcrf.gov/>), a data resource composed of an integrated biology knowledge base and analysis tools to extract meaningful biological information from large quantities of genes and protein collections. A p -value < 0.05 was set as the cut-off criterion⁴.

RNA-seq and clinical information data from The Cancer Genome Atlas (TCGA)

We used TCGAbiolinks, an R/Bioconductor software (<http://bioconductor.org/packages/release/bioc/html/TCGAbiolinks.html>)¹⁷ and the

interphase TCGAbiolinksGUI¹⁸ to download genomic and clinical data of both normal and solid tumor tissues for two different types of cancer from TCGA. Selected cancer types were lung squamous cell carcinoma (LUSC) and lung adenocarcinoma (LUAD). We retrieved level data for raw count mRNA and miRNA expression (Illumina HiSeq 2000). Co-expressed upregulated and downregulated DEGs from the gene expression profiles were combined and identified with a Venn Diagram 2.1.0 (<http://bioinfogp.cnb.csic.es/tools/venny/index.html>). DNA methylation analyses were performed using MEXPRESS dataset (<https://mexpress.be/?ref=labworm>). The cancer dataset, consisting of DNA methylation data (Illumina Infinium Human Methylation 450 K Bead array, Illumina, USA) and the β value, was considered as significantly hypermethylated only if the value was found in more than 5% of the tumors¹⁹. Copy number alteration analysis was performed using the cBio Cancer Genomics Portal (<http://cbioportal.org>).

Lung cancer expression analyses

To obtain individual gene-protein data, relevant information from The Cancer Proteome Atlas (TCPA) website (<https://tcpaportal.org/tcpa/analysis.html>) was used as the primary source of information for reverse phase protein array (RPPA) analysis. Several other web resources were used as source of information while some more were used as analysis tools for lung cancer expression studies: Immunohistochemistry image-based protein data for both normal and cancer samples are available at the Human Protein Atlas (<https://www.proteinatlas.org/>). LOCATE database for protein subcellular location was included on the analysis (http://locate.imb.uq.edu.au/cgi-bin/sort_search.cgi). Survival analysis of the TCGA data was performed using the Survival module of the Tumor Immune Estimation Resource (TIMER) and Prediction of clinical outcomes from genomics (PRECOG). Kaplan–Meier plots were drawn using TIMER to explore the association between clinical outcome and gene expression, and to visualize survival differences.

Statistical analyses

Statistical analyses involving copy number variation were performed using GraphPad Prism 7 software. A two-way ANOVA and a two-tailed unpaired *t* test were used to compare the means between groups.

Results

Identification of differentially expressed genes, gene ontology enrichment, and functional classification

We obtained gene expression data belonging to specimens across two cancer types, LUAD and LUSC, from TCGA; these data were preprocessed using standard methods. After the identification of DEGs, a DAVID analysis was performed using them. Downregulated genes in both lung cancers belong to “complement and coagulation cascades” and “cell adhesion molecules (CAMs)” pathways. While “cell cycle” and “DNA replication” were the most active pathways in both lung cancers (supplementary Tables 1-4).

As Schwann cells act on both of the aforementioned upregulated pathways, we selected datasets from the GEO database containing gene expression profiles of both early and late passage human Schwann cells exposed to cancer growth factors heregulin and forskolin (GSE4030). These expression profiles were used to identify DEGs with the aid of the online tool GEO2R. We found 638 upregulated and 1250 downregulated genes. Then, we performed a GO term enrichment and functional classification by KEGG analysis, using DAVID platform, to investigate the biological and functional roles of these DEGs. Upregulated DEG enrichment included “neuroactive ligand-receptor interaction,” while “pathways in cancer” and “focal adhesion” were enriched for downregulated DEGs (supplementary Tables 5-6).

To facilitate the analysis of the large throughput of DEGs, a protein classification analysis was performed using the PANTHER classification system. According to the study, upregulated genes categories were identified, in which hydrolase (PC00121), enzyme modulator (PC00095), nucleic acid binding (PC00171), receptor (PC00197), transcription factor (PC00218), transporter (PC00227), and signaling molecule (PC00207) are the top seven most abundant protein classes. However, protease (PC00190) is the top one most abundant protein class among downregulated DEGs (Figure 1 A-B).

Overview of the cancer transcriptomic analysis

We conducted a systematic and integrative analysis to explore cancer type-specific and Schwann cell specific DEGs, to construct a cancer network. We first determined DEGs by comparing gene expression levels between tumor and normal samples. A Venn diagram was

then constructed to visualize the overlap between DEG genes, both upregulated and downregulated, from both cancer types and from Schwann cells. Results are shown in Figure 1 C-F. Among upregulated genes from LUSC and LUAD, we identified 84 and 70 co-expressed DEGs with Schwann cells, respectively.

We also ran a KEGG analysis to investigate pathways with major expression changes in studied cell lines, based on previously identified DEGs. The analysis revealed that “neuroactive ligand-receptor interaction” and “p53 signaling pathway” were among the most active pathways in LUSC. In contrast, LUAD samples show “neuroactive ligand-receptor interaction” pathway as mainly downregulated, while “p53 signaling pathway” is upregulated (supplementary Tables 7-10). *GRM1*, *CHRM3*, *GABRA5*, *GPR50*, and *PTH2R* were the common upregulated genes associated with the “neuroactive ligand-receptor interaction” pathway; *CCNE1*, *CDKN2A*, and *PERP* were commonly associated to “p53 signaling pathway”.

To confirm our results, we performed a differentially expressed miRNA analysis over cancer data. Data from identified miRNAs target genes were crossed with DEGs data from Schwann cells (Figure 1 G-J). We found that downregulated miRNAs had target genes associated with “neuroactive ligand-receptor interaction” in LUAD and “pathways in cancer” in both cancers (supplementary Tables 11-12). In contrast, upregulated miRNAs had target genes associated with the “axon guidance” pathway in both lung cancers (supplementary Tables 13-14). Genes from the “axon guidance” pathway, common to all our analyses, were *ROBO2* and *SLIT2* genes. Robo2 and Slit2 proteins were highly expressed in normal tissue compared to cancer samples (data not shown).

Hallmarks of cancer analysis

In order to understand the mechanism by which Schwann cells aid in neoplastic development, we analyzed the behavior of genes associated with cell differentiation processes (*GATA3*, *CDH1*, and *CDH2*), apoptosis (*CASP3*, *CASP9*, *BAX*, and *BCL2*), motility (*CXCR2*, *CXCL5*, *MMP9*, and *CCL12*), and cell proliferation (*MKI67*). While *CDH1* and *CDH2* showed an increased mRNA expression in LUSC samples, *CDH1* protein expression was decreased (data not shown). Also, *MMP9* and *MKI67* were overexpressed in both lung cancers (supplementary Figure 1-2).

Analysis of genes involved in dedifferentiation of Schwann cells

Schwann cells produce cell differentiation maintenance proteins (*SOX10*, *S100*, *EGR2*, *MBP*, and *MPZ*) that, after nerve damage, diminish their expression, provoking cellular dedifferentiation. Consequently, the expression of a new set of proteins that form non-myelinated cells, *SOX10*, *GAP43*, *S100*, *NCAM1*, *NGFR1*, and *GFAP*, is augmented. We observed increased expression of *GAP43* and *GFAP* genes in both lung cancers, whereas *NGFR1* was upregulated only in LUSC cells (supplementary Figure 1-2).

Methylation and protein analyses

Methylation analysis of the *CDH1*, *CDH2*, *MMP9*, *MKI67*, *GFAP*, *GAP43*, *ROBO2*, and *SLIT2* genes from tumor samples demonstrated that all of them were methylated in their promoter regions unlike those from normal tissues. However, there was no significant correlation between methylation and *GFAP* gene expression in lung cancers. Whereas there was a positive correlation between methylation and *GAP43* gene expression in LUSC samples (supplementary Figures 3-24).

Copy number alteration

Copy number alteration data demonstrated that *CDH1*, *CDH2*, *GFAP*, *PERP*, and *ROBO2* had a higher mRNA expression than normal tissues; increased expression was associated with gain or amplification alterations in LUAD cells (supplementary Figure 25). Similarly, in LUSC cells, *CCNE1*, *CDH1*, *CDKN2A*, *GAP43*, and *PERP* had a higher mRNA expression associated with gain or amplification alterations (Figure 2).

Cancer protein expression patterns correspond to pathway activation levels

We also performed an RPPA protein analysis. Only *CDH1* and *CDH2* protein expression data were available for analysis. We observed that *CDH2* was overexpressed in LUSC compared to LUAD. Additionally, no significant difference was found in *CDH1* analysis (supplementary Figure 26).

In order to analyze the pathway by which Schwann cells induce neoplastic and their

own cell proliferation and migration, we evaluated the expression of Mek1 (MEK1 and MEK1_pS217S221), Erk2, Akt (PRAS40_pT246, AKT_pT308 and AKT_pS473), Raf (CRAF and CRAF_pS338), and Gsk3 β (GSK3_pS9 and GSK3ALPHABETA_pS21S9) proteins. We observed higher expression of Erk2, Akt, cRaf and Gsk3 β proteins in LUSC when compared with LUAD. Only MEK1_pS217S221 presented higher expression in LUAD (supplementary Figure 26).

Prognostic analyses

Survival analyses showed that *CCNE1*, *MKI67*, and *GAP43* mRNA higher expression are associated with poor LUAD prognostic. Similarly, *SLIT2* higher mRNA expression is associated with poor prognostic in LUSC (supplementary Figure 27). Figure 4 illustrates the association between Schwann cells and LUSC.

Discussion

Cells surrounding a tumor form a molecular microenvironment known as stroma. Stroma formation is influenced by tumor cells and, in turn, it influences tumor growth, migration, and invasion³. Depending on the characteristics of the primary tumor, the stroma, and the intrinsic ability of metastatic tumor cells to adapt to a new location, malignant cells use distinct mechanisms for proliferation, survival, and dissemination. These cells often reactivate the expression of genes employed during embryogenesis^{3,9}. In order to leave the primary tumor and disseminate to distant organs, metastatic cells lose the ability to adhere to adjacent cells, enhancing their migratory and invasive capacity. This mechanism is accompanied by several modifications in the expression of genes, such as loss of epithelial receptor expression and increased expression of mesenchymal markers, a phenomenon also known as epithelial-mesenchymal transition^{9,20}.

We investigated the association between Schwann cells and those lung cancer types often associated with perineural invasion. Initially, we used the GEO DataSets platform from the GEO repository to identify a database reporting gene expression in Schwann cells in a neoplastic context. Briefly, the database contains the expression results from experiments in which two factors produced by tumor cells were added into cell cultures. Comparisons were made between samples from the first and third passages. We then used these data to perform differential gene expression analysis and crossed data from upregulated genes with differential expression data from LUAD and LUSC. After identifying the genes in common, we ran several analysis tools to identify molecular pathways associated to these genes. Interestingly, we noted that the “neuroactive ligand-receptor interaction” pathway was active in LUSC. Studies have demonstrated the association between neuroactive ligand-receptors in the control of Schwann cell differentiation as well as in neoplastic cell proliferation. For example, *GRM1* can activate the Ras/Mek1/Erk/Akt/Raf/Gsk3 β phosphorylation cascade^{21,22}, leading to an increase in cell proliferation and invasion. *GRM1* was upregulated in LUSC, suggesting that this gene participates in lung cancer development.

In these context, it has also been demonstrated that neuroactive ligand-receptors are active during Wallerian degeneration of peripheral nerves. Together with macrophages, Schwann cells remove axon and myelin debris, and clear a path for subsequent axonal regrowth and nerve regeneration²³. Tumor cells benefit from nerve regeneration machinery to promote cell proliferation, migration, and invasion. It has been reported that Schwann cells are induced to migrate to the region close to the tumor at the beginning of the carcinogenic

process. It was also suggested that Schwann cells promote neoplastic invasion by direct contact with cancer cells, since paracrine signaling and matrix remodeling are not yet sufficient to induce the migration process^{12,24}. Cell-cell contact between Schwann cells and tumor tissue is necessary to potentiate the ability of neoplastic cells to penetrate into the underlying tissue^{25,26}. After contact, the degradation of the extracellular matrix by Schwann cells provokes the formation of tunnels or bands coated with laminin, due to Schwann cells' capacity to express matrix metalloproteins, especially MMP2 and MMP9. The mechanism of extracellular matrix degradation that promotes neoplastic migration also depends on the production of NCAM1 and N-cadherin (CDH2) by Schwann cells^{26,27}.

In the present study, we analyzed the expression of genes associated with the hallmark of cancer. The importance of analyzing these genes derives from the hypothesis that there may be a correlation between the presence of Schwann cells and the aggressiveness of the neoplastic cell. Increased expression of genes related to cell differentiation (*CDH1* and *CDH2*), motility (*MMP9*), and proliferation (*MKI67*), mainly in LUSC, suggests this correlation. We observed that these genes are mutated and had higher expression in lung cancer samples when compared with normal tissue.

Decreased E-cadherin protein expression after contact of Schwann cells with the tumor resembles the mechanism followed by cells during axonal repair process. The loss of E-cadherin during the epithelial-mesenchymal transition in cancer is associated with a positive regulation of NCAM1 and CDH2^{12,25,26,28}. When E-cadherin is suppressed, NCAM1 and CDH2 are upregulated; they associate with the p59fyn protein, whose subsequent activation leads to inhibition of focal adhesion and an increase in cell migration. A study using oncogenic *K-ras* pancreatic cancer cell lines identified increased levels of polysialylated NCAM1 expression, which interacts with E-cadherin to create steric hindrance of homophilic binding and decrease cell adhesion²⁶. In our study, we observed upregulation of E-cadherin and CDH2 in both lung cancers. A CDH2 protein RPPA analysis showed that it is overexpressed in LUSC. Copy number alteration analysis also showed that amplification and gain are associated with E-cadherin and N-cadherin mRNA levels in both cancers. However, we showed that *CDH2* mRNA expression is higher in LUSC when compared to LUAD. No difference was observed neither in *NCAM1* mRNA nor in E-cadherin protein analyses.

Differentiation of myelinating Schwann cells may undergo interference from inhibitory pathways that negatively control the expression of genes responsible for myelin sheath formation. NOTCH1 and JUN stand out among the negative regulators of the myelination

program, in the same way as SOX-2 and PAX-3²⁹⁻³¹. The myelinating phenotype also involves the inactivation of a number of genes linked to the production of immature Schwann cell markers. Some transcription factors are responsible for ensuring proper maturation in Schwann cells. SOX-10 acts synergistically with a second factor, OCT-6, resulting in the expression of *KROX-20*. In turn, *KROX-20* is a key inducer of expression of myelin genes, such as *MBP*, *MPZ* and *PRX*. The maintenance of the myelinating phenotype therefore requires the continuous expression of *KROX-20* and *SOX-10*, considering that inactivation of both proteins results in dedifferentiation of Schwann cells³⁰.

Previous studies have shown that Schwann cells induce cellular aggressiveness in lung cancer³². During dedifferentiation, Schwann cells express proteins initially lost during the myelination process. Among these proteins are *Gap43*, *Ncam1*, *P75ntr (NGFR)*, *Gfap* and *Sox-2*²⁹. Data from our study showed that *GFAP*, *NGFR* and *GAP43* gene expression is increased in lung cancers, especially in LUSC. *GFAP* and *GAP43* copy number alterations are associated with higher mRNA levels in LUAD and LUSC, respectively. It is likely that Schwann cells in these tissues are dedifferentiated, aiding tumors in their mechanisms of cell proliferation, migration, and tissue invasion.

During the process of carcinogenesis, there is an inactivation of the *SLIT2* and *ROBO2* genes, being therefore considered as tumor suppressor genes³³. Both genes are extremely important during the process of nerve formation and repair. Both *SLIT2* and *ROBO2* have been reported to inhibit migration of Schwann cells³⁴. In the present study, we observed that *SLIT2* and *ROBO2* mRNAs are decreased in lung cancer samples when compared to normal tissue. Also, there is a participation of miRNAs and of methylation of their promoter regions in the regulation of these genes. Similarly, both genes are targets for upregulated miRNAs. Immunohistochemical expression analyses revealed low expression of both genes in the lung. Thus, we suggest that decreased expression of *SLIT2* and *ROBO2* genes in lung cancer may favor the migration of Schwann cells; consequently, favoring invasion by neoplastic tissue.

We next analyzed the Ras/Mek1/Erk/Akt/Raf/Gsk3 β phosphorylation cascade. This pathway is activated during the proliferation process of Schwann cells and neoplastic cells. We observed that the protein expression of all pathway genes is increased in LUSC when compared to LUAD.

In summary, we observed that the “neuroactive ligand-receptor interaction” pathway was upregulated in LUSC and downregulated in LUAD. The “p53 signaling pathway” was active in both lung cancers, since *CCNE1*, *CDKN2A*, and *PERP* were upregulated. Meanwhile,

upregulated miRNAs inactivate the “axon guidance” pathway, targeting *ROBO2* and *SLIT2* genes. Both genes are also associated with Schwann cells migration inhibition. Also, *GFAP* and *GAP43* are overexpressed, leading to Schwann cells dedifferentiation. Besides, both Schwann and cancer cells are stimulated via a phosphorylation cascade to proliferate and migrate. We also believe that Schwann cells’ dedifferentiation and proliferation are induced by neoplastic tissue; consequently, Schwann cells produce different factors that will participate in various processes of tumor progression. These processes may also be involved in tumor invasion into the perineural tissue, especially in LUSC.

Competing interests

The authors declare that they have no competing interests.

Ethics approval and consent to participate

Not applicable.

References

1. Gatenby, R. A. & Gillies, R. J. A microenvironmental model of carcinogenesis. *Nature Reviews Cancer* (2008). doi:10.1038/nrc2255
2. Noguti, J. *et al.* Metastasis from Oral Cancer: An Overview. *Cancer Genomics Proteomics* (2012). doi:9/5/329 [pii]
3. Huang, H. Z. and S. Role of mTOR Signaling in Tumor Cell Motility, Invasion and Metastasis. *Curr Protein Pept Sci* (2011). doi:10.1016/j.cmet.2011.03.023.Ouimet
4. Huang, D. W., Sherman, B. T. & Lempicki, R. A. Systematic and integrative analysis of large gene lists using DAVID bioinformatics resources. *Nat. Protoc.* **4**, 44–57 (2009).
5. Leemans, C. R., Snijders, P. J. F. & Brakenhoff, R. H. The molecular landscape of head and neck cancer. *Nature Reviews Cancer* (2018). doi:10.1038/nrc.2018.11
6. McCubrey, J. A. *et al.* Roles of the Raf/MEK/ERK pathway in cell growth, malignant transformation and drug resistance. *Biochimica et Biophysica Acta - Molecular Cell Research* **1773**, 1263–1284 (2007).
7. Hingorani, D. V. *et al.* Impact of MMP-2 and MMP-9 enzyme activity on wound healing, tumor growth and RACPP cleavage. *PLoS One* (2018). doi:10.1371/journal.pone.0198464
8. Yao, Q., Kou, L., Tu, Y. & Zhu, L. MMP-Responsive ‘Smart’ Drug Delivery and Tumor Targeting. *Trends in Pharmacological Sciences* (2018). doi:10.1016/j.tips.2018.06.003
9. Lo, H. C. & Zhang, X. H. F. EMT in Metastasis: Finding the Right Balance. *Developmental Cell* (2018). doi:10.1016/j.devcel.2018.05.033
10. Pastushenko, I. *et al.* Identification of the tumour transition states occurring during EMT. *Nature* (2018). doi:10.1038/s41586-018-0040-3
11. Aiello, N. M. *et al.* EMT Subtype Influences Epithelial Plasticity and Mode of Cell Migration. *Dev. Cell* (2018). doi:10.1016/j.devcel.2018.05.027
12. Azam, S. H. & Pecot, C. V. Cancer’s got nerve: Schwann cells drive perineural invasion.

Journal of Clinical Investigation (2016). doi:10.1172/JCI86801

13. Demir, I. E. *et al.* Investigation of schwann cells at neoplastic cell sites before the onset of cancer invasion. *J. Natl. Cancer Inst.* (2014). doi:10.1093/jnci/dju184
14. Edgar, R. & Lash, A. The Gene Expression Omnibus (GEO): A Gene Expression and Hybridization Repository. *NCBI Handb.* 0 (2002).
15. Bastos, H. P., Tavares, B., Pesquita, C., Faria, D. & Couto, F. M. Application of gene ontology to gene identification. *Methods Mol. Biol.* **760**, 141–157 (2011).
16. Kanehisa, M., Sato, Y., Kawashima, M., Furumichi, M. & Tanabe, M. KEGG as a reference resource for gene and protein annotation. *Nucleic Acids Res.* **44**, D457–D462 (2016).
17. Colaprico, A. *et al.* TCGAbiolinks: An R/Bioconductor package for integrative analysis of TCGA data. *Nucleic Acids Res.* **44**, e71 (2016).
18. Silva, T. C. *et al.* TCGAbiolinksGUI: A graphical user interface to analyze cancer molecular and clinical data. *F1000Research* **7**, 439 (2018).
19. Guo, S. *et al.* Identification and validation of the methylation biomarkers of non-small cell lung cancer (nslc). *Clin. Epigenetics* (2015). doi:10.1186/s13148-014-0035-3
20. Shaw, R. The epigenetics of oral cancer. *International Journal of Oral and Maxillofacial Surgery* (2006). doi:10.1016/j.ijom.2005.06.014
21. Namkoong, J. *et al.* Metabotropic glutamate receptor 1 and glutamate signaling in human melanoma. *Cancer Res.* (2007). doi:10.1158/0008-5472.CAN-06-3665
22. Wen, Y. *et al.* Activation of the glutamate receptor GRM1 enhances angiogenic signaling to drive melanoma progression. *Cancer Res.* (2014). doi:10.1158/0008-5472.CAN-13-1531
23. Cheng, Q., Wang, Y. X., Yu, J. & Yi, S. Critical signaling pathways during wallerian degeneration of peripheral nerve. *Neural Regen. Res.* (2017). doi:10.4103/1673-5374.208596
24. Kim, H. S. *et al.* Schwann Cell Precursors from Human Pluripotent Stem Cells as a Potential Therapeutic Target for Myelin Repair. *Stem Cell Reports* (2017). doi:10.1016/j.stemcr.2017.04.011

25. Napoli, I. *et al.* A Central Role for the ERK-Signaling Pathway in Controlling Schwann Cell Plasticity and Peripheral Nerve Regeneration In Vivo. *Neuron* (2012). doi:10.1016/j.neuron.2011.11.031
26. Deborde, S. *et al.* Schwann cells induce cancer cell dispersion and invasion. *J. Clin. Invest.* (2016). doi:10.1172/JCI82658
27. Deborde, S. & Wong, R. J. How Schwann cells facilitate cancer progression in nerves. *Cellular and Molecular Life Sciences* (2017). doi:10.1007/s00018-017-2578-x
28. Webber, C. A. *et al.* Schwann cells direct peripheral nerve regeneration through the Netrin-1 receptors, DCC and Unc5H2. *Glia* (2011). doi:10.1002/glia.21194
29. Gokey, N. G., Srinivasan, R., Lopez-Anido, C., Krueger, C. & Svaren, J. Developmental Regulation of MicroRNA Expression in Schwann Cells. *Mol. Cell. Biol.* (2012). doi:10.1128/MCB.06270-11
30. Beirowski, B., Wong, K. M., Babetto, E. & Milbrandt, J. mTORC1 promotes proliferation of immature Schwann cells and myelin growth of differentiated Schwann cells. *Proc. Natl. Acad. Sci.* (2017). doi:10.1073/pnas.1620761114
31. Clements, M. P. *et al.* The Wound Microenvironment Reprograms Schwann Cells to Invasive Mesenchymal-like Cells to Drive Peripheral Nerve Regeneration. *Neuron* (2017). doi:10.1016/j.neuron.2017.09.008
32. Zhou, Y. *et al.* Schwann cells augment cell spreading and metastasis of lung cancer. *Cancer Res.* (2018). doi:10.1158/0008-5472.CAN-18-1702
33. Gara, R. K. *et al.* Slit/Robo pathway: A promising therapeutic target for cancer. *Drug Discovery Today* (2015). doi:10.1016/j.drudis.2014.09.008
34. Carr, L., Parkinson, D. B. & Dun, X. P. Expression patterns of Slit and Robo family members in adult mouse spinal cord and peripheral nervous system. *PLoS One* (2017). doi:10.1371/journal.pone.0172736

Legends

Figure 1 - Molecular function and protein class terms of downregulated (A) and upregulated (B) among the differentially regulated genes in Schwann cells. Fig 1C-D - Venn Diagrams of combined overrepresented differentially expressed genes in Schwann cells and Lung adenocarcinoma (C and D), and Lung squamous cell carcinoma (E and F) cancer samples. Fig 1C is showing overlapping downregulated genes between Lung adenocarcinoma and Schwann cells. Fig 1D is showing overlapping upregulated genes between Lung adenocarcinoma and Schwann cells. Fig 1E is showing overlapping downregulated genes between Lung squamous cell carcinoma and Schwann cells. Fig 1F is showing overlapping upregulated genes between Lung squamous cell carcinoma and Schwann cells. Fig 1G-H - Venn Diagrams of downregulated miRNA target genes combined with upregulated genes in Lung adenocarcinoma (G) and Lung squamous cell carcinoma (H). The number in each intersecting region represents the number of overlapping genes. Fig 1I-J - Venn Diagrams of upregulated miRNA target genes combined with downregulated genes in Lung adenocarcinoma (I) and Lung squamous cell carcinoma (J). The number in each intersecting region represents the number of overlapping genes.

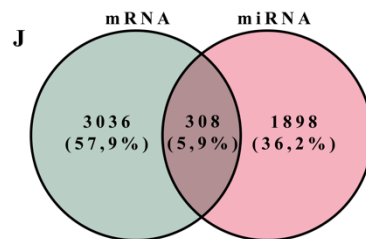
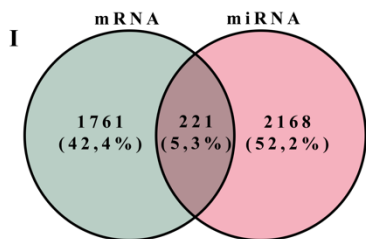
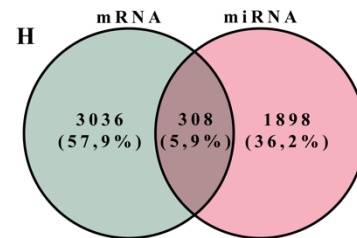
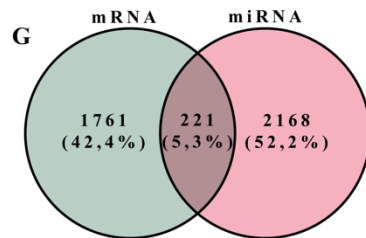
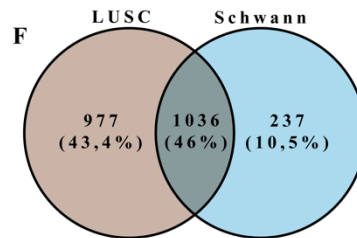
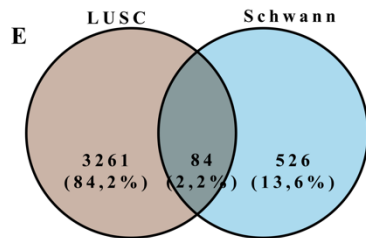
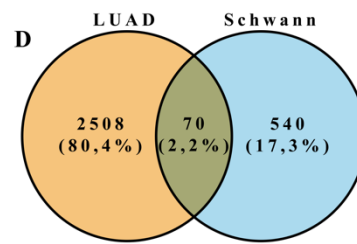
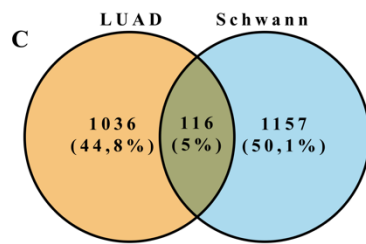
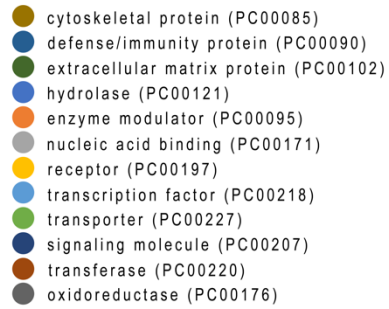
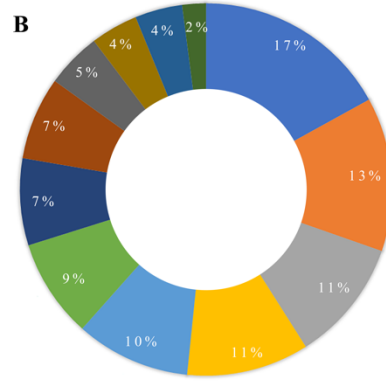
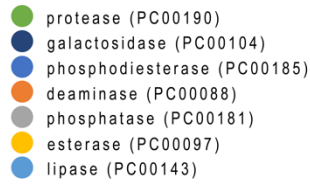
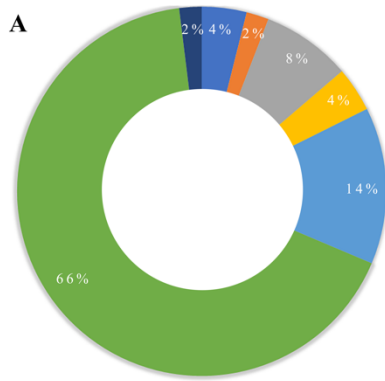


Figure 2- Copy number alteration and mRNA expression analysis of GAP43, GFAP, ROBO2 and SLIT2 genes in lung adenocarcinoma and lung squamous cell carcinoma.

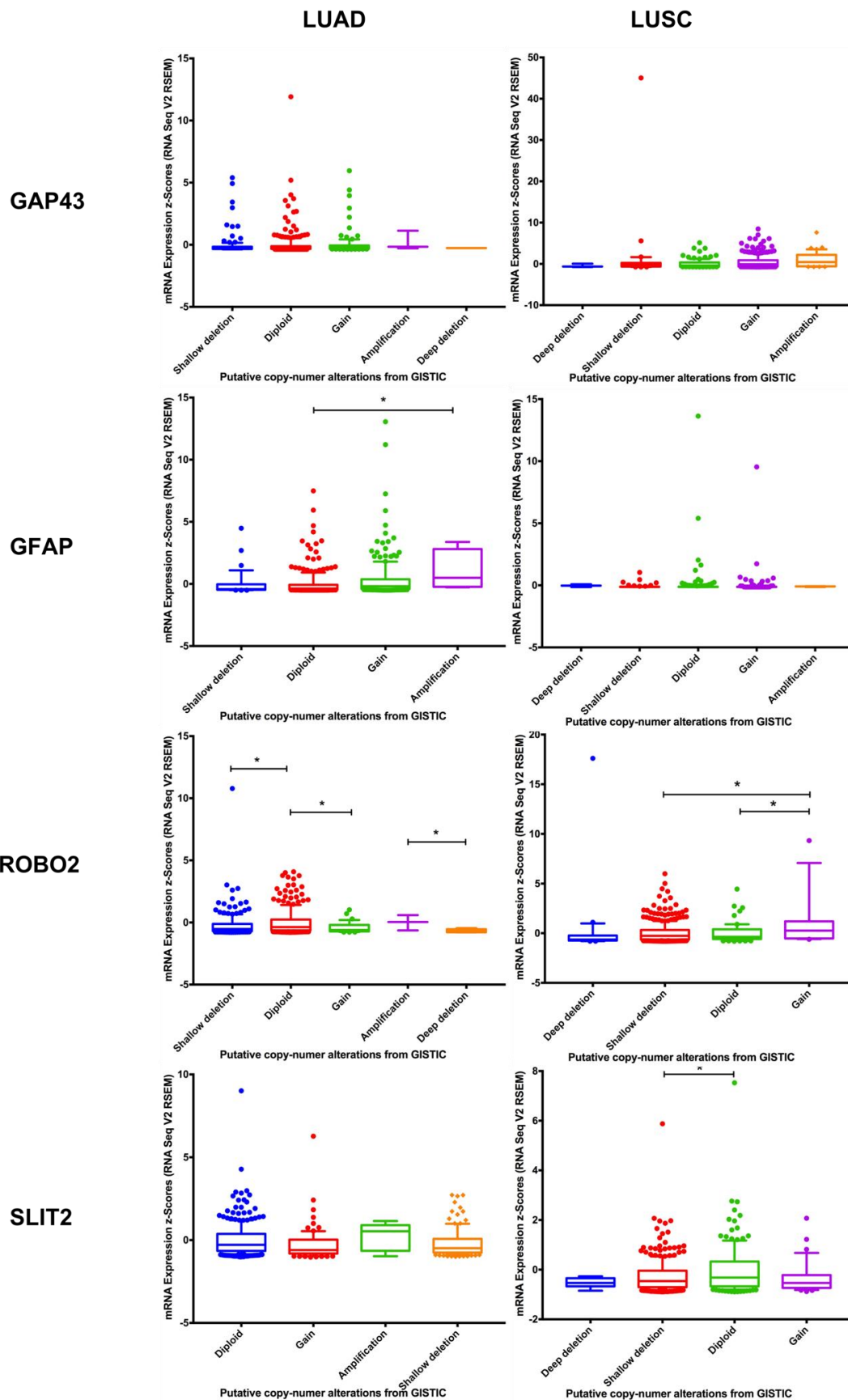
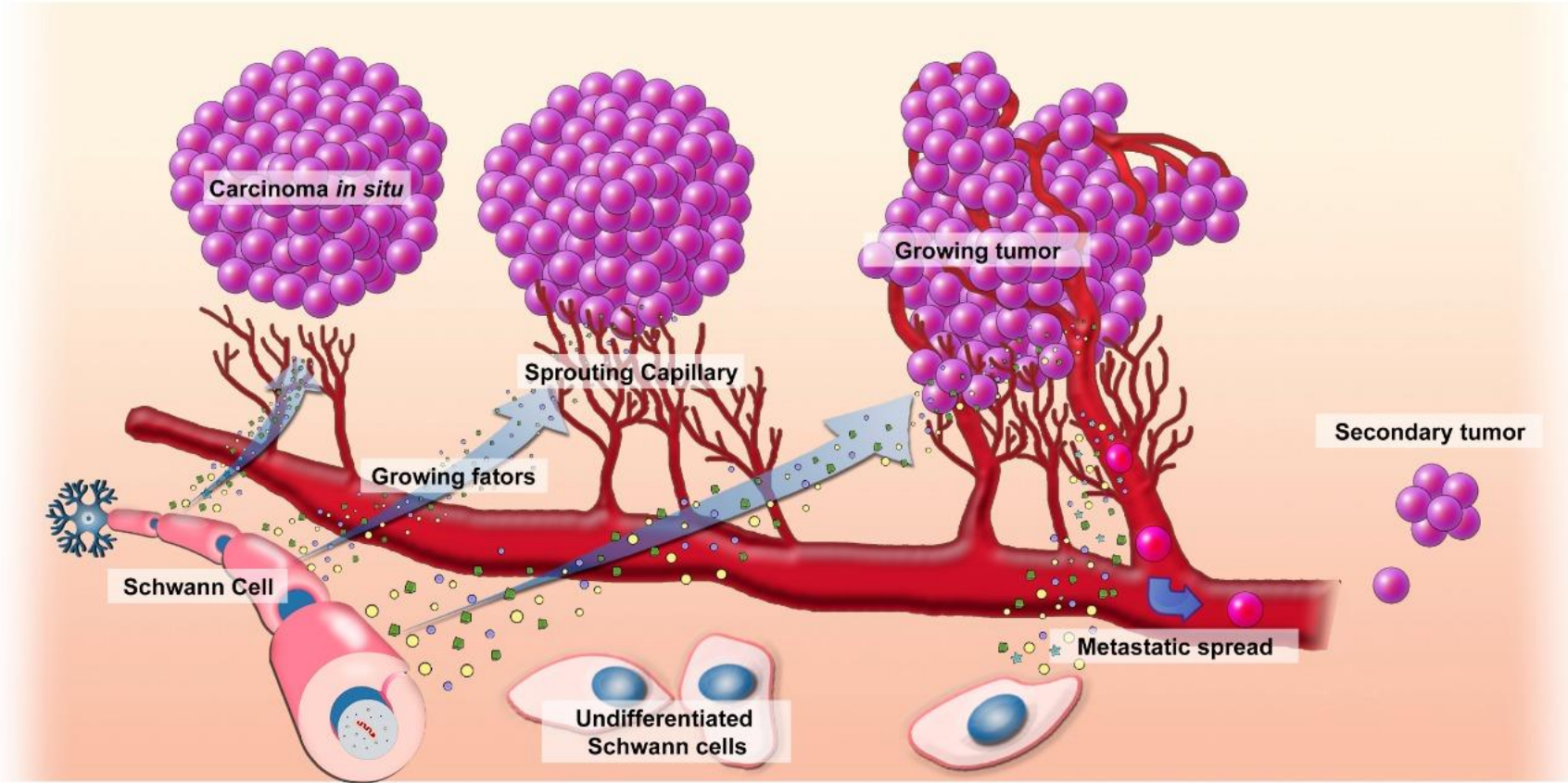


Figure 3- Mechanism of action of Schwann cells in the development of cancer.



Supplementary Table 1 -Functional annotation analysis of downregulated differentially expressed genes in Lung adenocarcinoma datasets using the DAVID tool.

Term	Count	PValue	Genes	Pop Hits	Fold Enrichment
hsa04610:Complement and coagulation cascades	17	2,02E-05	F11, C7, A2M, F10, C5AR1, MASP1, C6, F8, SERPING1, C1QA, C8B, VWF, C1QB, THBD, CFD, PROS1, CPB2	69	3,423022096
hsa04270:Vascular smooth muscle contraction	21	1,10E-04	RAMP3, ADCY4, RAMP2, NPR1, PRKCE, PRKG1, MYL9, AGTR1, ACTG2, PRKCQ, PTGIR, GNAQ, ADCY9, GUCY1A2, PLA2G1B, MYH11, CALCRL, PLA2G3, PLA2G5, MYLK, PPP1R14A	112	2,605020492
hsa04514:Cell adhesion molecules (CAMs)	21	0,00103288	SELP, ITGAL, CLDN18, PTPRM, CADM1, ICAM2, CLDN5, NFASC, CLDN11, HLA-E, CDH5, SIGLEC1, CD34, ITGA8, ESAM, JAM2, JAM3, NEGR1, SELE, SELPLG, SPN	132	2,210320417
hsa04080:Neuroactive ligand-receptor interaction	32	0,00245857	F2RL3, THRB, LEPR, PTH1R, FPR1, GRIN3B, FPR2, VIPR1, APLNR, AGTR1, EDNRB, AGTR2, PTGIR, S1PR1, NMUR1, S1PR4, CNR1, P2RY1, S1PR5, CALCRL, GHR, GRID1, C5AR1, PTGER4, PTGFR, ADRB2, ADRB1, P2RX1, SSTR1, GRIA1, P2RY14, CTSG	256	1,736680328
hsa04614:Renin-angiotensin system	6	0,0055758	AGTR1, ACE, AGTR2, MME, CPA3, CTSG	17	4,903567985
hsa02010:ABC transporters	9	0,0117617	ABCA8, ABCC9, ABCA9, ABCB1, CFTR, ABCA3, ABCG1, ABCA6, ABCG2	44	2,841840537
hsa04670:Leukocyte transendothelial	16	0,02073563	ITGAL, CLDN18, NCF2, NCF1, CLDN5, CLDN11, CXCL12, CDH5, MYL9, CYBB,	118	1,883856627

migration		ESAM, PIK3R5, RAPGEF4, JAM2, JAM3, PIK3R1		
hsa03320:PPAR signaling pathway	11	0,02420575	LPL, CD36, CYP27A1, SORBS1, OLR1, PPARG, RXRG, FABP4, SCD5, ACADL, FABP5	69 2,21489665
hsa04062:Chemokine signaling pathway	22	0,02578677	ADCY4, CCL2, FGR, NCF1, PREX1, HCK, CXCL3, CXCL2, CXCR1, GNG11, CXCR2, CXCL12, CCL14, CCL23, PPBP, ADCY9, ARRB1, RASGRP2, CX3CR1, PIK3R5, GRK5, PIK3R1	187 1,634522662
hsa04060:Cytokine-cytokine receptor interaction	28	0,03410983	CSF3, ACVRL1, CCL2, PDGFB, CXCL3, LEPR, CXCL2, BMPR2, CXCR1, CXCR2, TNFSF13, TNFSF12, IL7R, CXCL12, CCL23, PLEKHO2, FIGF, GHR, IL18R1, IL6, BMP2, FLT4, TGFBR2, LIFR, CCL14, PPBP, IL20RA, CX3CR1, IL3RA	262 1,484795395
hsa05020:Prion diseases	7	0,0361229	C1QA, EGR1, C1QB, C8B, C7, IL6, C6	35 2,778688525
hsa00590:Arachidonic acid metabolism	9	0,04474724	ALOX15, PTGIS, PTGDS, GPX3, PLA2G1B, LTC4S, ALOX5, PLA2G3, HPGDS, PLA2G5	56 2,232874707
hsa04350:TGF-beta signaling pathway	12	0,04546484	BMP2, SMAD9, ACVRL1, CDKN2B, ZFYVE9, SMAD6, LEFTY2, TGFBR2, BMPR2, ID4, DCN, ID3	87 1,916336914

Supplementary Table 2 -Functional annotation analysis of upregulated differentially expressed genes in Lung adenocarcinoma datasets using the DAVID tool.

Term	Count	PValue	Genes	Pop Hit	Fold Enrichment
hsa04110:Cell cycle	43	2,82E-09	E2F1, E2F2, E2F3, E2F5, DBF4, PRKDC, TTK, PKMYT1, CHEK1, CHEK2, SFN, PTTG1, CCNE2, CCNE1, CDC45, MCM7, CDKN2A, ORC6L, BUB1, CCNA2, CDC7, CDC6, CDK1, RBL1, SKP2, ESPL1, CDC20, MCM2, CDC25C, MCM3, CDK4, MCM4, ORC1L, CDC25A, MCM6, CCNB1, MAD2L1, CCNB2, PLK1, PCNA, BUB1B, MAD2L2, SMC1B	125	2,591466667
hsa03030:DNA replication	17	4,23E-06	LIG1, POLE, MCM2, MCM3, RNASEH2A, MCM4, MCM6, RFC5, PRIM1, DNA2, RFC3, RFC4, MCM7, POLE2, PRIM2, PCNA, FEN1	36	3,557407407
hsa04512:ECM-receptor interaction	26	5,15E-05	IBSP, TNC, COL3A1, ITGA11, ITGB4, COL2A1, VTN, ITGB3, CHAD, HMMR, LAMB3, ITGB8, COMP, COL6A3, SV2A, COL11A2, COL11A1, THBS2, SPP1, THBS4, ITGA2, COL5A2, COL5A1, LAMA1, COL1A2, COL1A1	84	2,331746032
hsa00270:Cysteine and methionine metabolism	13	9,00E-04	DNMT3A, LDHB, LDHA, AHCY, SRM, IL4I1, CTH, GOT1, SDS, MAT1A, DNMT1, DNMT3B, CBS	34	2,880392157
hsa00330:Arginine and proline metabolism	17	9,64E-04	PYCRL, ODC1, ALDH18A1, CKMT1B, SRM, AGMAT, CPS1, PYCR1, ABP1, CKMT1A, GOT1, CKM, ALDH1B1, P4HA1, P4HA3, GAMT, OAT, ADC	53	2,416352201
hsa00250:Alanine, aspartate and glutamate	12	0,00139536	ADSSL1, GOT1, ACY3, GFPT1, IL4I1, GPT, CAD, ASNS, CPS1, GAD1, GPT2, PPAT	31	2,916129032

metabolism						
hsa00010:Glycolysis / Gluconeogenesis	18	0,0014841	3	ALDOA, LDHB, LDHA, ALDOB, PFKP, ADH1C, ALDH3B2, PGAM2, PCK1, ALDH3A1, GPI, TPI1, G6PC, ALDH1B1, PKM2, ENO3, GAPDH, ENO1	60	2,26
hsa00601:Glycosphingolipi d biosynthesis	10	0,0033785		B4GALT3, B4GALT2, FUT9, B3GALT5, B3GNT4, FUT6, FUT3, B3GNT3, FUT2, B4GALT4	25	3,01333333
hsa04115:p53 signaling pathway	18	0,0061972	4	CDK1, LRDD, CHEK1, CHEK2, PMAIP1, SFN, CDK4, GTSE1, CCNB1, CCNE2, CCNE1, CCNB2, CDKN2A, SERPINB5, RRM2, BAI1, PERP, IGFBP3	68	1,99411764
hsa00051:Fructose and mannose metabolism	11	0,0103373	8	ALDOA, TPI1, AKR1B15, SORD, GMDS, AKR1B10, GMPPA, ALDOB, PFKP, TSTA3, MTMR7, PMM2	34	2,43725490
hsa04950:Maturity onset diabetes of the young	9	0,0124429		HNF1A, HNF4A, BHLHA15, FOXA3, MNX1, NEUROD1, IGF2, HNF4G, PDX1	25	2,712
hsa00260:Glycine, serine and threonine metabolism	10	0,0160460	8	CTH, SHMT2, SDS, GCAT, DMGDH, GAMT, PSAT1, PSPH, CBS, GLDC	31	2,43010752
hsa03440:Homologous recombination	9	0,0249713	3	XRCC3, XRCC2, BLM, EME1, SHFM1, BRCA2, RAD54B, RAD54L, RAD51	28	2,42142857
hsa00533:Keratan sulfate biosynthesis	6	0,0288538	1	B4GALT3, B4GALT2, FUT8, CHST6, CHST4, B4GALT4	14	3,22857142
hsa00140:Steroid hormone biosynthesis	12	0,0343766		AKR1C3, AKR1C2, UGT1A6, UGT1A10, UGT1A9, AKR1C4, HSD17B2, HSD17B1, CYP11B1, SRD5A3, UGT2B4, SRD5A1, UGT2B15, AKR1C1	46	1,96521739
hsa00512:O-Glycan biosynthesis	9	0,0370701	8	GALNT3, GCNT3, GALNT7, GALNT6, GALNT4, B3GNT6, C1GALT1, GALNT14, ST6GALNAC1	30	2,26

hsa05219:Bladder cancer	11	0,0437757	1	E2F1, E2F2, E2F3, CDKN2A, PGF, MMP9, ERBB2, CDH1, EGF, CDK4, MMP1	42	1,97301587	3
hsa00830:Retinol metabolism	13	0,0467652	4	BCMO1, CYP2C18, CYP2B6, ADH1C, RDH5, UGT1A10, UGT1A6, UGT1A9, RDH10, LRAT, DGAT1, DGAT2, CYP2A6, UGT2B4, UGT2B15	54	1,81358024	7
hsa00980:Metabolism of xenobiotics by cytochrome P450	14	0,0473776	6	CYP2C18, CYP2B6, ADH1C, ALDH3B2, CYP2E1, ALDH3A1, AKR1C3, UGT1A10, UGT1A6, AKR1C2, UGT1A9, AKR1C4, UGT2B4, UGT2B15, AKR1C1, MGST1	60	1,75777777	8

Supplementary Table 3 -Functional annotation analysis of downregulated differentially expressed genes in Lung squamous cell carcinoma datasets using the DAVID tool.

Term	Count	PValue	Genes	Po p Hit s	Fold Enrichme nt
hsa04610:Complement and coagulation cascades	31	1,15E-10	C3AR1, C7, A2M, MASP1, C3, F13A1, C6, C5, C1QC, FGG, SERPINA1, C2, CFI, CFD, F11, CR1, F10, C5AR1, C4A, F8, SERPING1, C4BPA, C1QA, C1QB, VWF, C8B, CD55, TFPI, SERPIND1, CPB2, PROS1	69	3,5864446 11
hsa04514:Cell adhesion molecules (CAMs)	44	8,51E-10	HLA-DQB1, ITGAL, CADM3, CLDN18, CADM1, HLA-DRB1, CLDN5, ITGB2, HLA-DMB, SDC4, HLA-DMA, CDH5, ITGAM, CD22, HLA-DRB5, ESAM, CD4, HLA-DPB1, HLA-DOA, SELPLG, NEGR1, SPN, ICAM1, SELP, PTPRC, PTPRM, ICAM2, HLA-E, HLA-DQA2, CLDN23, HLA-DQA1, SIGLEC1, NCAM2, ITGA9, CD86, CD34, ITGA8, CLDN2, HLA-DPA1, JAM2, JAM3, SELE, CD226, HLA-DRA	132	2,6609105 18
hsa04640:Hematopoietic cell lineage	30	2,22E-07	CSF3, IL1R1, HLA-DRB1, CSF1, MME, ANPEP, IL7R, ITGAM, FCGR1C, FCGR1A, CSF3R, CD22, HLA-DRB5, CD4, CSF2RA, CSF1R, IL6, CR1, CD1C, ITGA1, IL6R, IL11RA, CD1E, CD55, CD37, CD36, CD34, CD33, EPOR, IL3RA, HLA-DRA	86	2,7846737 98
hsa05416:Viral myocarditis	25	2,37E-06	HLA-DQB1, PRF1, ITGAL, CAV1, HLA-DRB1, ITGB2, HLA-DMB, HLA-DMA, HLA-DRB5, HLA-DPB1, HLA-DOA, ICAM1, HLA-E, HLA-DQA2, HLA-DQA1, LAMA2, CD86, CD55, SGCG, MYH11, SGCD, HLA-DPA1, SGCA, HLA-DRA, MYH10	71	2,8108209 7
hsa04060:Cytokine-cytokine receptor	58	1,18E-05	ACVRL1, PDGFB, IL6ST, LEPR, TNFSF15, CXCR1, CXCR2, TNFSF13, TNFSF12, CXCL12, TGFB2, CSF3R, CSF2RB, CSF2RA, IL18RAP, LIFR, IL6R, IL11RA, TNFRSF10C, PPBP, TNFRSF10D, CCR2, CX3CR1, TNFSF12-TNFSF13, CSF3, CCL3, IL1R1, CCL2,	262	1,7671695 81

interaction			CXCL5, CSF1, CCR1, CXCL3, CXCL2, BMPR2, IL7R, CCL4, LIF, TNFRSF1B, IL12RB1, CCL21, IL10RA, PLEKHO2, FIGF, CSF1R, IL18R1, IL6, BMP2, FLT1, FLT4, TGFB2, EDA2R, HGF, CCL18, KDR, CCL17, CCL13, CCL14, CXCL16, EPOR, IL3RA		
hsa04062:Chemokine signaling pathway	45	1,61E-05	ADCY4, PRKCZ, CCL3, CCL2, GNAI2, CXCL5, FGR, PREX1, CXCL3, CCR1, CXCL2, NCF1C, NFKBIA, CXCR1, GNG11, CXCR2, CCL4, CXCL12, DOCK2, CCL21, RASGRP2, GNG2, PIK3R5, SHC3, PLCB2, GNG7, PIK3CG, ITK, NCF1, HCK, WAS, CCL18, ELMO1, PRKCB, CCL17, GNGT2, CCL13, CCL14, PPBP, ADCY9, ARRB2, ARRB1, CXCL16, CCR2, CX3CR1, GRK5	187	1,9209781 81
hsa05310:Asthma	14	1,62E-05	FCER1A, HLA-DQB1, HLA-DRB1, HLA-DMB, HLA-DMA, HLA-DQA2, HLA-DQA1, HLA-DRB5, MS4A2, FCER1G, HLA-DPA1, HLA-DPB1, HLA-DOA, HLA-DRA	29	3,8537324 74
hsa04270:Vascular smooth muscle contraction	31	2,82E-05	ADCY4, ADORA2A, PPP1R12B, MRVI1, PRKG1, MYL9, EDNRA, AGTR1, ACTG2, PTGIR, GUCY1A2, PLA2G1B, GUCY1A3, CALCRL, PLCB2, PPP1R14A, RAMP3, RAMP2, PLA2G10, NPR1, PRKCE, ITPR1, PRKCB, PRKCQ, ADCY9, GNAQ, MYH11, CACNA1C, CACNA1D, PLA2G5, MYLK	112	2,2095060 55
hsa05332:Graft-versus-host disease	16	3,38E-05	HLA-DQB1, PRF1, IL6, HLA-DRB1, HLA-DMB, HLA-E, HLA-DMA, HLA-DQA2, HLA-DQA1, CD86, HLA-DRB5, HLA-DPA1, HLA-DPB1, HLA-DOA, KLRD1, HLA-DRA	39	3,2749667 91
hsa05322:Systemic lupus erythematosus	27	1,37E-04	HLA-DQB1, C7, HLA-DRB1, C3, C6, C5, HLA-DMB, C1QC, HLA-DMA, FCGR1C, FCGR1A, HLA-DRB5, HLA-DPB1, C2, FCGR3A, HLA-DOA, FCGR3B, C4A, HLA-DQA2, HLA-DQA1, C1QA, C8B, C1QB, CD86, HLA-DPA1, FCGR2A, CTSG, HLA-DRA	99	2,1771086 06
hsa04672:Intestinal immune network for IgA production	17	1,84E-04	HLA-DQB1, IL6, HLA-DRB1, TNFSF13, TNFSF12, PIGR, HLA-DMB, HLA-DMA, CXCL12, HLA-DQA2, HLA-DQA1, TGFB2, CD86, HLA-DRB5, HLA-DPA1, HLA-DPB1, TNFSF12-TNFSF13, HLA-DOA, HLA-DRA	49	2,7695191 11
hsa05330:Allograft	14	2,39E-04	HLA-DQB1, PRF1, HLA-DRB1, HLA-DMB, HLA-E, HLA-DMA, HLA-DQA2, HLA-DQA1,	36	3,1043956

rejection			CD86, HLA-DRB5, HLA-DPA1, HLA-DPB1, HLA-DOA, HLA-DRA			04
hsa04940:Type I diabetes mellitus	15	3,63E-04	HLA-DQB1, PRF1, HLA-DRB1, PTPRN2, HLA-DMB, HLA-E, HLA-DMA, HLA-DQA2, HLA-DQA1, CD86, HLA-DRB5, HLA-DPA1, HLA-DPB1, HLA-DOA, HLA-DRA	42		2,8509755 55
hsa05414:Dilated cardiomyopathy	24	7,06E-04	ADCY4, SLC8A1, TNNC1, ITGA1, CACNG4, ITGA10, CACNB4, TTN, CACNA2D2, TGFB2, LAMA2, ITGA9, DES, ADRB1, SGCG, ADCY9, PLN, ITGA8, ITGA7, RYR2, SGCD, CACNA1C, CACNA1D, SGCA	92		2,0824517 1
hsa05410:Hypertrophic cardiomyopathy (HCM)	22	0,001398	SLC8A1, IL6, TNNC1, ITGA1, CACNG4, ITGA10, CACNB4, TTN, CACNA2D2, TGFB2, LAMA2, ITGA9, ACE, DES, SGCG, ITGA8, ITGA7, RYR2, SGCD, CACNA1C, CACNA1D, SGCA	85	78	2,0661187 55
hsa04614:Renin-angiotensin system	8	0,002901	AGTR1, ACE, AGTR2, MME, CPA3, ANPEP, ENPEP, CTSG	17	77	3,7565795 55
hsa05320:Autoimmune thyroid disease	14	0,008318	HLA-DQB1, PRF1, HLA-DRB1, HLA-DMB, HLA-E, HLA-DMA, HLA-DQA2, HLA-DQA1, CD86, HLA-DRB5, HLA-DPA1, HLA-DPB1, HLA-DOA, HLA-DRA	51	8	2,1913380 74
hsa04670:Leukocyte transendothelial migration	25	0,009943	ITGAL, CLDN18, GNAI2, CLDN5, NCF1C, ITGB2, CXCL12, CDH5, ITGAM, MYL9, ESAM, PIK3R5, RAPGEF4, RAPGEF3, PIK3CG, ICAM1, ITK, NCF2, NCF1, NCF4, CLDN23, PRKCB, CYBB, CLDN2, JAM2, JAM3	118	56	1,6912566 85
hsa04612:Antigen processing and presentation	19	0,012583	HLA-DQB1, CIITA, HLA-DRB1, IFI30, CTSS, HLA-DMB, HLA-E, HLA-DMA, HLA-DQA2, HLA-DQA1, CD74, B2M, HLA-DRB5, CD4, HLA-DPA1, HLA-DPB1, HLA-DOA, KLRD1, HLA-DRA	83	02	1,8273722 83
hsa05412:Arrhythmic right ventricular cardiomyopathy	17	0,023573	SLC8A1, ITGA1, CACNG4, ITGA10, CACNB4, CACNA2D2, LAMA2, ITGA9, DES, SGCG, ITGA8, ITGA7, RYR2, SGCD, CACNA1C, CACNA1D, SGCA	76	62	1,7856110 06

(ARVC)

hsa04530:Tight junction	26	0,024583 98	PRKCZ, CLDN18, GNAI2, MRAS, CLDN5, MYL9, RRAS, PARD6B, MAGI3, MAGI1, MPDZ, PRKCE, CLDN23, PRKCB, EPB41L2, EPB41L3, PRKCQ, TJP1, CGN, MYH11, CLDN2, TJP3, JAM2, JAM3, MYH10, SPTAN1	134	12	1,5488882
hsa05020:Prion diseases	10	0,024776 95	C1QA, EGR1, C1QB, NCAM2, C8B, C7, IL6, C6, C5, C1QC	35	44	2,2807804
hsa04960:Aldosterone-regulated sodium reabsorption	11	0,026348 7	PIK3CG, ATP1B2, HSD11B1, NR3C2, PIK3R5, NEDD4L, ATP1A2, SCNN1G, SCNN1B, SLC9A3R2, PRKCB	41	66	2,1417084
hsa03320:PPAR signaling pathway	15	0,043643 93	ACOX2, LPL, OLR1, PPARG, RXRG, ACADL, ACSL1, CD36, SORBS1, CYP27A1, HMGCS2, FABP3, FABP4, ACSL4, ACSL5	69	25	1,7353764
hsa04666:Fc gamma R-mediated phagocytosis	19	0,044920 25	PIK3CG, DNMT3, PTPRC, WASF3, NCF1, HCK, NCF1C, PIP5K1B, PRKCE, WAS, PRKCB, DOCK2, GAB2, FCGR1C, CFL2, FCGR1A, PLA2G4F, PIK3R5, FCGR2A, FCGR3A, PPAP2B	95	11	1,5965463
hsa04020:Calcium signaling pathway	31	0,045462 62	GNA14, ADCY4, ERBB4, CYSLTR1, ADORA2A, TNNC1, EDNRA, AGTR1, EDNRB, PDE1B, PLCB2, SLC8A1, BST1, PTGFR, ITPR1, PRKCB, ADRB2, P2RX7, PLCE1, ADRB1, P2RX1, ADCY9, GNAQ, PLN, TBXA2R, CACNA1H, RYR2, CACNA1C, CACNA1D, MYLK, PTAFR	176	08	1,4060493

Supplementary Table 4 -Functional annotation analysis of upregulated differentially expressed genes in Lung squamous cell carcinoma datasets using the DAVID tool.

Term	Count	PValue	Genes	Populations	Fold Enrichment
hsa04110:Cell cycle	54	7,45E-13	E2F1, E2F2, E2F3, DBF4, PKMYT1, TTK, PTTG1, CCNE2, CCNE1, CDC45, MCM7, CDKN2A, CCNA1, CCNA2, CDC7, CDK1, CDC6, RBL1, SKP2, CDK6, ESPL1, MCM2, MCM3, CDK4, MCM4, MCM5, ORC1L, CDK2, MCM6, MAD2L1, BUB1B, ORC5L, ANAPC7, MAD2L2, YWHAZ, PRKDC, CHEK1, CHEK2, SFN, ORC6L, BUB1, TFDP2, TFDP1, CDC20, ATR, CDC25C, CDC25A, CCNB1, HDAC2, CCNB2, HDAC1, PLK1, PCNA, SMC1B	125	2,715352287
hsa03030:DNA replication	25	9,11E-12	RNASEH1, POLA2, RPA3, PRIM1, MCM7, POLE2, POLE3, PRIM2, FEN1, LIG1, POLE, MCM2, RNASEH2A, MCM3, MCM4, MCM5, MCM6, RFC5, DNA2, RFC3, RFC4, RFC2, POLD1, POLD2, PCNA	36	4,364956737
hsa04115:p53 signaling pathway	27	6,14E-06	BID, LRDD, RPRM, CHEK1, SFN, CHEK2, PMAIP1, GTSE1, SESN3, CCNE2, CCNE1, CDKN2A, BAI1, TP53AIP1, CDK1, CYCS, CDK6, ATR, CDK4, CDK2, TP73, CCNB1, CCNB2, SERPINB5, RRM2, PERP, IGFBP3	68	2,495728205
hsa00480:Glutathione metabolism	21	3,38E-05	GSTA1, ODC1, GCLC, GGCT, PGD, GCLM, GSS, GSTM1, GPX2, GSTM2, GSR, GSTM3, GSTM4, G6PD, OPLAH, RRM2, RRM1, IDH2, GSTO2, GPX7, SMS	50	2,639925834
hsa03410:Base excision repair	16	1,29E-04	APEX2, UNG, NEIL3, LIG1, POLE, LIG3, POLB, SMUG1, POLE2, POLE3, POLD1, POLD2, PCNA, TDG, PARP1, FEN1	35	2,873388663

hsa05217:Basal cell carcinoma	21	1,64E-04	FZD9, WNT5A, DVL3, WNT10A, WNT16, WNT10B, WNT5B, LEF1, FZD3, GLI2, FZD7, FZD6, GLI1, WNT2B, SMO, FZD10, WNT7B, WNT4, WNT3, WNT11, PTCH2	55	77	2,3999325
hsa03430:Mismatch repair	12	3,26E-04	RFC5, EXO1, MSH6, RFC3, RFC4, RFC2, MSH2, POLD1, LIG1, POLD2, PCNA, RPA3	23	74	3,2794109
hsa00010:Glycolysis / Gluconeogenesis	21	6,17E-04	ALDOA, LDHA, ALDOC, PGAM1, HK2, PFKP, ADH1C, ALDH3B2, PGAM2, ADH7, PCK1, ALDH3A1, PGM2, GPI, TPI1, PKM2, ENO2, ENO3, PGK1, GAPDH, ENO1	60	95	2,1999381
hsa05200:Pathways in cancer	75	6,70E-04	FGF19, E2F1, E2F2, E2F3, HRAS, PGF, MMP9, FGF11, FGF12, GLI2, MMP1, ACVR1C, GLI1, CCNE2, CCNE1, WNT4, WNT3, CDKN2A, SLC2A1, TGFA, NOS2, CCNA1, FGF3, EGFR, WNT10A, RET, PLD1, WNT10B, CYCS, SKP2, LEF1, FADD, CDK6, CDK4, CDK2, RAD51, JUP, SMO, PIAS3, LAMC2, WNT11, WNT5A, BID, CKS1B, WNT16, WNT5B, FGFR3, EGLN3, TFG, CDH1, LAMB3, RAC3, EGF, TRAF4, PIK3R2, FZD9, MSH6, DVL3, MSH2, BRCA2, ITGA2, FZD3, BIRC5, COL4A6, FZD7, FZD6, WNT2B, LAMA1, CBLC, FZD10, WNT7B, HDAC2, ITGA6, HDAC1, PTCH2	328	52	1,4372418
hsa04114:Oocyte meiosis	32	6,81E-04	YWHAZ, ADCY2, PKMYT1, AURKA, PTTG1, PRKX, CCNE2, CCNE1, CALML3, FBXO43, BUB1, STAG3, FBXO5, CAMK2B, CALML5, CDK1, SGOL1, CHP2, IGF2, ESPL1, CDC20, CDC25C, CDK2, CCNB1, RPS6KA6, MAD2L1, CCNB2, MAPK12, PLK1, ANAPC7, MAD2L2, SMC1B	110	58	1,8285200
hsa00240:Pyrimidine metabolism	28	0,001290	POLR2H, CTPS, PNPT1, DTYMK, CAD, POLA2, POLR2D, TK1, PRIM1, TYMS, POLE2, NT5M, POLE3, PRIM2, ENTPD3, UCK2, POLR3G, POLE, POLR1C, POLR2J3, NME4, UMPS, NME2, NME1-NME2, NME1, RRM2, POLD1, POLD2, RRM1, TXNRD1	95	33	1,8525795
hsa00250:Alanine, aspartate and glutamate metabolism	13	0,001794	GLS2, GOT2, ADSSL1, ALDH4A1, ADSL, IL4I1, GPT, CAD, ASNS, CPS1, GAD1, GPT2, PPAT	31	49	2,6358706

hsa04340:Hedgehog signaling pathway	19	0,001826 44	WNT5A, WNT10A, WNT16, WNT10B, WNT5B, GLI2, PRKX, ZIC2, GLI1, WNT2B, SMO, WNT7B, WNT4, WNT3, WNT11, PTCH2, BMP7, BMP8B, BMP8A	56	2,1325931 49
hsa04512:ECM-receptor interaction	25	0,002176 7	TNC, COL3A1, ITGB4, ITGA11, ITGA2, COL2A1, COL5A2, COL5A1, COL4A6, HMMR, LAMA1, LAMB3, SDC1, ITGA6, ITGB8, COMP, COL1A2, LAMC2, SV2B, SV2A, COL1A1, COL11A2, THBS2, COL11A1, SPP1	84	1,8706957 44
hsa03440:Homologous recombination	12	0,002414 16	XRCC3, XRCC2, BLM, POLD1, POLD2, EME1, SHFM1, BRCA2, RAD54B, RAD54L, RAD51, RPA3	28	2,6938018 72
hsa00360:Phenylalanine metabolism	10	0,004337 44	GOT2, DDC, NAA20, LCLAT1, ALDH3B2, IL4I1, PAH, PNPLA3, MIF, ALDH3A1	22	2,8570625 91
hsa00230:Purine metabolism	37	0,008018 09	XDH, POLR2H, GDA, ADCY2, PNPT1, POLA2, POLR2D, HPRT1, AK3L1, ADA, PPAT, PRIM1, POLE2, ATIC, POLE3, NT5M, PRIM2, ENTPD3, ADCY10, ENTPD2, POLR3G, ADSSL1, POLE, POLR1C, GMPS, POLR2J3, GART, NME4, NME2, NME1-NME2, NME1, RRM2, POLD1, PKM2, POLD2, RRM1, ADSL, PAICS, PRPS2	153	1,5200319 93
hsa00980:Metabolism of xenobiotics by cytochrome P450	18	0,010032 69	GSTA1, CYP2C18, CYP2S1, ADH1C, ALDH3B2, ADH7, CYP2E1, UGT1A1, ALDH3A1, AKR1C3, GSTM1, UGT1A7, GSTM2, AKR1C2, UGT1A10, UGT1A6, UGT1A9, GSTM3, GSTM4, UGT1A8, UGT2A1, GSTO2, AKR1C1	60	1,8856613 1
hsa00030:Pentose phosphate pathway	10	0,011405 98	PGM2, ALDOA, GPI, TALDO1, G6PD, ALDOC, PGD, PFKP, TKTL1, PRPS2	25	2,5142150 8
hsa00330:Arginine and proline metabolism	16	0,015259 79	PYCRL, ODC1, ALDH18A1, CKMT1B, AGMAT, CPS1, GLS2, GOT2, ABP1, PYCR1, CKMT1A, P4HA1, P4HA3, ALDH4A1, GAMT, NOS2, SMS	53	1,8975208 15
hsa04310:Wnt	35	0,018971	WNT5A, WNT16, WNT5B, MMP7, PRKX, WNT4, CSNK2A1, WNT3, RAC3, CACYBP, CAMK2B, FZD9, WNT10A, TBL1XR1, DVL3, WNT10B, VANGL1, VANGL2, CHP2, LEF1,	151	1,4569127

signaling pathway	7	FZD3, CSNK2A1P, PORCN, FZD7, WNT2B, FZD6, DKK4, SENP2, WNT7B, FZD10, DKK1, SFRP1, SFRP2, WNT11, RUVBL1, TBL1X	12
hsa04916:Melanogenesis	25	0,019310 WNT5A, HRAS, WNT16, ADCY2, WNT5B, POMC, PRKX, WNT4, WNT3, MC1R, CALML3, CAMK2B, CALML5, TUBB3, FZD9, DVL3, WNT10A, WNT10B, LEF1, FZD3, FZD7, FZD6, WNT2B, WNT7B, FZD10, WNT11	1,5872569 99 95
hsa05219:Bladder cancer	13	0,026466 E2F1, EGFR, E2F2, E2F3, HRAS, FGFR3, PGF, MMP9, CDH1, CDK4, MMP1, CDKN2A, EGF	1,9455235 42 74
hsa00670:One carbon pool by folate	7	0,030346 TYMS, MTHFD2, SHMT2, ALDH1L1, DHFR, ATIC, GART	2,7499227 16 44
hsa05222:Small cell lung cancer	21	0,036949 E2F1, E2F2, CKS1B, E2F3, CYCS, SKP2, ITGA2, CDK6, CDK4, CDK2, COL4A6, CCNE2, LAMA1, CCNE1, LAMB3, ITGA6, PIAS3, LAMC2, NOS2, TRAF4, PIK3R2	1,5713844 84 25

Supplementary Table 5 -Functional annotation analysis of downregulated differentially expressed genes in Schwann cells datasets using the DAVID tool.

Term	Count	PValue	Genes	Populations	Fold Enrichment	Bonferroni
hsa05200:Pathways in cancer	31	6,88E-04	WNT5A, FGFR1, FGF18, FGF7, WNT5B, PGF, FGF11, BCL2L1, TGFB1, TCF7L1, CTNNB1, IGF1R, BCL2, HHIP, WNT8B, FN1, EGFR, TGFB1, CBL, RUNX1T1, LEF1, BIRC5, FZD5, STK4, CDK2, PRKCB, PLCG2, PDGFRA, JAK1, WNT9A, ITGA2B	328	1,8995830 52	0,0962221 32
hsa04510:Focal adhesion	22	8,54E-04	EGFR, FLT1, PGF, COL3A1, ITGB4, ITGA11, ITGB5, ACTN2, CTNNB1, PRKCB, IGF1R, CCND3, CCND2, RASGRF1, COMP, BCL2, COL6A3, PDGFRA, RELN, COL1A1, FN1, ITGA2B	201	2,1998702 14	0,1180162 84
hsa05412:Arrhythmic right ventricular cardiomyopathy (ARVC)	11	0,003953	SLC8A1, SGCG, ITGB4, ITGA11, LEF1, ITGB5, ACTN2, CACNA1C, TCF7L1, ITGA2B, CTNNB1	76	2,9090389 02	0,4414132 64
hsa04520:Adherens junction	11	0,004350	EGFR, IGF1R, FGFR1, TGFB1, LMO7, LEF1, ACTN2, INSR, TCF7L1, FARP2, CTNNB1	77	2,8712591 76	0,4732119 52
hsa05217:Basal cell carcinoma	9	0,005228	WNT5A, WNT5B, LEF1, WNT9A, HHIP, FZD5, TCF7L1, CTNNB1, WNT8B	55	3,2888968 74	0,5372666 18

hsa04115:p53 signaling pathway	10	0,005918	44	CCNB2, CCND3, CCND2, RRM2, ATR, GADD45B, IGFBP3, GTSE1, CDK2, TP53AIP1	68	2,9557079	0,5821343	75	33
hsa05210:Colorectal cancer	11	0,008085	27	EGFR, IGF1R, BCL2, TGFB1, CTNNB1, PDGFRA, LEF1, BIRC5, FZD5, TCF7L1,	84	2,6319875	0,6968010	78	67
hsa04914:Progesterone-mediated oocyte maturation	11	0,009509	96	PGR, IGF1R, ADCY4, RPS6KA6, CCNB2, ANAPC5, ADCY8, BUB1, PDE3A, CDC25C, CDK2	86	2,5707785	0,7545481	64	23
hsa04114:Oocyte meiosis	12	0,019583	01	PGR, IGF1R, ADCY4, RPS6KA6, CCNB2, ANAPC5, ADCY8, BUB1, FBXO5, PTTG2, CDC25C, CDK2	110	2,1925979	0,9453749	16	38
hsa04340:Hedgehog signaling pathway	8	0,019615	51	WNT5A, WNT5B, WNT9A, HHIP, LRP2, BMP7, IHH, WNT8B	56	2,8712591	0,9456404	76	78
hsa04512:ECM-receptor interaction	10	0,022288	93	COMP, COL6A3, COL3A1, ITGB4, ITGA11, ITGB5, RELN, COL1A1, ITGA2B, FN1	84	2,3927159	0,9636128	8	41
hsa04916:Melanogenesis	11	0,023901	53	WNT5A, ADCY4, WNT5B, ADCY8, LEF1, WNT9A, FZD5, TCF7L1, PRKCB, CTNNB1, WNT8B	99	2,2332015	0,9714527	81	94
hsa04020:Calcium signaling pathway	16	0,027179	1	EGFR, PTGER1, ADCY4, SLC8A1, NOS1, ADCY8, CACNA1I, PTGFR, PRKCB, EDNRA, AGTR1, ATP2A3, RYR3, PLCG2, PDGFRA, CACNA1C	176	1,8271649	0,9825885	3	45
hsa05414:Dilated cardiomyopathy	10	0,037444	29	ADCY4, SLC8A1, SGCG, ADCY8, ITGB4, ITGA11, ITGB5, CACNA1C, TGFB1, ITGA2B	92	2,1846537	0,9963389	21	66
hsa04110:Cell cycle	12	0,044604	37	CDC45, CCNB2, CCND3, ANAPC5, CCND2, BUB1, PTTG2, ATR, CDC25C, GADD45B, CDK2, TGFB1	125	1,9294861	0,9987783	66	76

hsa05014: Amyotrophic lateral sclerosis (ALS)	0,045586	7	66	ALS2, SLC1A2, NOS1, GRIA2, BCL2, RAB5A, BCL2L1	2,6545603	0,9989498
					53	7 16

Supplementary Table 6 -Functional annotation analysis of upregulated differentially expressed genes in Schwann cells datasets using the DAVID tool.

Term	Count	PValue	Genes	Pop Hits	Fold Enrichment
hsa04080:Neuroactive ligand-receptor interaction	24	1,95E-06	CSH1, MCHR1, F2RL3, GABRG3, PTH2R, GRIK1, GABRA4, GABRB2, GLRA3, GABRA5, BRS3, FPR3, GRM1, TAAR8, GH2, GH1, SSTR5, APLNR, P2RY10, CHRM3, GRIA2, CHRM1, ADRA1A, GPR50	256	3,075604839
hsa04950:Maturity onset diabetes of the young	4	0,0384673	4 HES1, HHEX, HNF1A, FOXA2	25	5,249032258
hsa00350:Tyrosine metabolism	5	0,0430019	3 DDC, PNMT, ADH1B, DBH, FAH	44	3,728005865

Supplementary Table 7 - Functional annotation analysis of downregulated differentially expressed overlapped genes in Schwann cells and Lung adenocarcinoma datasets using the DAVID tool.

Term	Count	PValue	Genes	Pop Hits	Fold Enrichment
hsa04080:Neuroactive ligand-receptor interaction	24	1,95E-06	CSH1, MCHR1, F2RL3, GABRG3, PTH2R, GRIK1, GABRA4, GABRB2, GLRA3, GABRA5, BRS3, FPR3, GRM1, TAAR8, GH2, GH1, SSTR5, APLNR, P2RY10, CHRM3, GRIA2, CHRM1, ADRA1A, GPR50	256	3,0756048 4
hsa04950:Maturity onset diabetes of the young	4	0,0384673	4 HES1, HHEX, HNF1A, FOXA2	25	5,2490322 6
hsa00350:Tyrosine metabolism	5	0,0430019	3 DDC, PNMT, ADH1B, DBH, FAH	44	3,7280058 7
hsa00740:Riboflavin metabolism	3	0,0828751	3 ACP5, MTMR7, ACP	16	6,1512096 8
hsa04020:Calcium signaling pathway	10	0,0848993	2 ATP2B2, PLCB4, CHRM3, CHRM1, ADRA1A, GNAS, CACNA1E, CAMK2B, CACNA1C, GRM1	176	1,8640029 3

Supplementary Table 8 - Functional annotation analysis of upregulated differentially expressed overlapped genes in Schwann cells and Lung adenocarcinoma datasets using the DAVID tool.

Term	Count	PValue	Genes	Pop Hits	Fold Enrichment
hsa04115:p53 signaling pathway	3	0,02105574	CCNE1, CDKN2A, PERP	68	12,4632353
hsa00340:Histidine metabolism	2	0,09279159	DDC, ACY3	29	19,4827586

Supplementary Table 9 - Functional annotation analysis of downregulated differentially expressed overlapped genes in Schwann cells and Lung squamous cell carcinoma datasets using the DAVID tool.

Term	Count	PValue	Genes	Pop Hits	Fold Enrichment
hsa04270:Vascular smooth muscle contraction	4	0,05024756	AGTR1, ADCY4, MYH11, PPP1R14A	112	4,65659341
hsa04340:Hedgehog signaling pathway	3	0,06506959	WNT9A, HHIP, IHH	56	6,98489011

Supplementary Table 10 - Functional annotation analysis of upregulated differentially expressed overlapped genes in Schwann cells and Lung squamous cell carcinoma datasets using the DAVID tool.

Term	Count	PValue	Genes	Pop Hits	Fold Enrichment
hsa04080:Neuroactive ligand-receptor interaction	5	0,02607792	PTH2R, CHRM3, GABRA5, GPR50, GRM1	256	4,13818359
hsa04115:p53 signaling pathway	3	0,03721193	CCNE1, CDKN2A, PERP	68	9,34742647

Supplementary Table 11 - Functional annotation analysis of downregulated miRNA target genes combined with upregulated genes in Lung adenocarcinoma datasets using the DAVID tool.

Term	Count	PValue	Genes	Pop Hits	Fold Enrichment
hsa04360:Axon guidance	8	8,85E-04	SEMA5A, DCC, SEMA6A, SEMA6D, CFL2, ROBO2, CXCL12, SLIT2	129	5,0055371
hsa04010:MAPK signaling pathway	10	0,0046364	DUSP1, FGF14, JUN, PTPN5, MRAS, NTRK2, TGFBR2, RRAS, CACNB4, DUSP8	267	3,02300696
hsa04520:Adherens junction	4	0,0668683	PTPRM, WASF3, TGFBR2, LMO7	77	4,19294991

Supplementary Table 12 - Functional annotation analysis of upregulated miRNA target genes combined with downregulated genes in Lung adenocarcinoma datasets using the DAVID tool.

Term	Count	PValue	Genes	Pop Hits	Fold Enrichment
hsa04080:Neuroactive ligand-receptor interaction	9	0,0051273	GPR83, CALCR, MCHR1, GABRR1, SSTR3, PRLR, PTH2R, GRIK3, GRIN2A	256	3,25035511
hsa05200:Pathways in cancer	9	0,0211608	E2F1, E2F2, CKS1B, RET, HSP90B1, SLC2A1, SKP2, FGF11, WNT8B	328	2,53686253
hsa05222:Small cell lung cancer	4	0,0590702	5 E2F1, E2F2, CKS1B, SKP2	84	4,4025974

Supplementary Table 13 - Functional annotation analysis of downregulated miRNA target genes combined with upregulated genes in Lung squamous cell carcinoma datasets using the DAVID tool.

hsa05414:Dilated cardiomyopathy	12	0,0013487	2	ITGA9, ADRB1, ADCY9, ITGA1, RYR2, SGCD, CACNB4, TTN, CACNA1C, CACNA1D, CACNA2D2, TGFB2	92	3,1285890	1
hsa04270:Vascular smooth muscle contraction	13	0,0021556	5	ADORA2A, PRKG1, PRKCE, ITPR1, PRKCB, PRKCQ, GNAQ, ADCY9, GUCY1A2, CALCRL, CACNA1C, PLCB2, CACNA1D	112	2,7840717	7
hsa05410:Hypertrophic cardiomyopathy (HCM)	11	0,0025059	2	ITGA9, IL6, ITGA1, RYR2, SGCD, CACNB4, TTN, CACNA1C, CACNA1D, CACNA2D2, TGFB2	85	3,1040510	5
hsa04020:Calcium signaling pathway	16	0,0059957	4	GNA14, ERBB4, BST1, ADORA2A, ITPR1, PRKCB, EDNRB, PLCE1, ADRB2, ADRB1, GNAQ, ADCY9, RYR2, CACNA1C, PLCB2, CACNA1D	176	2,1805317	3
hsa04530:Tight junction	13	0,0092404	4	PARD6B, CLDN18, MAGI3, MAGI1, MPDZ, PRKCE, PRKCB, EPB41L2, PRKCQ, EPB41L3, TJP1, JAM2, MYH10	134	2,3269853	6
hsa04540:Gap junction	10	0,0109533	9	TJP1, ADRB1, GNAQ, ADCY9, GUCY1A2, PRKG2, PRKG1, PLCB2, ITPR1, PRKCB	89	2,6950392	2
hsa04060:Cytokine-cytokine receptor interaction	20	0,0117725	3	IL18R1, IL6, BMP2, CXCL5, IL6ST, FLT4, LEPR, CSF1, TGFB2, BMP2, LIFR, IL6R, HGF, CXCL12, TGFB2, KDR, CCL13, TNFRSF10D, PLEKHO2, CSF2RA	262	1,8309808	4
hsa04010:MAPK signaling pathway	20	0,0141980	3	MEF2C, FGF7, FGF14, TGFB2, CACNB4, CACNA2D2, TGFB2, PRKCB, FOS, BDNF, DUSP1, RASGRP3, RPS6KA2, JUN, MAP3K8, CACNA1C, NFATC2,	267	1,7966928	1

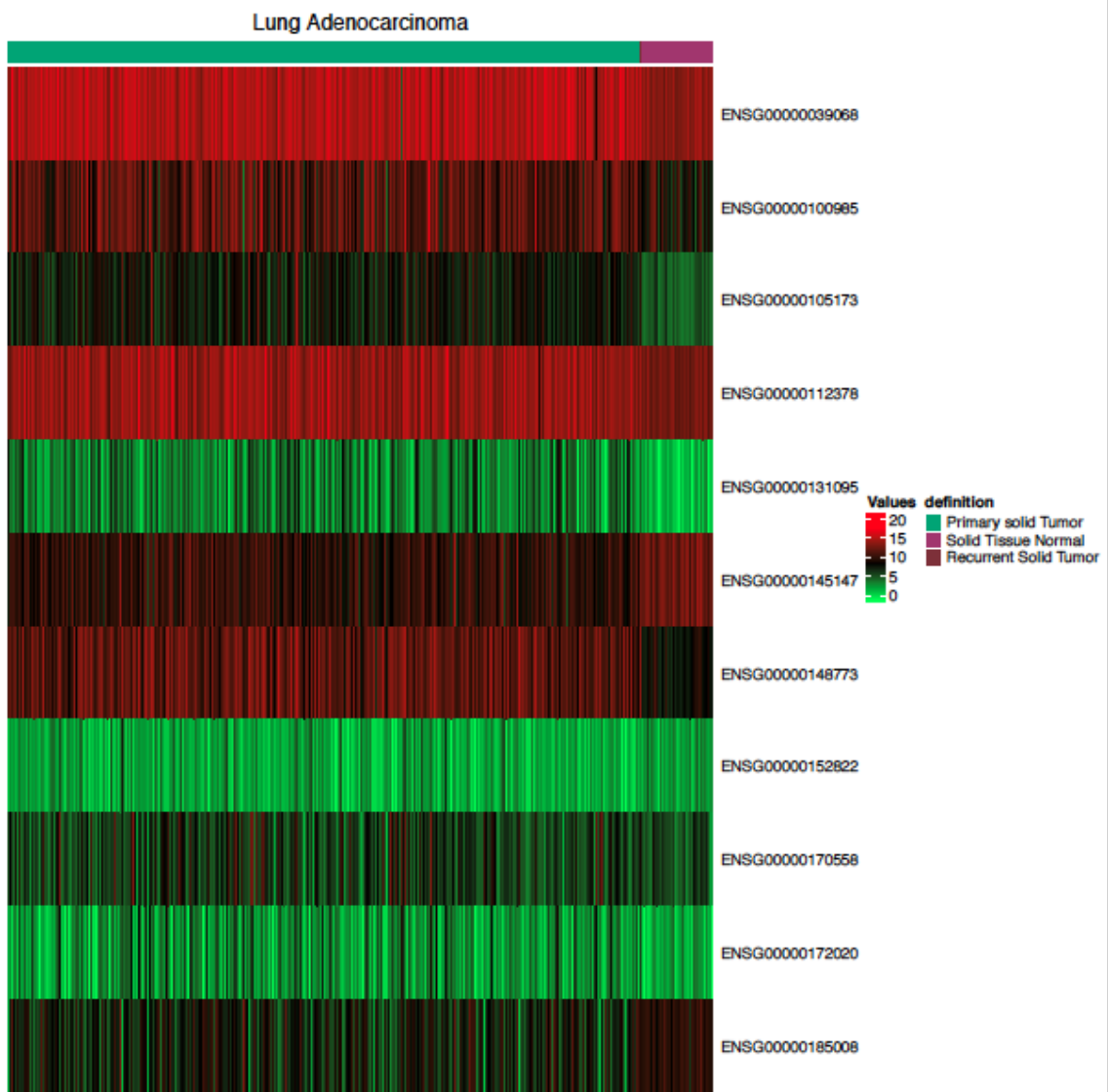
RAPGEF2, CACNA1D, FGF2

hsa04360:Axon guidance	12	0,0175176	2	SEMA5A, PLXNC1, NRP1, SEMA3G, ABLIM3, CFL2, SEMA3E, ROBO2, UNC5C, NFATC2, CXCL12, SLIT2	129	2,2312417	7
hsa04514:Cell adhesion molecules (CAMs)	12	0,0204618	8	NCAM2, ITGA9, CLDN18, PTPRM, CADM1, CD34, HLA-DPA1, JAM2, SDC4, NEGR1, HLA-DQA2, HLA-DQA1	132	2,1805317	3
hsa04730:Long-term depression	8	0,0233513	2	GNAQ, GRIA1, GUCY1A2, PRKG2, PRKG1, PLCB2, ITPR1, PRKCB	69	2,7809680	1
hsa04640:Hematopoietic cell lineage	9	0,0254004	1	CD55, IL6, CD34, CSF1, FCGR1A, ITGA1, IL6R, CSF2RA, CD1E	86	2,5101469	9
hsa04630:Jak-STAT signaling pathway	13	0,0266301	8	PIK3CG, SPRY1, IL6, SOCS2, SOCS3, IL6ST, STAT5A, LEPR, LIFR, IL6R, CSF2RA, SPRY4, CISH	155	2,0117163	7
hsa05200:Pathways in cancer	22	0,0297606	3	PIK3CG, IL6, BMP2, FGF7, FGF14, STAT5A, MITF, TGFBR2, RUNX1T1, HGF, FZD5, FZD4, TGFB2, DAPK1, PRKCB, FOS, ETS1, JUN, RARA, AXIN2, FGF2, CSF2RA	328	1,6088069	5
hsa05412:Arrhythmogenic right ventricular cardiomyopathy (ARVC)	8	0,0371737	5	ITGA9, ITGA1, RYR2, SGCD, CACNB4, CACNA1C, CACNA1D, CACNA2D2	76	2,5248262	2
hsa04930:Type II diabetes mellitus	6	0,0437676	6	PIK3CG, SOCS2, SOCS3, CACNA1C, PRKCE, CACNA1D	47	3,0620232	8
hsa04912:GnRH signaling pathway	9	0,0495942	1	GNAQ, ADCY9, JUN, HBEGF, CACNA1C, PLCB2, CACNA1D, ITPR1, PRKCB	98	2,2027820	6

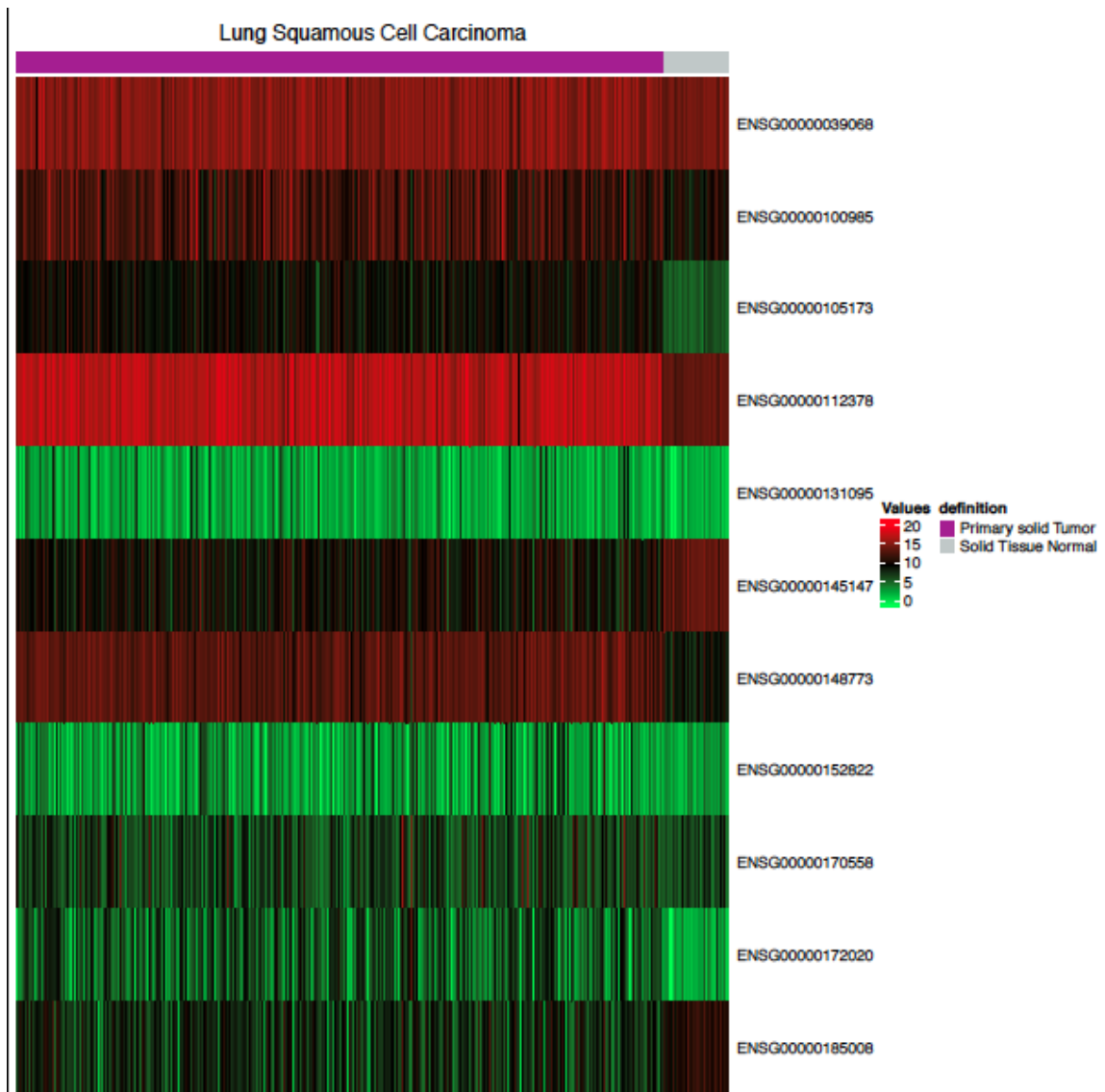
Supplementary Table 14 - Functional annotation analysis of upregulated miRNA target genes combined with downregulated genes in Lung squamous cell carcinoma datasets using the DAVID tool.

Term	Count	PValue	Genes	Pop Hits	Fold Enrichment
hsa00030:Pentose phosphate pathway	5	8,37E-04	PGM2, GPI, G6PD, PGD, PRPS2	25	11,3
hsa04110:Cell cycle	7	0,0216048	8 E2F2, YWHAZ, YWHAQ, SKP2, CDK6, MCM4, CDK2	125	3,164
hsa05200:Pathways in cancer	12	0,0268979	1 EGFR, BID, WNT5A, E2F2, CKS1B, WNT7B, SKP2, FGF11, TFG, LEF1, CDK6, CDK2	328	2,06707317
hsa04310:Wnt signaling pathway	7	0,0479839	1 WNT5A, TBL1XR1, WNT7B, DKK1, SFRP1, SFRP2, LEF1	151	2,6192053
hsa05222:Small cell lung cancer	5	0,0587607	9 E2F2, CKS1B, SKP2, CDK6, CDK2	84	3,36309524

Supplementary Figure 1- Heatmap of differentially expressed genes in LUSC samples.



Supplementary Figure 2- Heatmap of differentially expressed genes in LUAD samples.



Supplementary Figure 3- Methylation analysis of GRM1 gene in Lung adenocarcinoma. The highlighted probes are promoter gene region.

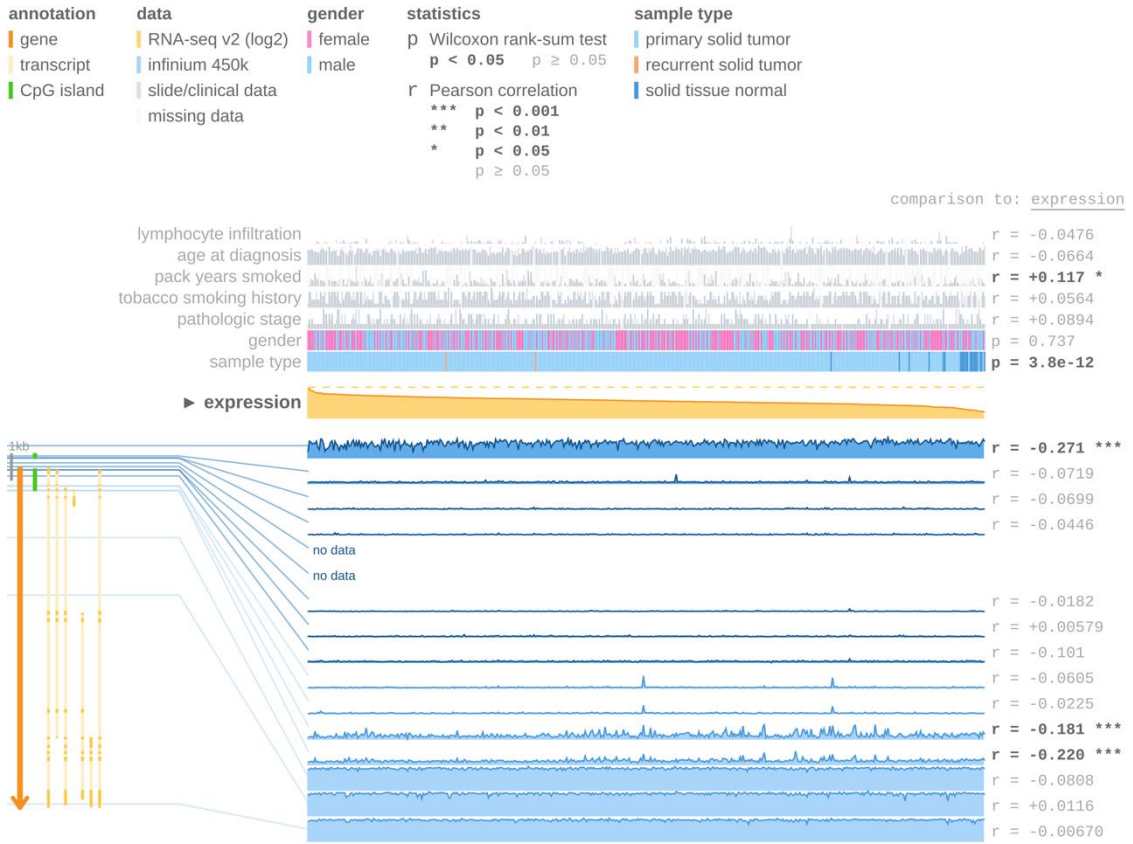
Supplementary Figure 4- Methylation analysis of GRM1 gene in Lung squamous cell carcinoma. The highlighted probes are promoter gene region.



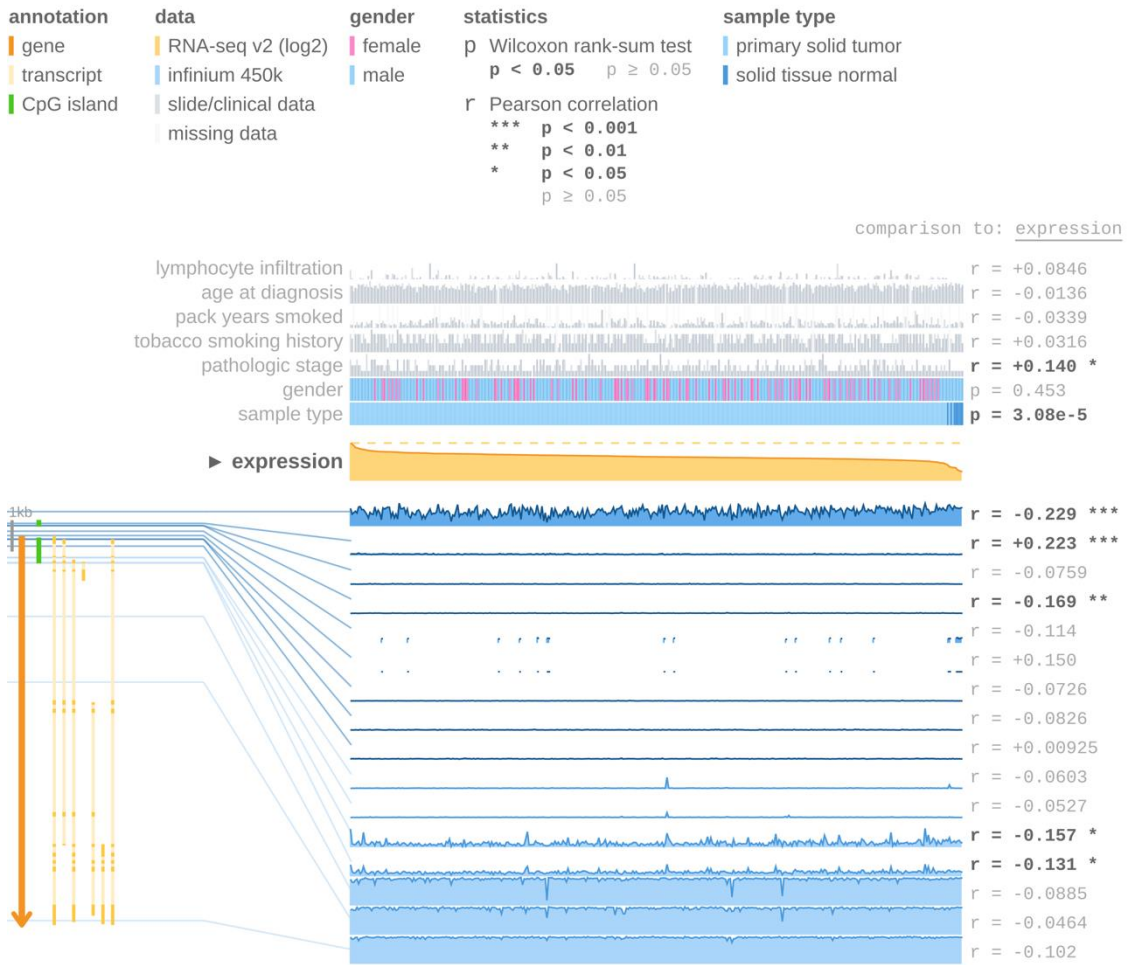
Supplementary Figure 5- Methylation analysis of CCNE1 gene in Lung adenocarcinoma. The highlighted probes are promoter gene region.



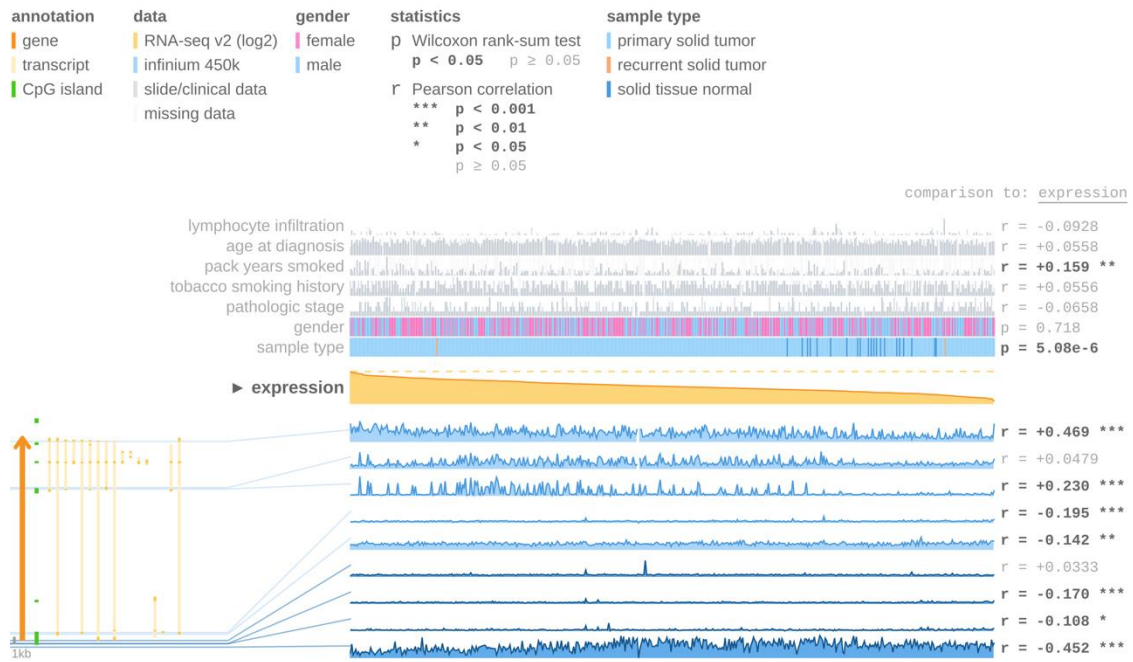
Supplementary Figure 6- Methylation analysis of CCNE1 gene in Lung squamous cell carcinoma. The highlighted probes are promoter gene region.



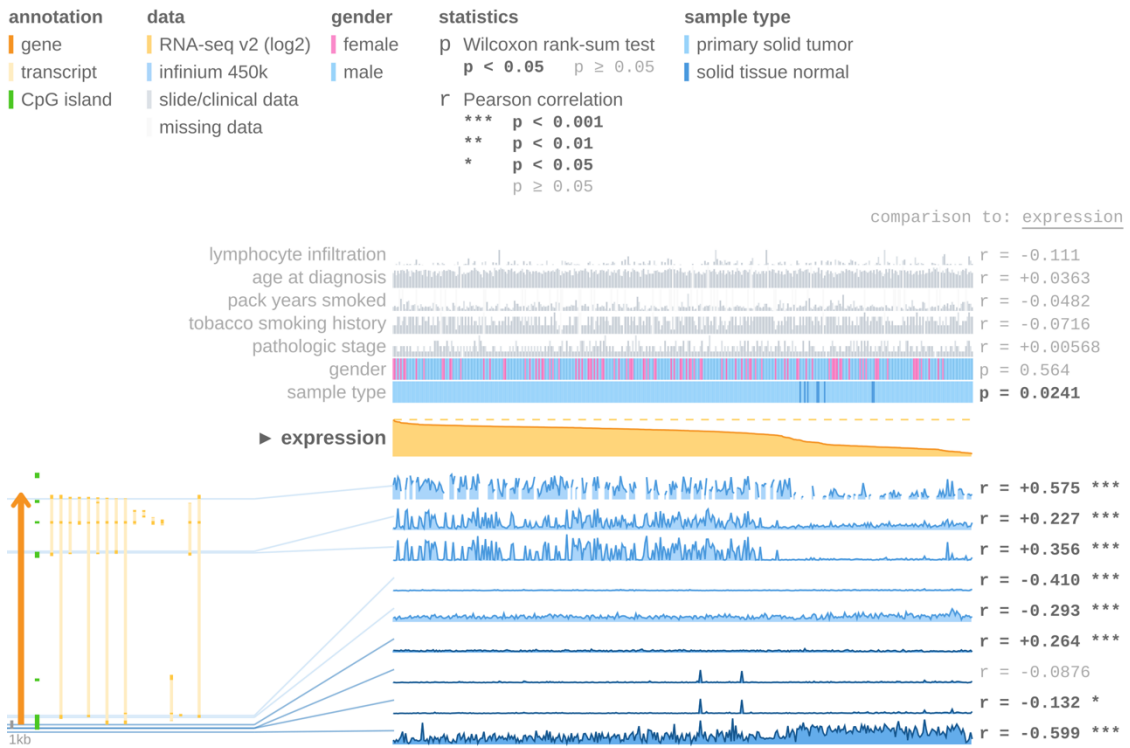
Supplementary Figure 7- Methylation analysis of CDKN2A gene in Lung adenocarcinoma. The highlighted probes are promoter gene region.



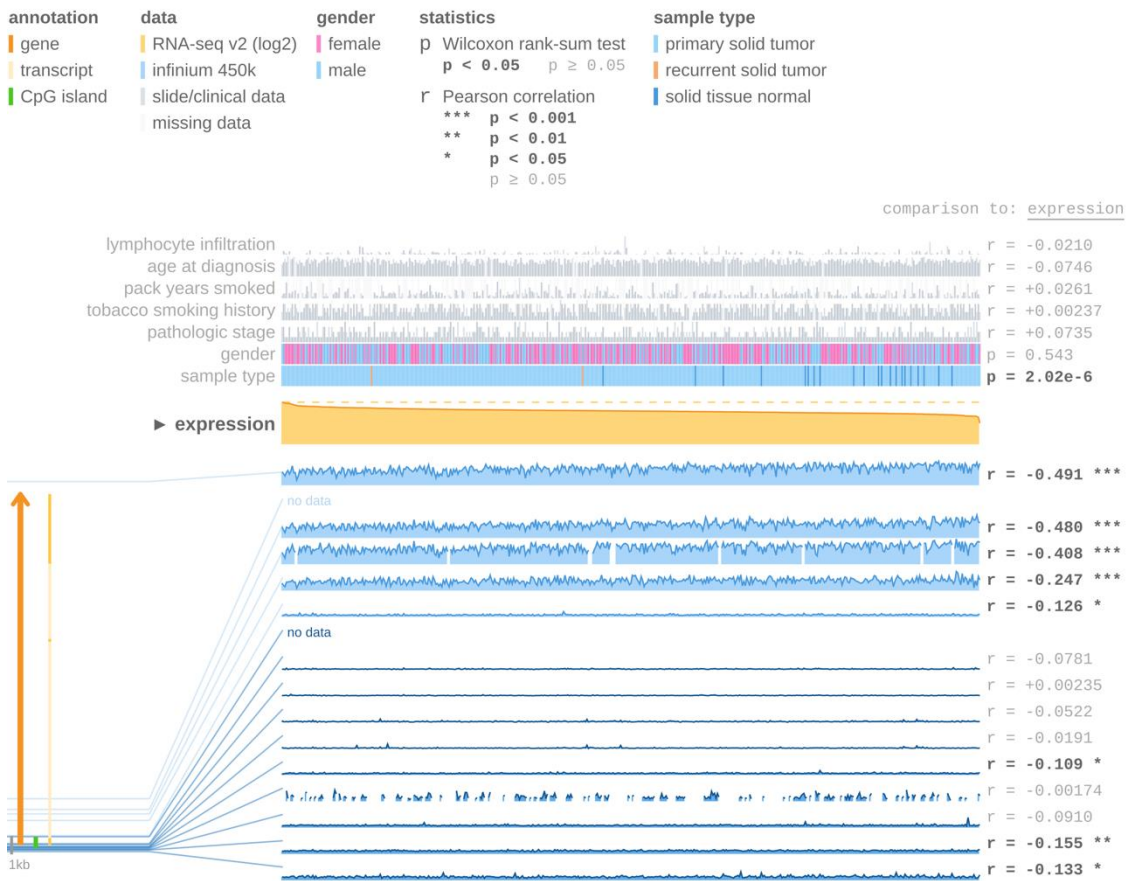
Supplementary Figure 8- Methylation analysis of CDKN2A gene in Lung squamous cell carcinoma. The highlighted probes are promoter gene region.



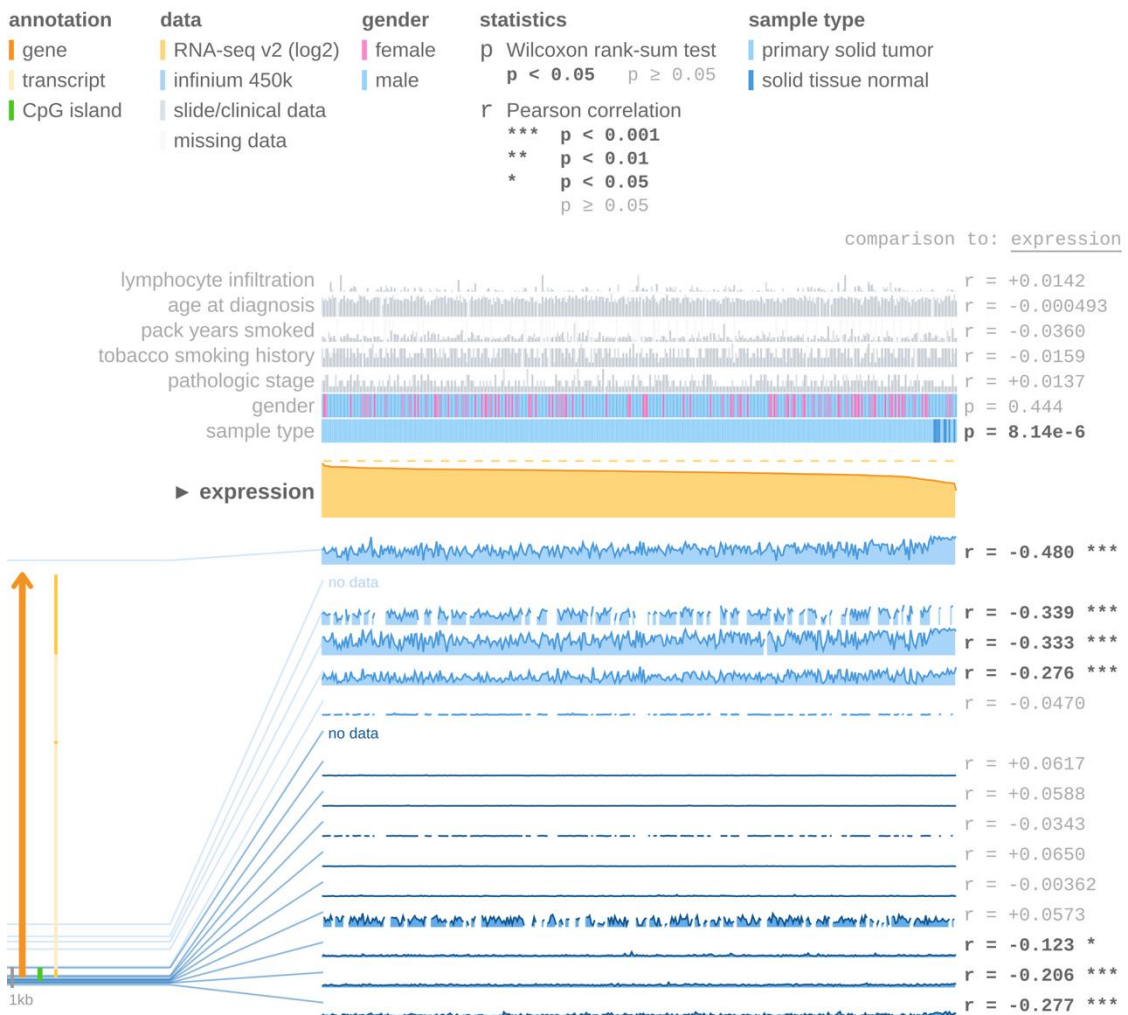
Supplementary Figure 9- Methylation analysis of PERP gene in Lung adenocarcinoma. The highlighted probes are promoter gene region.



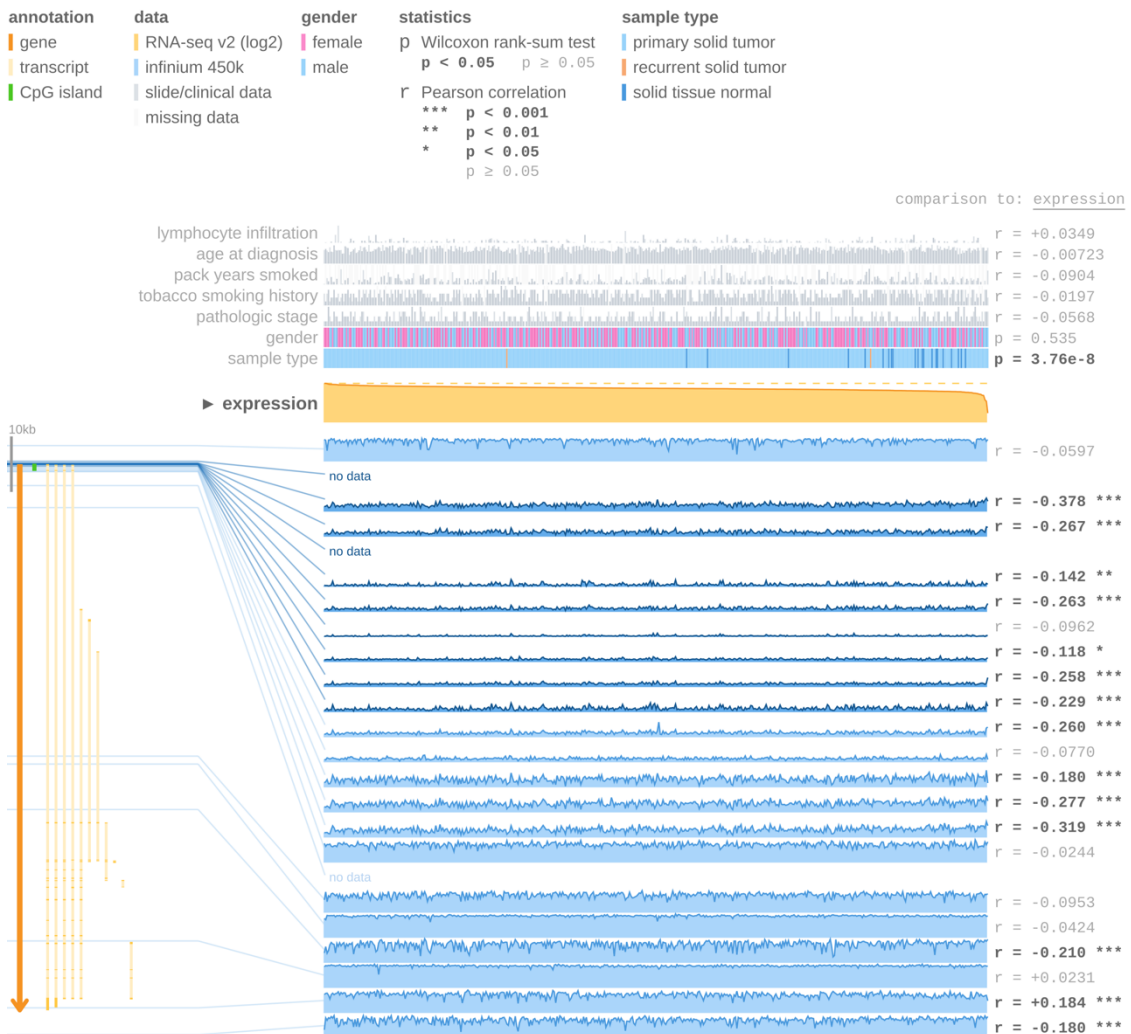
Supplementary Figure 10- Methylation analysis of PERP gene in Lung squamous cell carcinoma. The highlighted probes are promoter gene region.



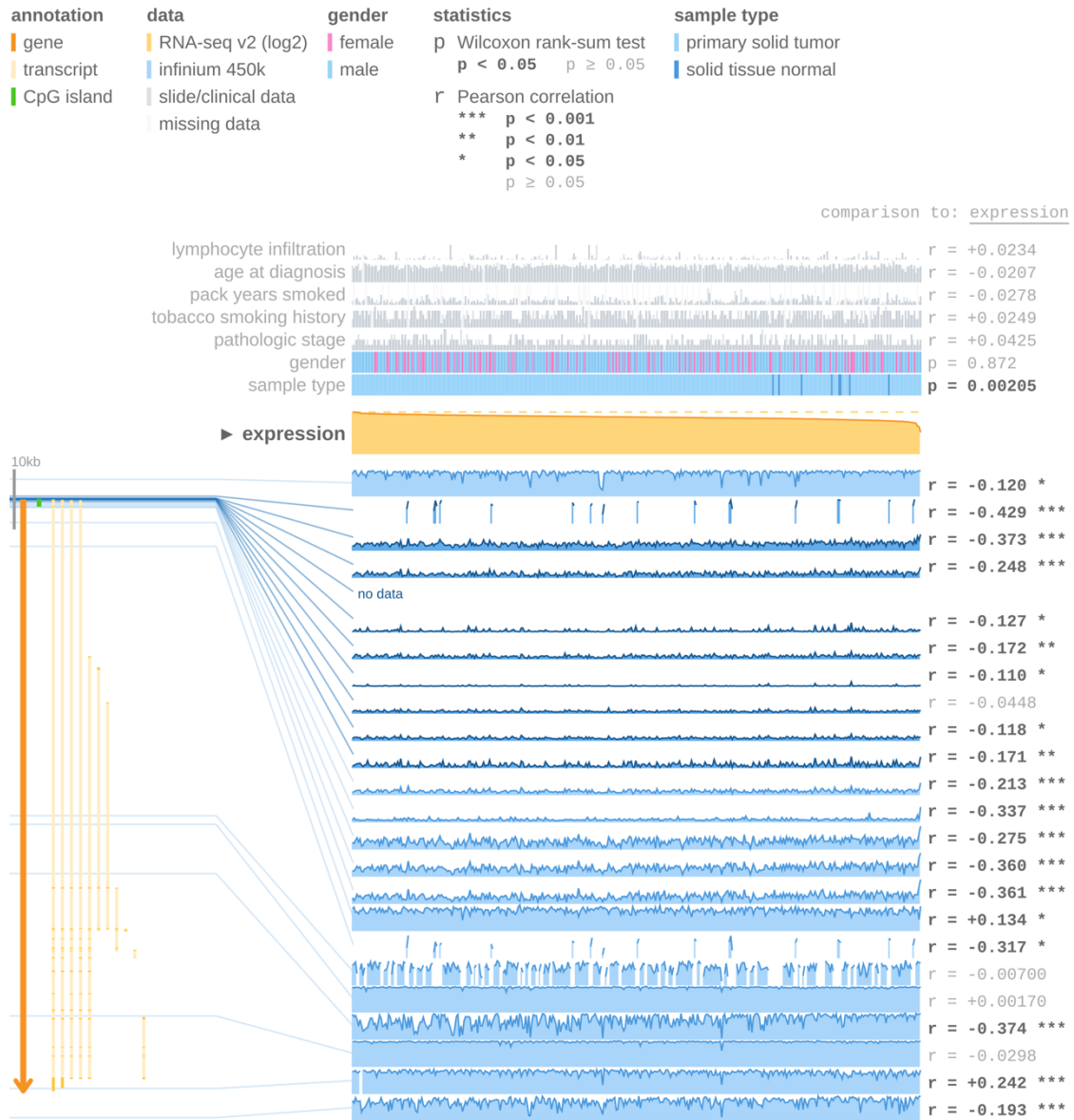
Supplementary Figure 11- Methylation analysis of CDH1 gene in Lung adenocarcinoma. The highlighted probes are promoter gene region.



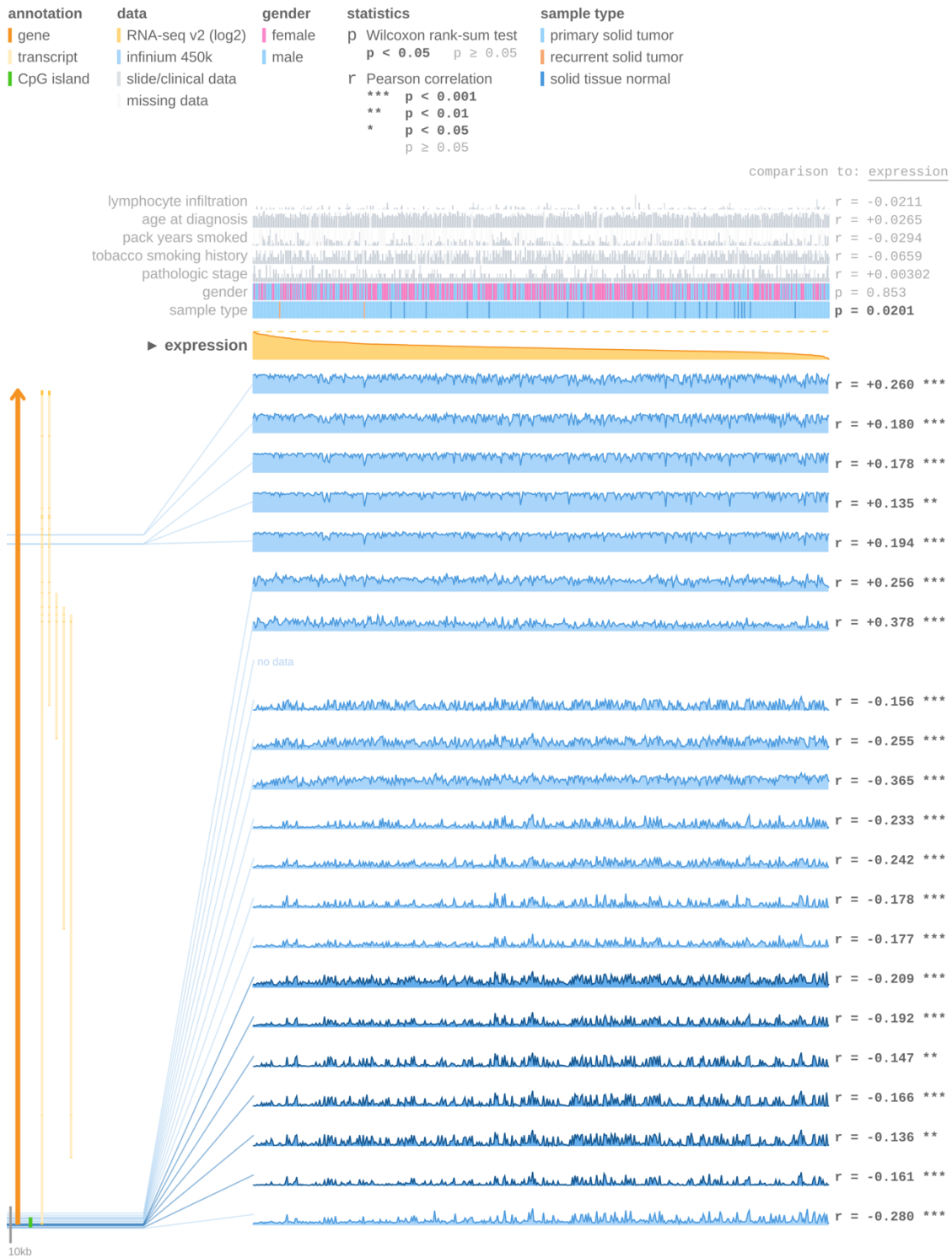
Supplementary Figure 12- Methylation analysis of CDH1 gene in Lung squamous cell carcinoma. The highlighted probes are promoter gene region.



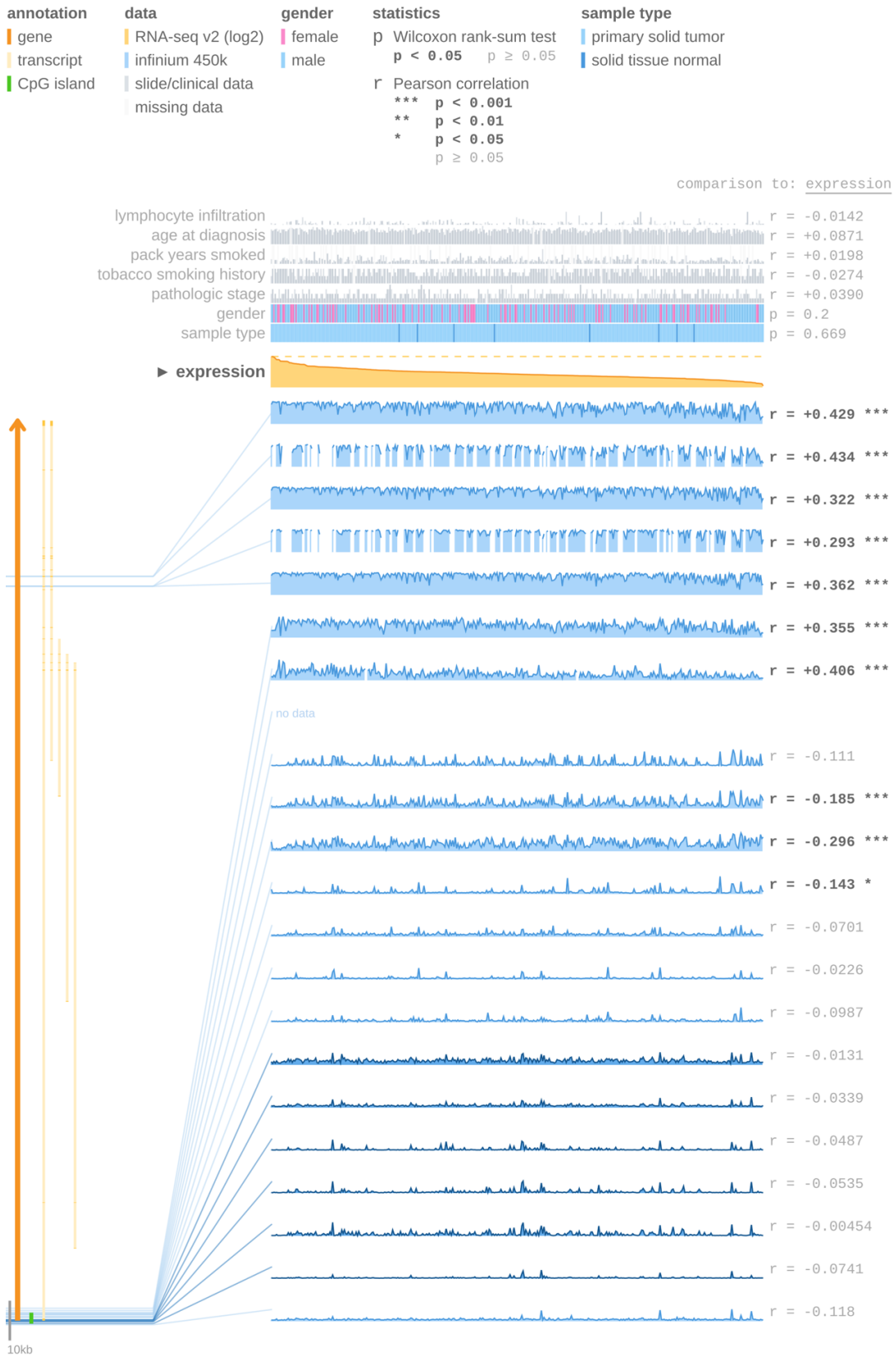
Supplementary Figure 13- Methylation analysis of CDH2 gene in Lung adenocarcinoma. The highlighted probes are promoter gene region.



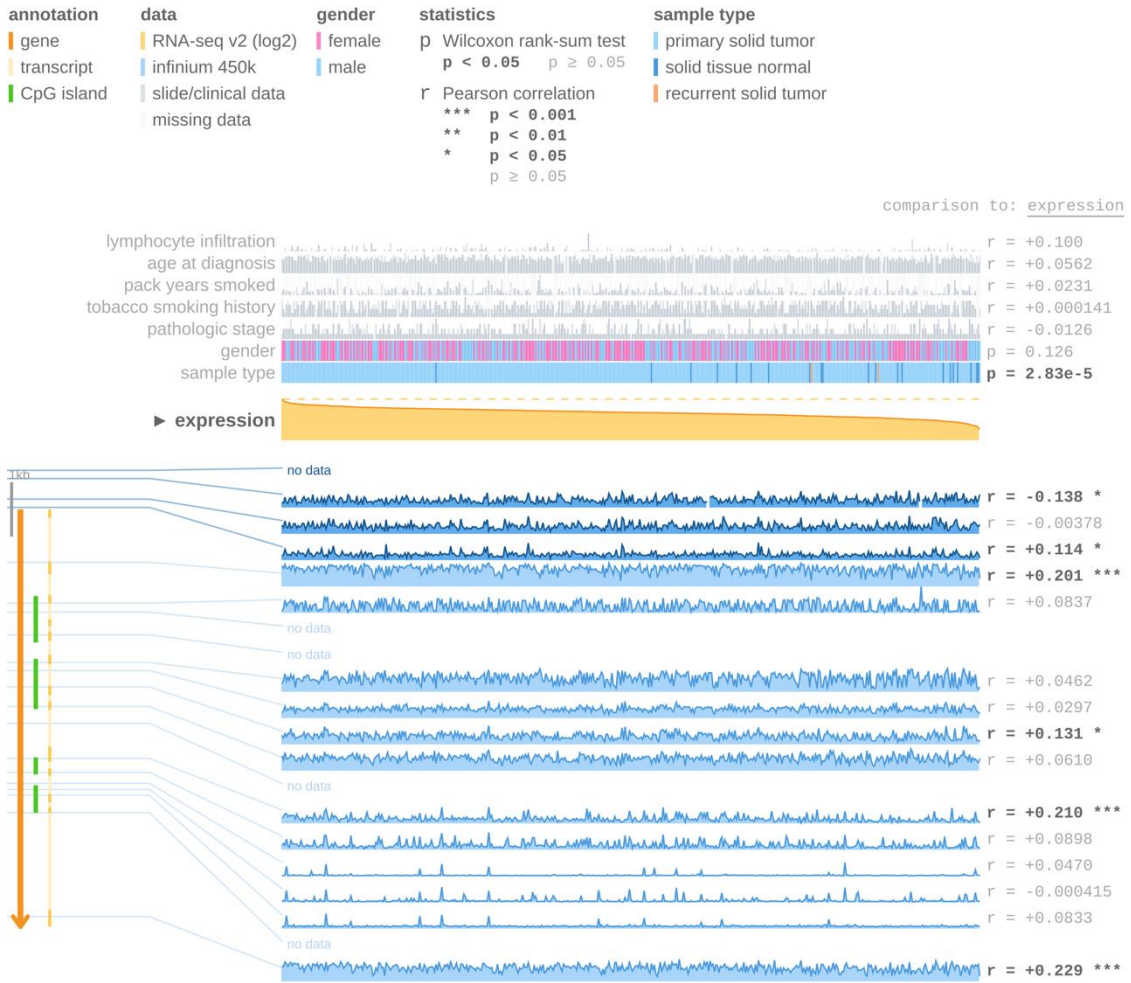
Supplementary Figure 14- Methylation analysis of CDH2 gene in Lung squamous cell carcinoma. The highlighted probes are promoter gene region.



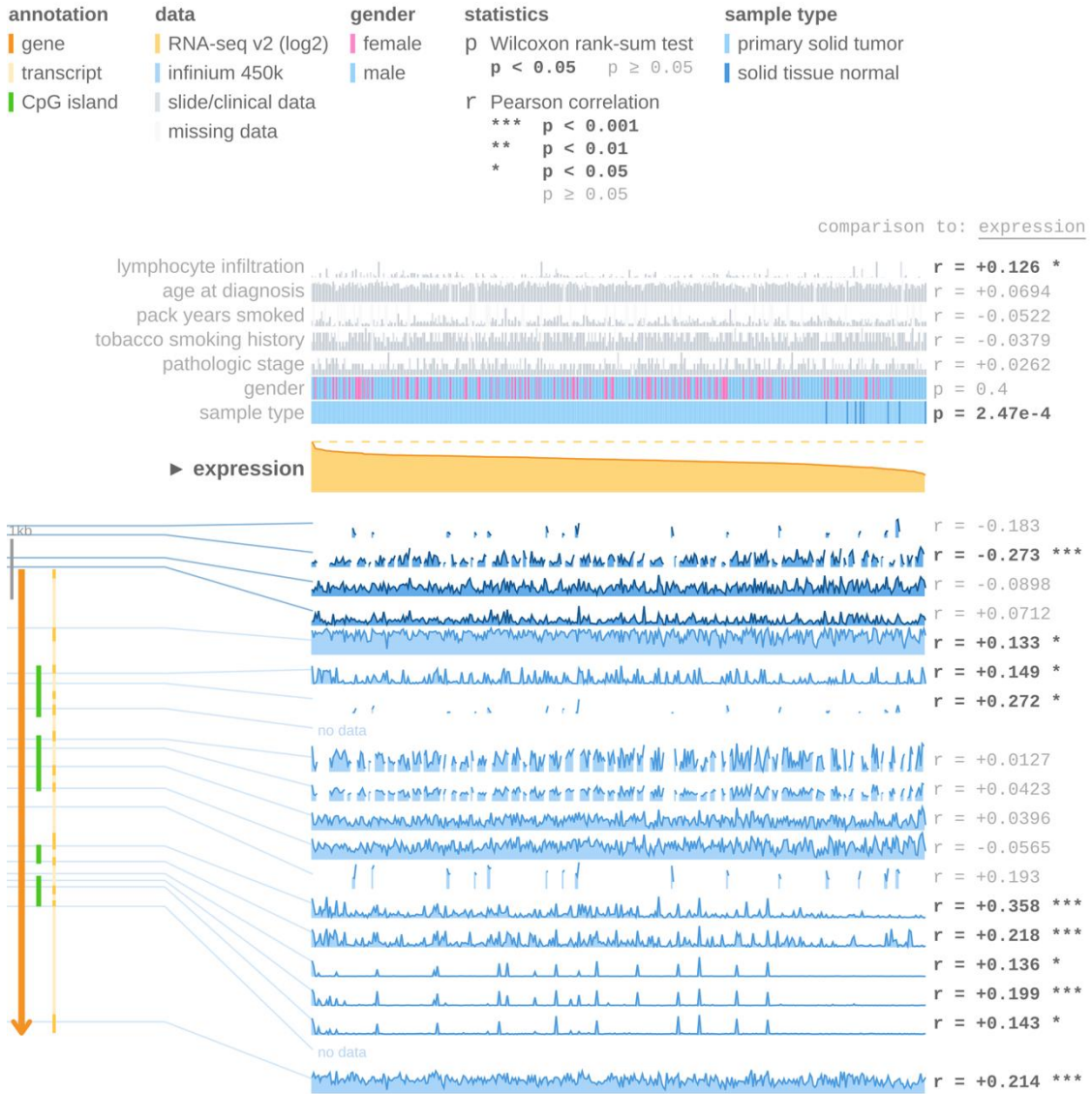
Supplementary Figure 15- Methylation analysis of MMP9 gene in Lung adenocarcinoma. The highlighted probes are promoter gene region.



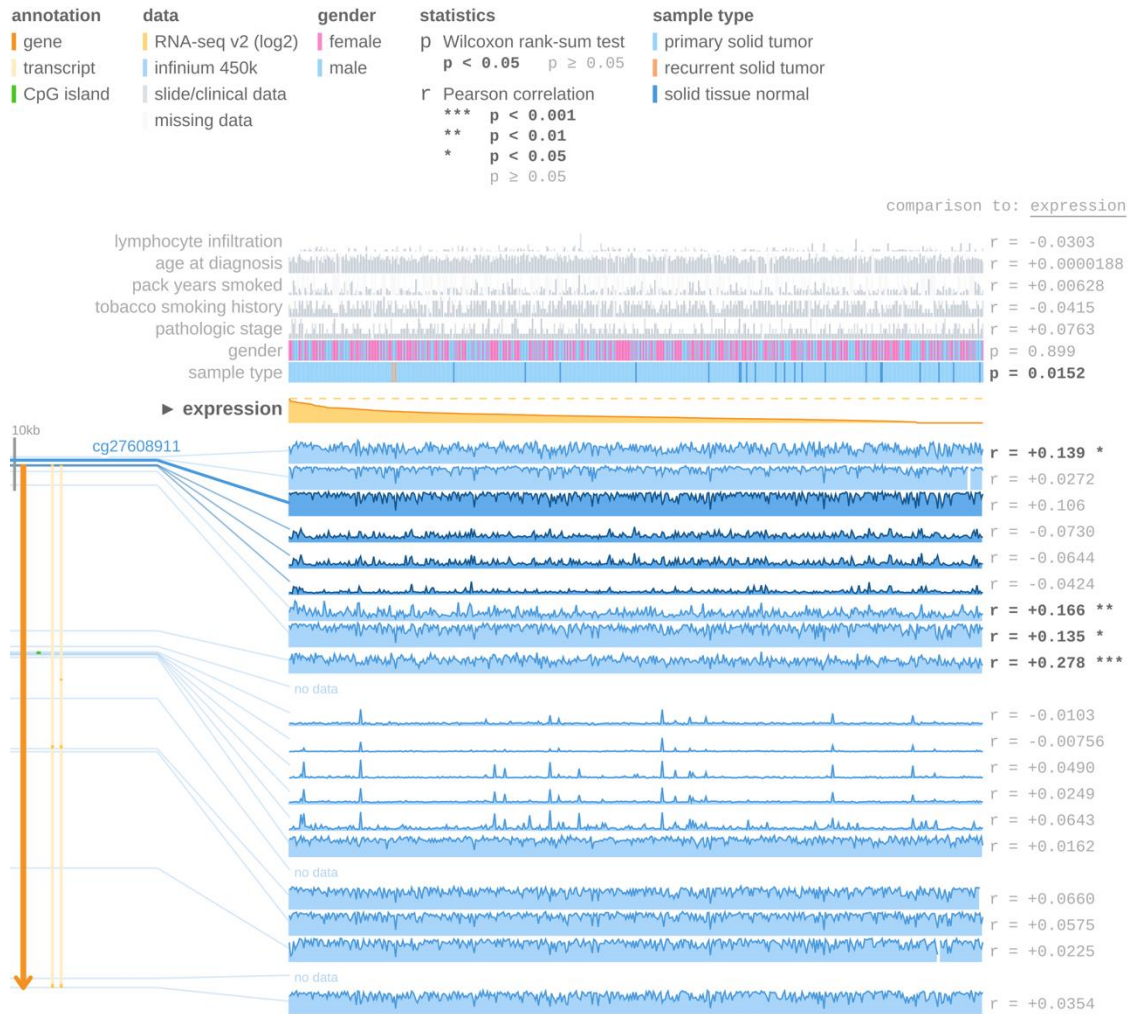
Supplementary Figure 16- Methylation analysis of MMP9 gene in Lung squamous cell carcinoma. The highlighted probes are promoter gene region.



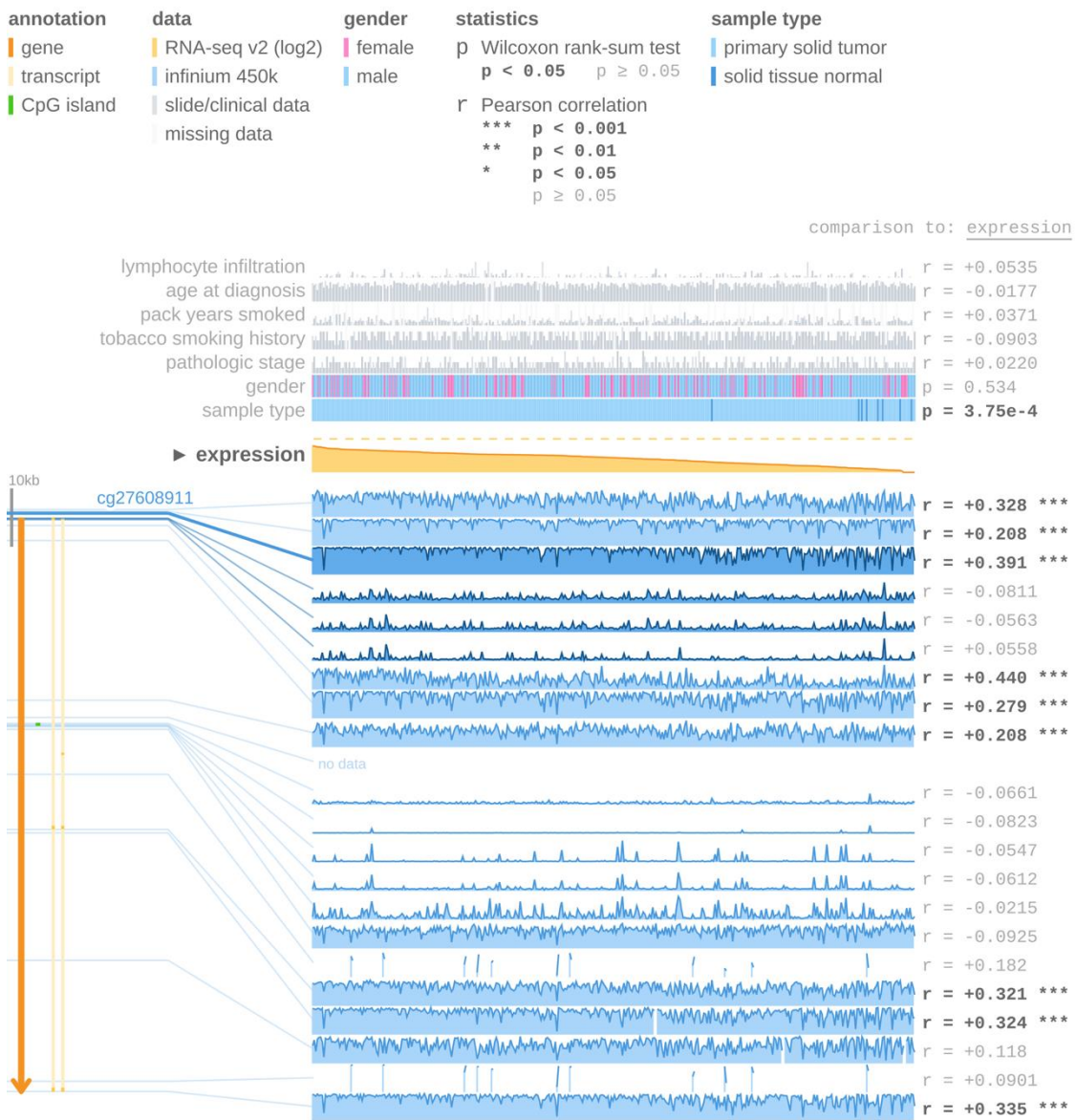
Supplementary Figure 17- Methylation analysis of GAP43 gene in Lung adenocarcinoma. The highlighted probes are promoter gene region.



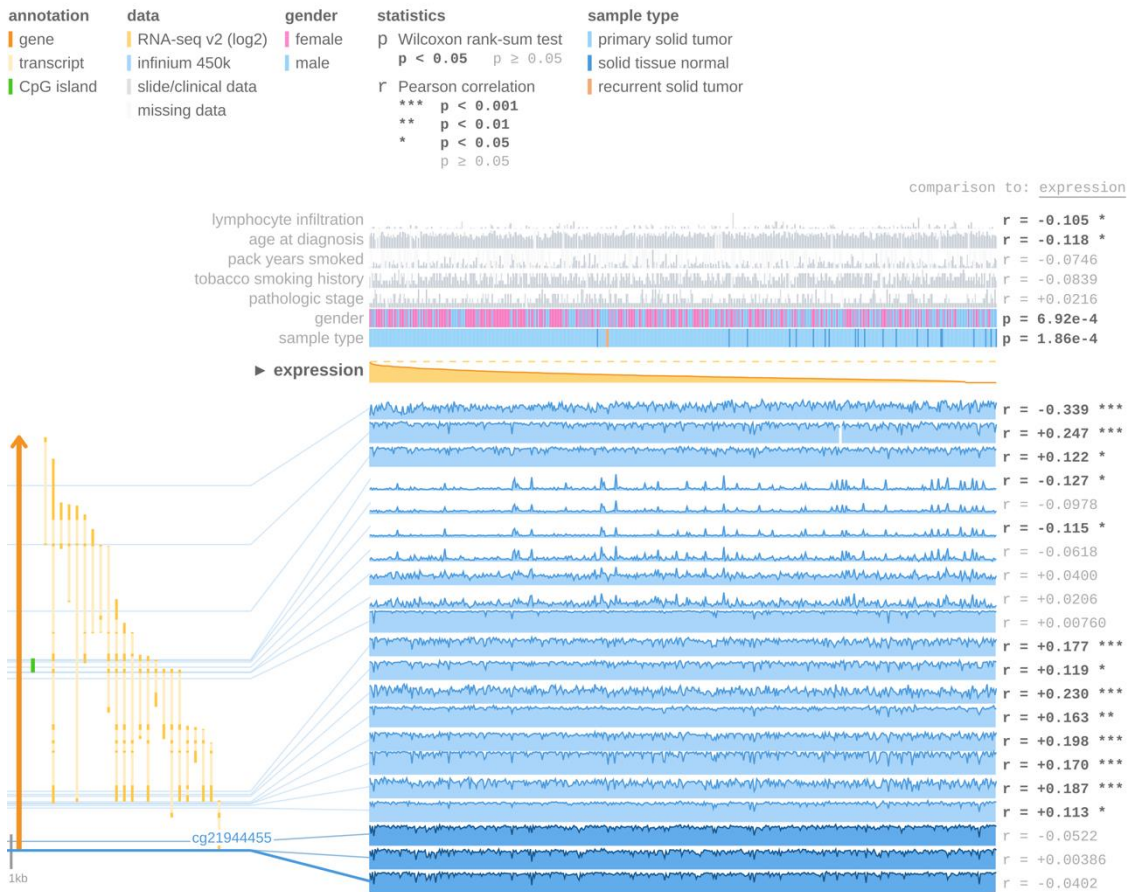
Supplementary Figure 18- Methylation analysis of GAP43 gene in Lung squamous cell carcinoma. The highlighted probes are promoter gene region.



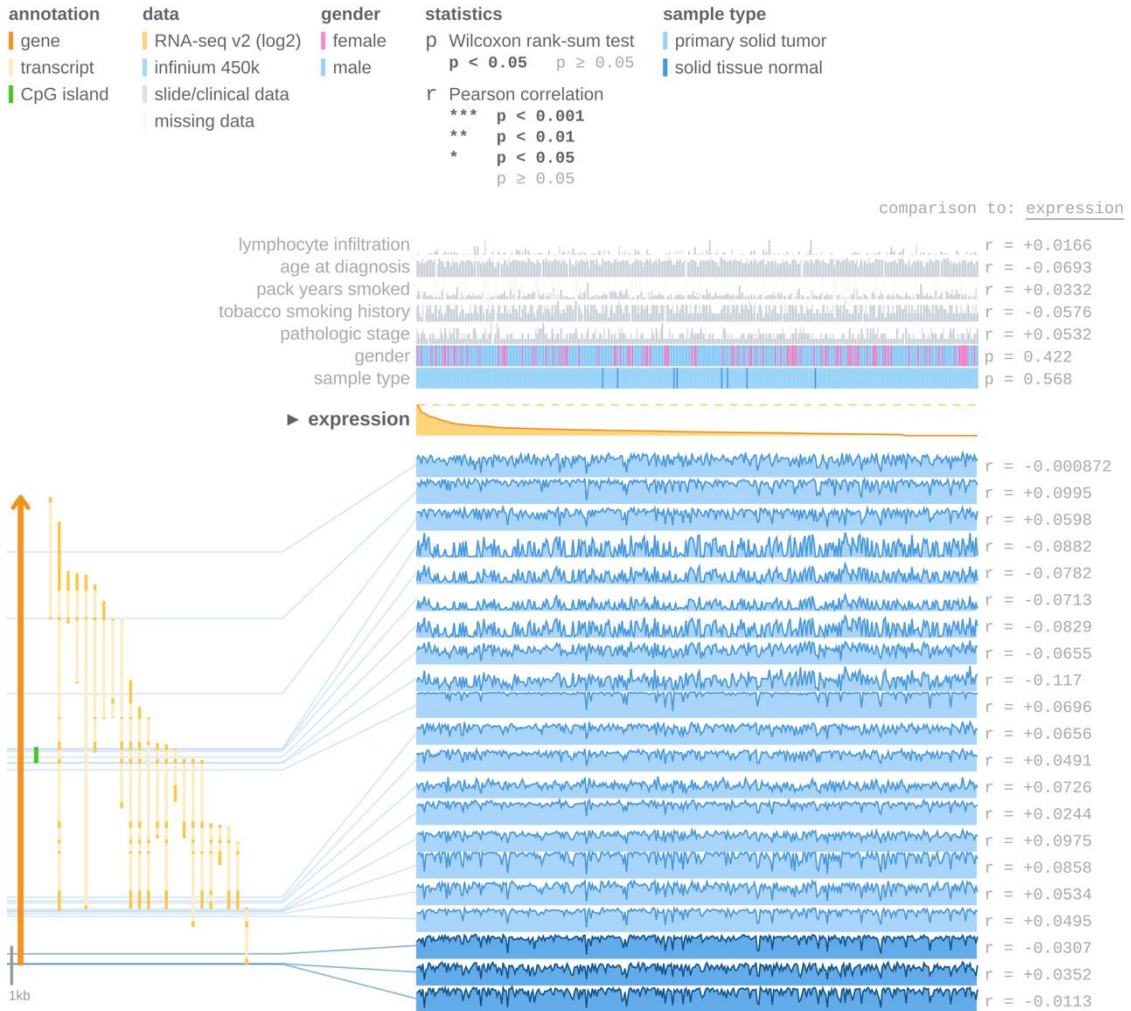
Supplementary Figure 19- Methylation analysis of GFAP gene in Lung adenocarcinoma. The highlighted probes are promoter gene region.



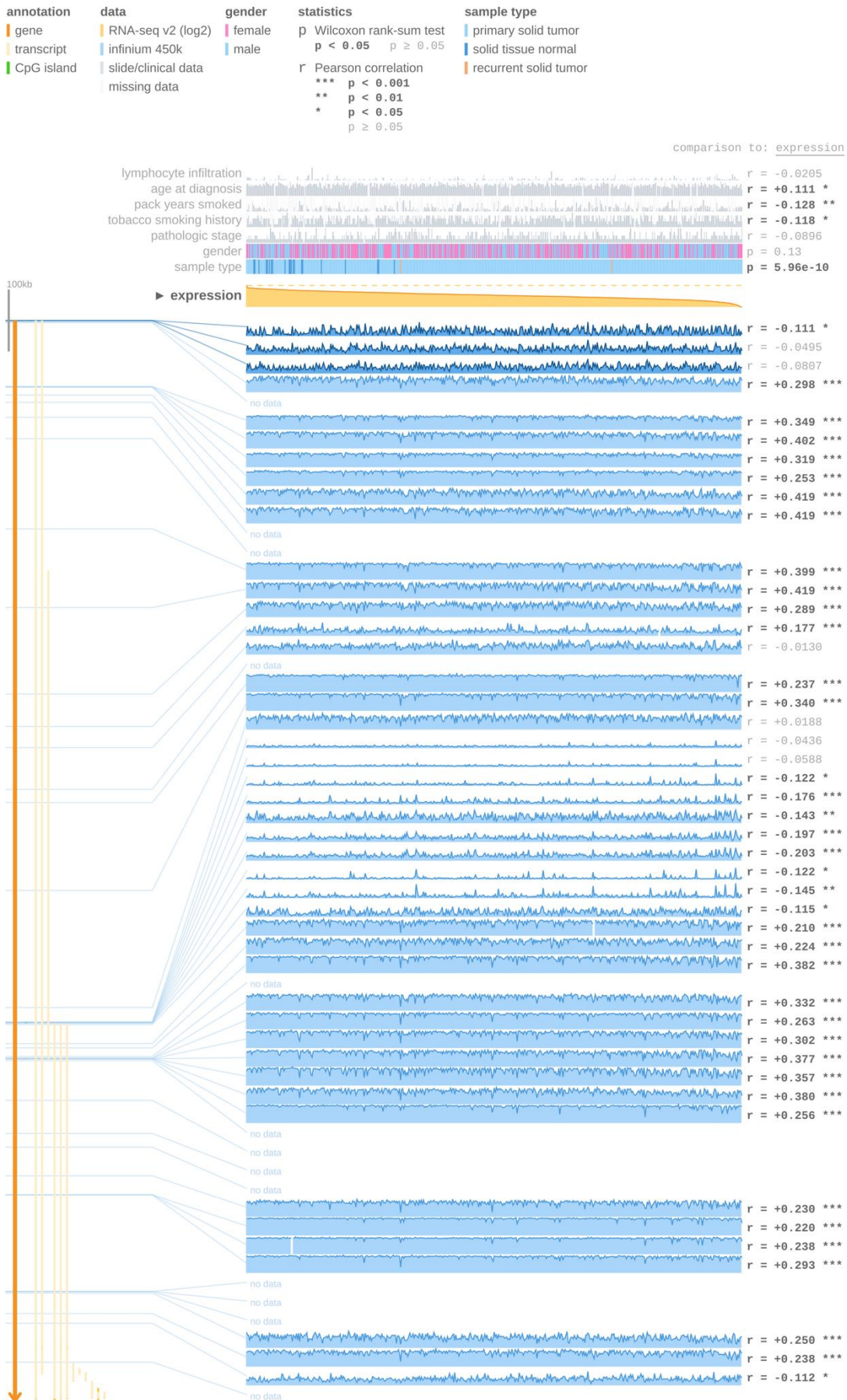
Supplementary Figure 20- Methylation analysis of GFAP gene in Lung squamous cell carcinoma. The highlighted probes are promoter gene region.



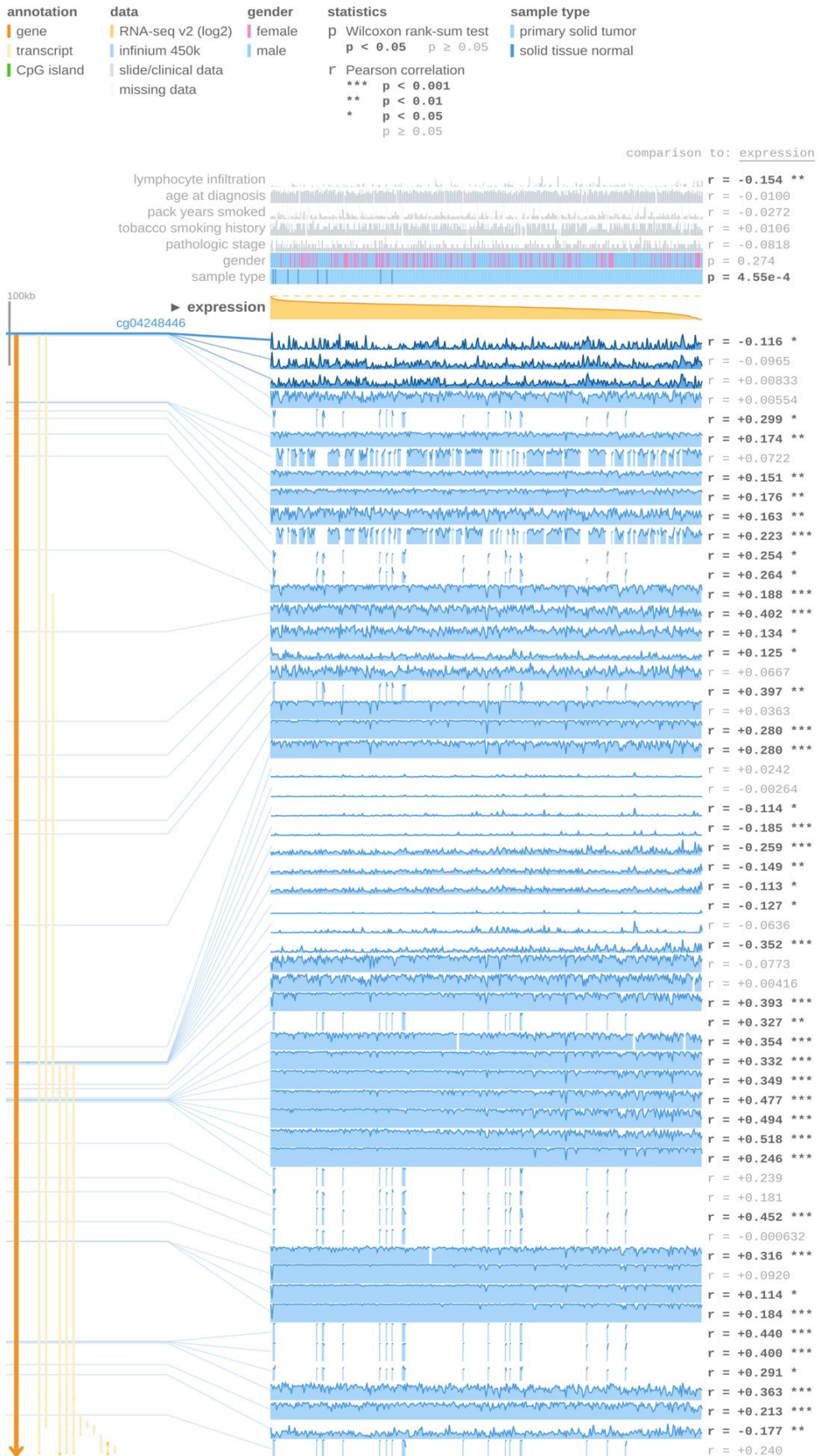
Supplementary Figure 21- Methylation analysis of ROBO2 gene in Lung adenocarcinoma. The highlighted probes are promoter gene region.



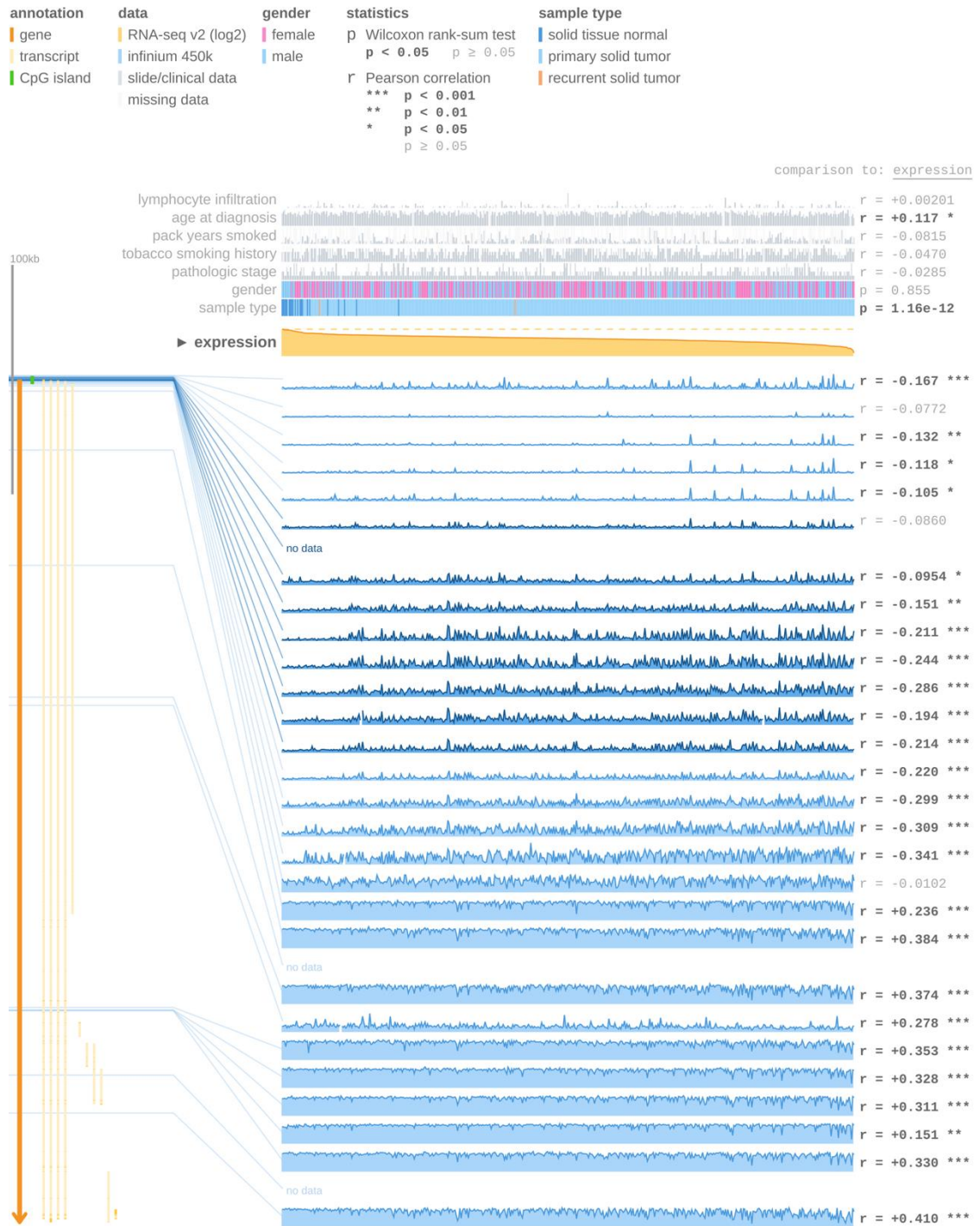
Supplementary Figure 22- Methylation analysis of ROBO2 gene in Lung squamous cell carcinoma. The highlighted probes are promoter gene region.



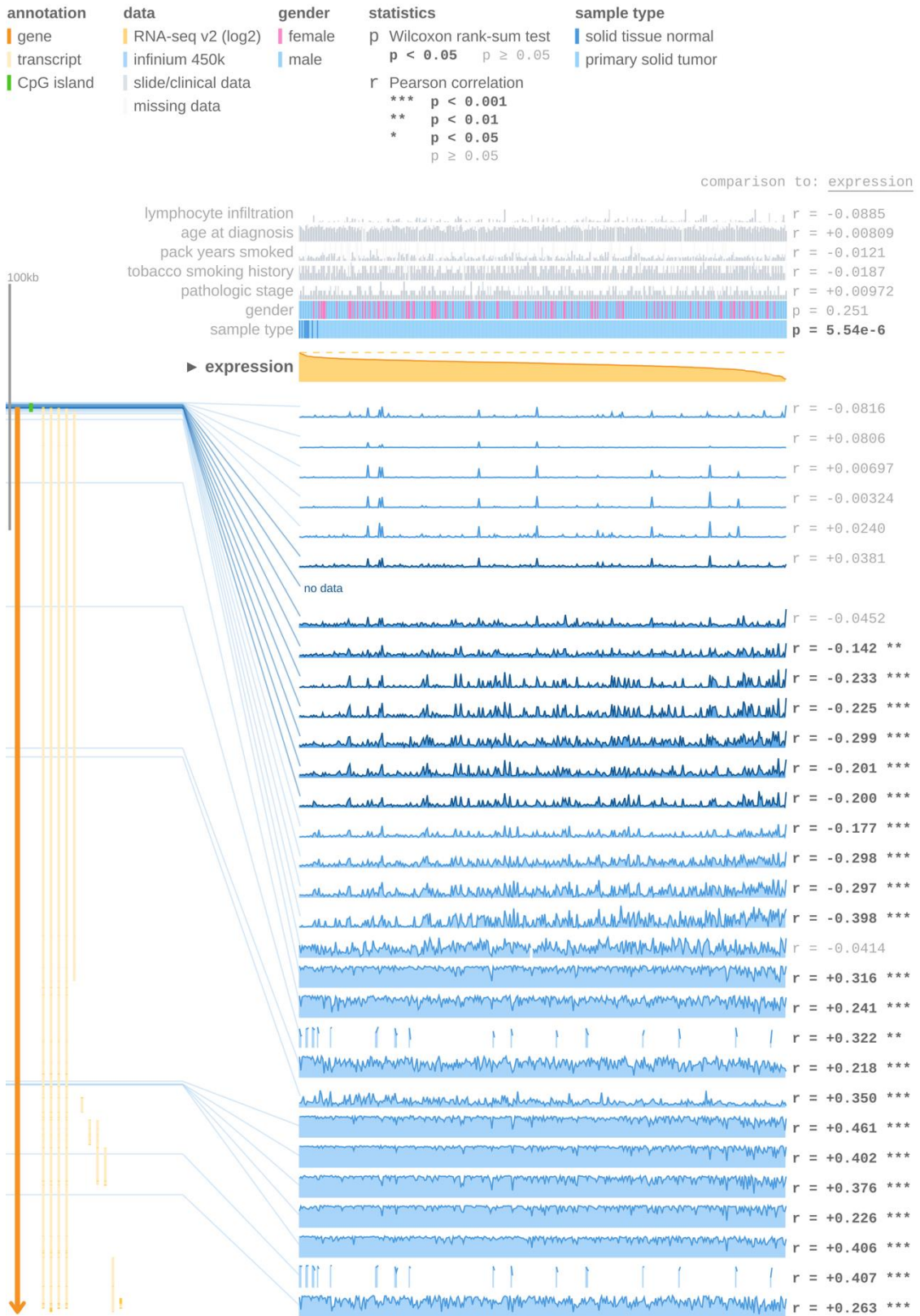
Supplementary Figure 23- Methylation analysis of SLIT2 gene in Lung adenocarcinoma. The highlighted probes are promoter gene region.



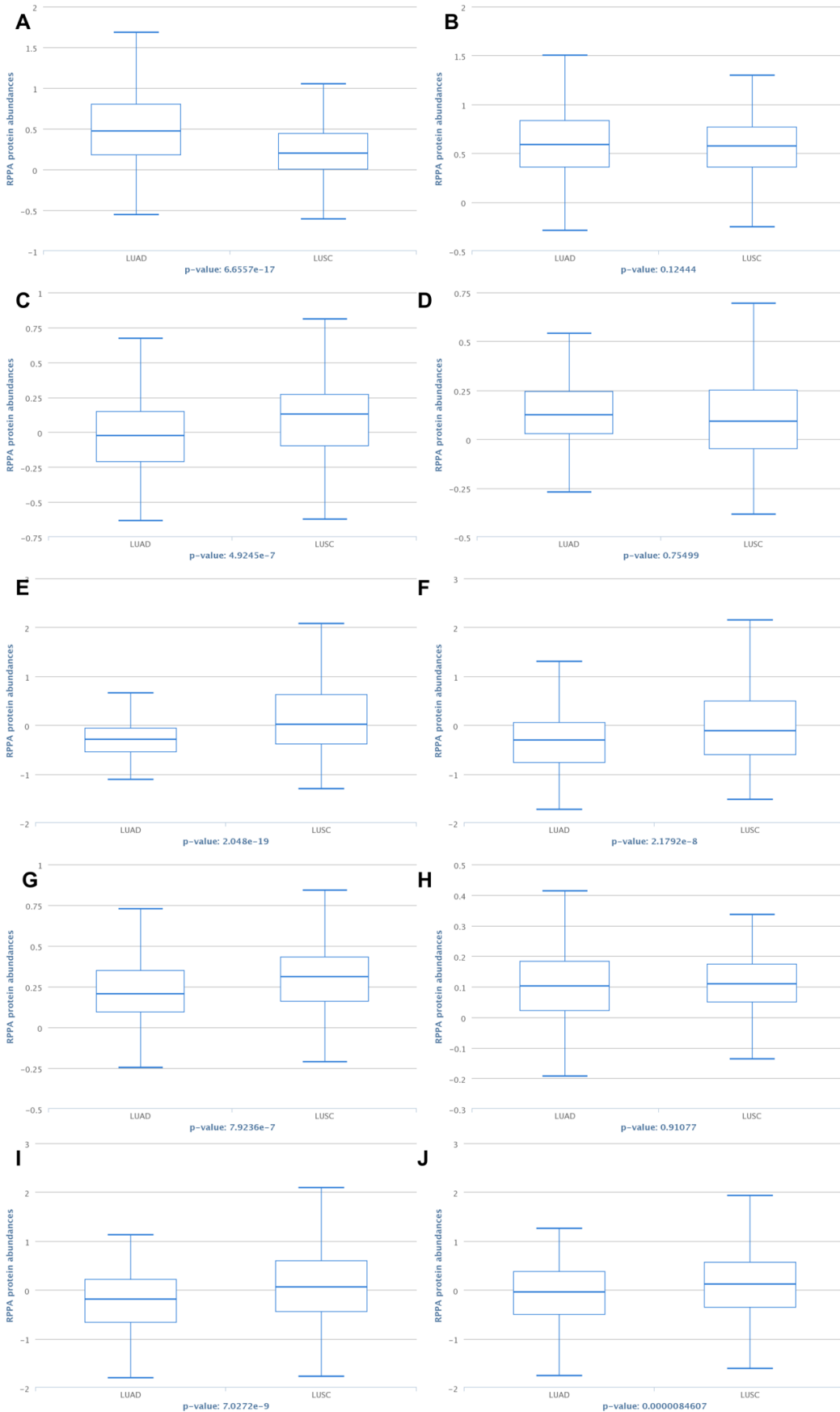
Supplementary Figure 24- Methylation analysis of SLIT2 gene in Lung squamous cell carcinoma. The highlighted probes are promoter gene region.

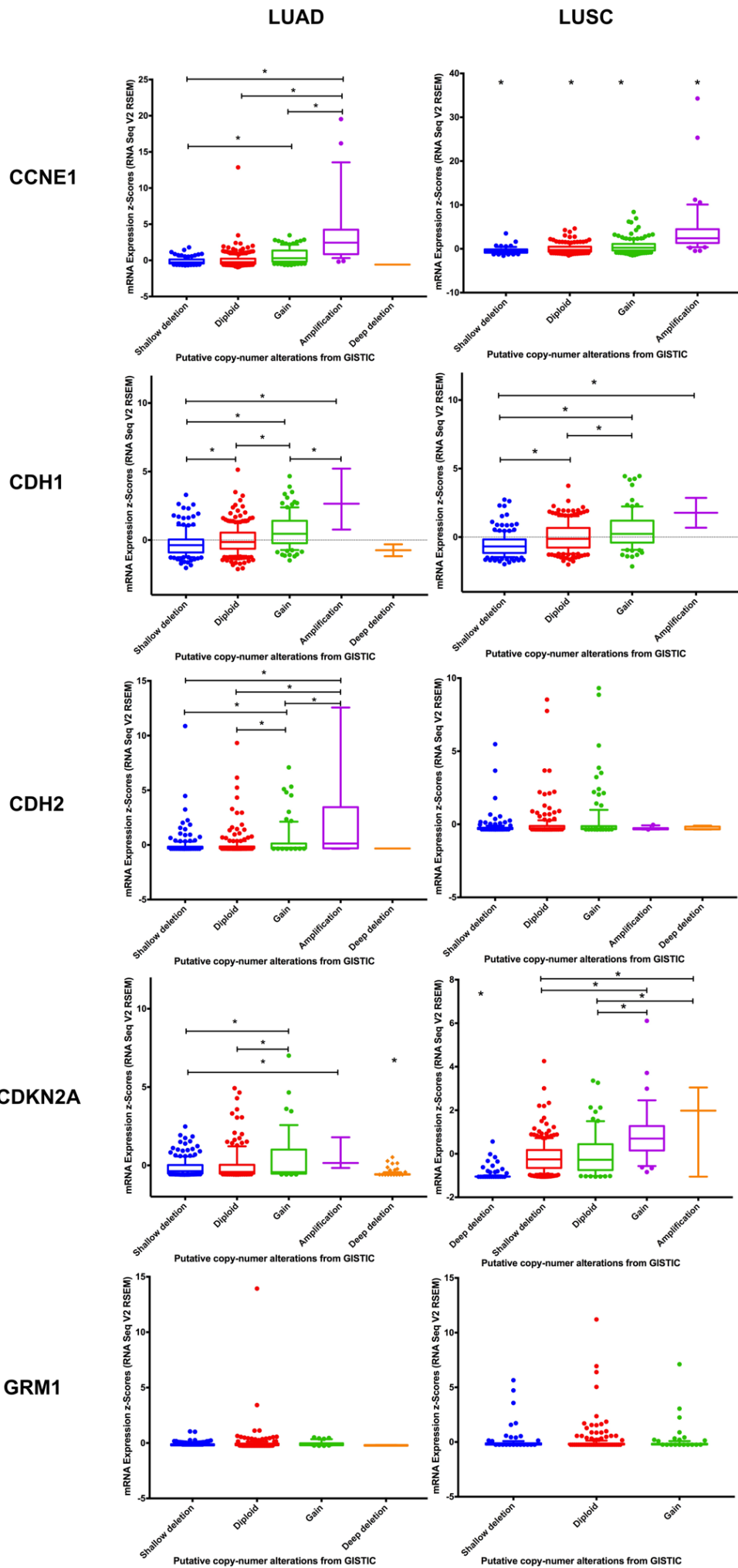


Supplementary Figure 25- Copy number alteration and mRNA expression analysis in lung adenocarcinoma and lung squamous cell carcinoma.

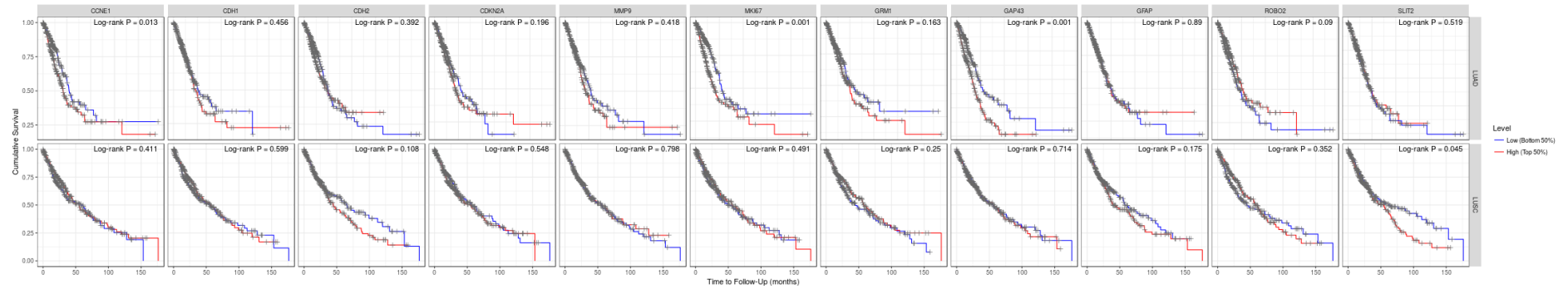


Supplementary Figure 26- RIPA analysis of MEK1 (A), MEK1_pS217S221 (B), Erk2 (C), PRAS40_pT246 (D), AKT_pT308 (E), AKT_pS473 (F), CRAF (G), CRAF_pS338 (H), GSK3_pS9 (I), GSK3ALPHABETA_pS21S9 (J) proteins in lung adenocarcinoma and lung squamous cell





Supplementary Figure 27- TIMER Survival analyses in lung adenocarcinoma and lung squamous cell carcinoma.



Scientific reports

Author Contributions statement

Title of Manuscript:

Are Schwann cells associated with lung cancer progression control? Insights from the meta-analysis of transcriptomics data

Contribution Author(S)

Study concepts: Victor Menezes Silva, Jessica Alves Gomes, Genilda Castro de Omena Neta, Karen da Costa Paixão, Ana Kelly Fernandes Duarte, Gabriel Cerqueira Braz da Silva, Ricardo Jansen Santos Ferreira, Rafael Danyllo da Silva Miguel, Aline Cavalcanti de Queiroz, Carlos Alberto de Carvalho Fraga

Study design: Victor Menezes Silva, Jessica Alves Gomes, Genilda Castro de Omena Neta, Karen da Costa Paixão, Rafael Danyllo da Silva Miguel, Aline Cavalcante de Queiroz, Carlos Alberto de Carvalho Fraga

Data acquisition: Victor Menezes Silva, Jessica Alves Gomes, Aline Cavalcante de Queiroz, Carlos Alberto de Carvalho Fraga

Quality control of data and algorithms: Victor Menezes Silva, Jessica Alves Gomes, Genilda Castro de Omena Neta, Karen da Costa Paixão, Ana Kelly Fernandes Duarte, Gabriel Cerqueira Braz da Silva, Aline Cavalcante de Queiroz, Carlos Alberto de Carvalho Fraga

Data analysis and interpretation: Victor Menezes Silva, Jessica Alves Gomes, Carlos Alberto de Carvalho Fraga

Statistical analysis: Victor Menezes Silva, Carlos Alberto de Carvalho Fraga

Manuscript preparation: Victor Menezes Silva, Carlos Alberto de Carvalho Fraga

Manuscript editing: Victor Menezes Silva, Jessica Alves Gomes, Genilda Castro de Omena Neta, Karen da Costa Paixão, Ana Kelly Fernandes Duarte, Gabriel Cerqueira Braz da Silva, Ricardo Jansen Santos Ferreira, Rafael Danyllo da Silva Miguel, Aline Cavalcante de Queiroz, Carlos Alberto de Carvalho Fraga

Manuscript review: Victor Menezes Silva, Jessica Alves Gomes, Genilda Castro de Omena Neta, Karen da Costa Paixão, Ana Kelly Fernandes Duarte, Gabriel Cerqueira Braz da Silva, Ricardo Jansen Santos Ferreira, Rafael Danyllo da Silva Miguel, Aline Cavalcante de Queiroz, Carlos Alberto de Carvalho Fraga

Name and Title of Corresponding Author: Carlos Alberto de Carvalho Fraga


Address: Av. Manoel Severino Barbosa, Bom Sucesso, Arapiraca, AL

Address: **Postcode and country:** 57309-005, Brazil

Tel No: +5582 991931405

Fax No:

Email: carlos.fraga@arapiraca.ufal.br



4. REFERÊNCIAS

- AIELLO, N. M. *et al.* EMT Subtype Influences Epithelial Plasticity and Mode of Cell Migration. **Developmental Cell**, 2018.
- ALLODI I.; UDINA E.; NAVARRO X. Specificity of peripheral nerve regeneration: interactions at the axon level. **Prog Neurobiol**, 2012.
- AZAM, S. H.; PECOT, C. V. Cancer's got nerve: Schwann cells drive perineural invasion. **Journal of Clinical Investigation**, 2016.
- BENITO, C. *et al.* STAT3 Controls the Long-Term Survival and Phenotype of Repair Schwann Cells during Nerve Regeneration. **The Journal of Neuroscience**, 2017.
- BOCKMAN D. E; BÜCHLER M.; BEGER H.G. Interaction of pancreatic ductal carcinoma with nerves leads to nerve damage. **Gastroenterology**, 1994.
- BOYD J.G.; GORDON T. Neurotrophic factors and their receptors in axonal regeneration and functional recovery after peripheral nerve injury. **Mol Neurobiol**, 2003.
- BRASIL. Ministério da Saúde. Instituto Nacional de Câncer. **Estimativa 2018: incidência de câncer no Brasil**. Rio de Janeiro: Inca, 2017.
- BROOM, L., WORLEY, A., GAO, F., HERNANDEZ, L. D., ASHTON, C. E., SHIH, L. C., & VANDERHORST, V. G. Translational methods to detect asymmetries in temporal and spatial walking metrics in parkinsonian mouse models and human subjects with Parkinson's disease. **Scientific reports**, 2019.
- BUNIMOVICH, Y. L., KESKINOV, A. A., SHURIN, G. V., & SHURIN, M. R. Schwann cells: a new player in the tumor microenvironment. **Cancer immunology, immunotherapy**, 2016.
- CHEN, G., RAMÍREZ, J. C., DENG, N., QIU, X., WU, C., ZHENG, W. J., & WU, H. Restructured GEO: restructuring Gene Expression Omnibus metadata for genome dynamics analysis. **Database: the journal of biological databases and curation**, 2019.
- CHEN, S. H., ZHANG, B. Y., ZHOU, B., ZHU, C. Z., SUN, L. Q., & FENG, Y. J. Perineural invasion of cancer: a complex crosstalk between cells and molecules in the perineural niche. **American journal of cancer research**, 2019.
- CHEN, R.; COHEN, L.G.; HALLETT. M. Nervous system reorganization following injury. **Neuroscience**, 2002.
- CLEMENTS, M. P. *et al.* The Wound Microenvironment Reprograms Schwann Cells to Invasive Mesenchymal-like Cells to Drive Peripheral Nerve Regeneration. **Neuron**, 2017.
- COLAPRICO, A. *et al.* TCGAbiolinks: An R/Bioconductor package for integrative

- analysis of TCGA data. **Nucleic Acids Research**, v. 44, n. 8, p. e71, 2016.
- CONSTANTIN, A. M.; TACHE, S. Stimulating factors for the regeneration of peripheral nerves. **Clujul Medical**, v. 85, n. 1, p. 12–19, 2012.
- DE OLIVEIRA, M.V.M. *et al.* Immunohistochemical expression of interleukin-4, -6, -8, and -12 in inflammatory cells in surrounding invasive front of oral squamous cell carcinoma. **Head and Neck**, v. 31, n. 11, 2009.
- DEBORDE, Sylvie *et al.* Schwann cells induce cancer cell dispersion and invasion. **Journal of Clinical Investigation**, 2016.
- DEBORDE, Sylvie; WONG, Richard J. How Schwann cells facilitate cancer progression in nerves. **Cellular and Molecular Life Sciences**, 2017.
- DEMIR, Ihsan Ekin *et al.* Investigation of schwann cells at neoplastic cell sites before the onset of cancer invasion. **Journal of the National Cancer Institute**, 2014.
- DOMENECH-ESTEVEZ, E. *et al.* Akt Regulates Axon Wrapping and Myelin Sheath Thickness in the PNS. **Journal of Neuroscience**, 2016.
- DORON-MANDEL E.; FAINZILBER M.; TERENCE M. Growth control mechanisms in neuronal regeneration. **FEBS Lett**, 2015.
- DROMAIN, C., PAVEL, M. E., RUSZNIEWSKI, P., LANGLEY, A., MASSIEN, C., BAUDIN, E., CAPLIN, M. E. Tumor growth rate as a metric of progression, response, and prognosis in pancreatic and intestinal neuroendocrine tumors. **BMC cancer**, 19(1), 2019.
- DU, Y., CHENG, Y., & SU, G. The essential role of tumor suppressor gene ING4 in various human cancers and non-neoplastic disorders. **Bioscience reports**, 39(1), 2019.
- EL SOURY M., FORNASARI B., MORANO M., GRAZIO E., RONCHI G., INCARNATO D., *et al.* Soluble Neuregulin1 down-regulates myelination genes in schwann cells. *Front. Mol. Neurosci.* 11:157. 2018.
- ESPAÑA-FERRUFINO A, LINO-SILVA LS, SALCEDO-HERNÁNDEZ RA. Extramural perineural invasion in pT3 and pT4 gastric carcinomas. **J PatholTransl Med.** 52:79–84. 2018.
- EVANS, G. R. D. Challenges to nerve regeneration. **Seminars in Surgical Oncology**, v. 19, p. 312-18, 2000.
- FENG, Y., HU, X., LIU, G., LU, L., ZHAO, W., SHEN, F., MA, K., SUN, C., ZHANG, B. M3 muscarinic acetylcholine receptors regulate epithelial-mesenchymal transition, perineural invasion, and migration/metastasis in cholangiocarcinoma through the AKT pathway. **Cancer cell international**, 18, 173. 2018.
- FLEDERICH, R. *et al.* Targeting myelin lipid metabolism as a potential therapeutic strategy in a model of CMT1A neuropathy. **Nature communications**, 9(1), 3025. 2018.

- FRIK, J. *et al.* Cross-talk between monocyte invasion and astrocyte proliferation regulates scarring in brain injury. **EMBO reports**, 2018.
- FURLANA, A., ADAMEYKO, I. Schwann cell precursor: a neural crest cell in disguise? **Developmental Biology**. 10.1101. 2018.
- GARMAN, R. H. Histology of the Central Nervous System. **Toxicologic Pathology**. [S.l: s.n.], 2011.
- GATENBY, R. A.; GILLIES, R. J. A microenvironmental model of carcinogenesis. **Nature Reviews Cancer**. [S.l: s.n.], 2008.
- GAUDET A. D.; POPOVICH P. G.; RAMER M. S. Wallerian degeneration: gaining perspective on inflammatory events after peripheral nerve injury. **J Neuroinflammation**, 2011.
- GEMINIANI, A. *et al.* A Multiple-Plasticity Spiking Neural Network Embedded in a Closed-Loop Control System to Model Cerebellar Pathologies. **International Journal of Neural Systems**, 2018.
- GOKEY, N. G. *et al.* Developmental Regulation of MicroRNA Expression in Schwann Cells. **Molecular and Cellular Biology**, 2012.
- GORDON, T., WOOD, P., & SULAIMAN, O. Long-Term Denervated Rat Schwann Cells Retain Their Capacity to Proliferate and to Myelinate Axons in vitro. **Frontiers in cellular neuroscience**, 12, 511. 2019.
- GORDON T.; FU S. Y. Long-term response to nerve injury. **Adv Neurol**. 72:185-99, 1997;
- GRIFFIN J.W.; THOMPSON, W.J. Biology and pathology of nonmyelinating Schwann cells. **Glia**, v. 56, p. 1518-31, 2008.
- GRÜNDKER, C., LÄSCHE, M., HELLINGER, J. W., & EMONS, G. Mechanisms of Metastasis and Cell Mobility - The Role of Metabolism. **Geburtshilfe und Frauenheilkunde**, 79(2), 184-188. 2019
- GUO, S. *et al.* Identification and validation of the methylation biomarkers of non-small cell lung cancer (nscl). **Clinical Epigenetics**, 2015.
- HE, D., WANG, X., ZHANG, Y., ZHAO, J., HAN, R., & DONG, Y. DNMT3A/3B overexpression might be correlated with poor patient survival, hypermethylation and low expression of ESR1/PGR in endometrioid carcinoma: an analysis of The Cancer Genome Atlas. **Chinese medical journal**, 132(2), 2019
- HEINEN A.; BEYER F.; TZEKOVA N.; HARTUNG H. P.; KÜRY P. Fingolimod induces the transition to a nerve regeneration promoting Schwann cell phenotype, **Experimental Neurology**, 2015.
- HINGORANI, D. V. *et al.* Impact of MMP-2 and MMP-9 enzyme activity on wound healing, tumor growth and RACPP cleavage. **PLoS ONE**, 2018.

HSU, Y. Y., CLYNE, M., WEI, C. H., KHOURY, M. J., & LU, Z. Using deep learning to identify translational research in genomic medicine beyond bench to bedside. **Database : the journal of biological databases and curation**, 2019.

HUANG, L., WU, R. L., & XU, A. M. Epithelial-mesenchymal transition in gastric cancer. **American journal of translational research**, 7(11), 2141-58. 2015.

JESSEN K. R.; MIRSKY R.; LLOYD A. C. Schwann cells: development and role in nerve repair. **Cold Spring Harb Perspect Biol**, 2015.

JESSEN, K. R.; MIRSKY, R. The repair Schwann cell and its function in regenerating nerves. **J Physiol**. 2016.

JOHNSON E. O.; ZOUBOS A.B.; SOUCACOS P. N. Regeneration and repair of peripheral nerves. **Injury, Int. J. Care Injured**. 36 Suppl 4: S24-29. 2005.

KANDEL, E.R.; SCHWARTS, J.H.; JESSEL, T.M. **Princípios da neurociência**. 4.ed. São Paulo: Manole; 2003.

KANG, Y. P., YOON J. H., LONG, N. P., KOO, G. B. *et al.* Spheroid-induced epithelial-mesenchymal transition provokes global alterations of breast cancer lipidome: A multi-layered omics analysis. **Front. Oncol**, 2. 2019

KATO, M., *et al.* A computational tool to detect DNA alterations tailored to formalin-fixed paraffin-embedded samples in cancer clinical sequencing. **Genome medicine**, 10(1), 2018.

KIM, I. W., JANG, H., KIM, J. H., KIM, M. G., KIM, S., & OH, J. M. Computational Drug Repositioning for Gastric Cancer using Reversal Gene Expression Profiles. **Scientific reports**, 9(1), 2019.

KOGURE, A., KOSAKA, N., & OCHIYA, T. Cross-talk between cancer cells and their neighbors via miRNA in extracellular vesicles: an emerging player in cancer metastasis. **Journal of biomedical science**, 26(1), 7. 2019.

KUANG AG, NICKEL JC, ANDRIOLE GL, CASTRO-SANTAMARIA R, FREEDLAND SJ, MOREIRA DM. Both acute and chronic inflammation are associated with lower perineural invasion in men with prostate cancer on repeat biopsy. **BJU Int**. 2019.

KUMAMARU, Hiromi *et al.* Activation of Intrinsic Growth State Enhances Host Axonal Regeneration into Neural Progenitor Cell Grafts. **Stem Cell Reports**, 2018.

LARNE, Olivia *et al.* MIR-183 in prostate cancer cells positively regulates synthesis and serum levels of prostate-specific antigen. **European Urology**, v. 68, n. 4, p. 581–588, 2015.

LO, H. C.; ZHANG, X. H.F. EMT in Metastasis: Finding the Right Balance. **Developmental Cell**. [S.l: s.n.]. , 2018

- MAGGI, S.P.; LOWE, J.B.; MACKINNON, S.E. Pathophysiology of nerve injury. **Clinical Plastic Surgery**, 30:109-126, 2003.
- MASCOLO, M. *et al.* Epigenetic dysregulation in oral cancer. **International Journal of Molecular Sciences**. [S.l: s.n.], 2012.
- MARTINS, R. S. *et al.* Mecanismos básicos da regeneração de nervos. **Arquivos Brasileiros de Neurocirurgia**, v. 24, n. 1, p. 20–25, 2005.
- MARKIEWICZ, A., TOPA, J., NAGEL, A., SKOKOWSKI, J., SEROCZYNSKA, B., STOKOWY, T., WELNICKA-JASKIEWICZ, M., ZACZEK, A. J. Spectrum of Epithelial-Mesenchymal Transition Phenotypes in Circulating Tumour Cells from Early Breast Cancer Patients. **Cancers**, 11(1), 59. 2019.
- MCCUBREY, J. A. *et al.* Roles of the Raf/MEK/ERK pathway in cell growth, malignant transformation and drug resistance. **Biochimica et Biophysica Acta - Molecular Cell Research**. [S.l: s.n.], 2007.
- MEISEL, J. S., NASKO, D. J., BRUBACH, B., CEPEDA-ESPINOZA, V., CHOPYK, J., CORRADA-BRAVO, H. Current progress and future opportunities in applications of bioinformatics for biodefense and pathogen detection: report from the Winter Mid-Atlantic Microbiome Meet-up, College Park, MD, January 10, 2018. **Microbiome**, 6(1), 197. 2018.
- MILLER, B. H. *et al.* Circadian and CLOCK-controlled regulation of the mouse transcriptome and cell proliferation. **Proceedings of the National Academy of Sciences**, 2007.
- MIYAZAKI, K., OYANAGI, J., HOSHINO, D., TOGO, S., KUMAGAI, H., & MIYAGI, Y. Cancer cell migration on elongate protrusions of fibroblasts in collagen matrix. **Scientific reports**, 9(1), 292. 2019.
- MOUSTAKAS, A., & HELDIN, C. H. Mechanisms of TGF β -Induced Epithelial-Mesenchymal Transition. **Journal of clinical medicine**, 5(7), 63. 2016.
- MULDER, N., *et al.* The development and application of bioinformatics core competencies to improve bioinformatics training and education. **PLoS computational biology**, 14(2), 2018.
- NAJI, A., FAVIER, B., DESCHASEAUX, F., ROUAS-FREISS, N., EITOKU, M., & SUGANUMA, N. Mesenchymal stem/stromal cell function in modulating cell death. **Stem cell research & therapy**, 10(1), 56. 2019.
- NAPOLI, I. *et al.* A Central Role for the ERK-Signaling Pathway in Controlling Schwann Cell Plasticity and Peripheral Nerve Regeneration In Vivo. **Neuron**, 2012.
- NAVARRO, X. Functional evaluation of peripheral nerve regeneration and target reinnervation in animal models: a critical overview. **Eur J Neurosci.**, 2015.
- NAVARRO, X.; VIVÓ, M.; VALERO-CABRE, A.; Neural plasticity after peripheral nerve injury and regeneration. **Progress in Neurobiology**, 82: 63–201, 2007.

- NOGUTI, J. *et al.* Metastasis from Oral Cancer: An Overview. **Cancer Genomics & Proteomics**, 2012.
- OGATA, T. Opposing Extracellular Signal-Regulated Kinase and Akt Pathways Control Schwann Cell Myelination. **Journal of Neuroscience**, 2004.
- PAKULA, M., MIKULA-PIETRASIK, J., WITUCKA, A., KOSTKA-JEZIorny, K., URUSKI, P., MOSZYŃSKI, R., NAUMOWICZ, E., SAJDAK, S., KSIĄŻEK, K. The Epithelial-Mesenchymal Transition Initiated by Malignant Ascites Underlies the Transmesothelial Invasion of Ovarian Cancer Cells. **International journal of molecular sciences**, 20(1), 137. 2019
- PASTUSHENKO, I. *et al.* Identification of the tumour transition states occurring during EMT. **Nature**, 2018.
- PAXTON, R. J., GARNER, W., DEAN, L. T., LOGAN, G., & ALLEN-WATTS, K. Health Behaviors and Lifestyle Interventions in African American Breast Cancer Survivors: A Review. **Frontiers in oncology**, 9, 3. 2019.
- PENAS, Clara; NAVARRO, Xavier. Epigenetic Modifications Associated to Neuroinflammation and Neuropathic Pain After Neural Trauma. **Frontiers in Cellular Neuroscience**, 2018.
- PETRUSKA J.C.; MENDELL L. M. The many functions of nerve growth factor: multiple actions on nociceptors. **Neurosci Lett.** 6;361(1-3):168-71, 2004.
- PORRELLO E. *et al.* Jab1 regulates Schwann cell proliferation and axonal sorting through p27. **J Exp Med** 211: 29–43. 2014.
- RAASAKKA, A. *et al.* Molecular structure and function of myelin protein P0 in membrane stacking. **Scientific reports**, 9(1), 642. 2019.
- RANDOLPH, G. J.; JAKUBZICK, C.; QU, Chunfeng. Antigen presentation by monocytes and monocyte-derived cells. **Current Opinion in Immunology**. [S.l: s.n.] , 2008.
- RASBAND, M. N., PELES E. The nodes of ranvier: Molecular assembly and maintenance. **Cold Spring Harb Perspect Biol** 10.1101. 2015
- ROSENWALD AG, PAULEY MA, WELCH L. The Course Source Bioinformatics Learning Framework. **CBE-Life Sci Educ**. 2016.
- ROSS, Michel H.; PAWLINA, Wojciech. **Ross histologia: texto e atlas: correlações com biologia celular e molecular**. 7. ed. Rio de Janeiro: Guanabara Koogan, 2016.
- SAKAUE, M., SIEBER-BLUM, M. Human epidermal neural crest stem cells as a source of Schwann cells. **Development** (Cambridge, England), 142(18), 2015.
- SALZER, J. L. Switching myelination on and off. **Journal of Cell Biology**. [S.l: s.n.] , 2008.
- SILVA, T. C. *et al.* TCGAbiolinksGUI: A graphical user interface to analyze cancer molecular and clinical data. **F1000Research**, v. 7, p. 439, 2018.

- SIMONS M, NAVE K-A. Oligodendrocytes: Myelination and axonal support. **Cold Spring Harb Perspect Biol**, 2015.
- SIQUEIRA, R. Lesões nervosas periféricas: uma revisão. **Revista Neurociências**, v. 15, n. 3, p. 226–233, 2007.
- SPAINHOUR, J. C., LIM, H. S., YI, S. V., & QIU, P. Correlation Patterns Between DNA Methylation and Gene Expression in The Cancer Genome Atlas. **Cancer informatics**, 2019.
- THOMAS, D., & RADHAKRISHNAN, P. Tumor-stromal crosstalk in pancreatic cancer and tissue fibrosis. **Molecular cancer**, 18(1), 14. 2019.
- TRICAUD N. Myelinating Schwann Cell Polarity and Mechanically-Driven Myelin Sheath Elongation. **Frontiers in cellular neuroscience**, 11, 2018.
- TSUBAKIHARA, Y., & MOUSTAKAS, A. Epithelial-Mesenchymal Transition and Metastasis under the Control of Transforming Growth Factor β . **International journal of molecular sciences**, 19(11), 2018.
- VILLARREAL-GARZA, C., LOPEZ-MARTINEZ, E. A., MUÑOZ-LOZANO, J. F., & UNGER-SALDAÑA, K. Locally advanced breast cancer in young women in Latin America. **Ecancermedicalscience**, 13, 894. 2019.
- WAGNER J, CHELARU F, KANCHERLA J, PAULSON JN, ZHANG A, FELIX V, *et al.* Metaviz: interactive statistical and visual analysis of metagenomic data. **Nucleic Acids Res**. 2018.
- WALLER, A. Experiments on the Section of the Glossopharyngeal and Hypoglossal Nerves of the Frog, and Observations of the Alterations Produced Thereby in the Structure of Their Primitive Fibres. **Philosophical Transactions of the Royal Society of London**, 1850.
- WANG, M., ZHAO, J., ZHANG, L., WEI, F., LIAN, Y., WU, Y., GONG, Z., ZHANG, S., ZHOU, J., CAO, K., GUO, C. Role of tumor microenvironment in tumorigenesis. **Journal of Cancer**, 8(5), 761-773. 2017.
- WEBBER, Christine A. *et al.* Schwann cells direct peripheral nerve regeneration through the Netrin-1 receptors, DCC and Unc5H2. **GLIA**, 2011.
- XIAO, YUNJUN *et al.* “Associations between dietary patterns and the risk of breast cancer: a systematic review and meta-analysis of observational studies”. **Breast cancer research: BCR** vol. 21,1 16. 29 Jan. 2019.
- YAO, Qing *et al.* MMP-Responsive ‘Smart’ Drug Delivery and Tumor Targeting. **Trends in Pharmacological Sciences**. [S.l: s.n.], 2018.
- ZHANG, K., LU, C., HUANG, X., CUI, J., LI, J., GAO, Y., LIANG, W., LIU, Y., SUN, Y., LIU, H., CHEN, L. Long noncoding RNA AOC4P regulates tumor cell proliferation and invasion by epithelial-mesenchymal transition in gastric cancer. **Therapeutic advances in gastroenterology**, 12, 2019.

ZHANG, X. *et al.* Schwann cells. **Neural Cell Biol.** [S.l: s.n.], 2017.

ZHOU H.; HUANG, S. Role of mTOR Signaling in Tumor Cell Motility, Invasion and Metastasis. **Curr Protein Pept Sci**, 2011.

ZHOU, Y. *et al.* Schwann cells augment cell spreading and metastasis of lung cancer. **Cancer Research**, 2018.

ZOCHODNE, D.W. The microenvironment of injured and regenerating peripheral nerves. **Muscle Nerve Suppl.**, v. 9, p. S33-38, 2000.

